

**Dynamics and Control of Spacecraft
with Retargeting Flexible Antennas**

by

Moon Kyu Kwak

Dissertation submitted to the Faculty of the
Virginia Polytechnic Institute and State University
in partial fulfillment of the requirements for the degree of
Doctor of Philosophy
in
Engineering Mechanics

APPROVED:

L. Meirovitch, Chairman

C. W. Smith

H. R. VanLandingham

S. L. Hendricks

D. P. Telionis

April 8, 1989

Blacksburg, Virginia

**Dynamics and Control of Spacecraft
with Retargeting Flexible Antennas**

by

Moon Kyu Kwak

L. Meirovitch, Chairman

Engineering Mechanics

(ABSTRACT)

This dissertation is concerned with the dynamics and control of spacecraft consisting of a rigid platform and a given number of retargeting flexible antennas. The mission consists of maneuvering the antennas so as to coincide with preselected lines of sight while stabilizing the platform in an inertial space and suppressing the elastic vibration of the antennas. The dissertation contains the derivation of the equations of motion by a Lagrangian approach using quasi-coordinates, as well as a procedure for designing the feedback controls. Assuming that antennas are flexible, distributed-parameter members, the state equations of motion are hybrid. Moreover, they are nonlinear. Following spatial discretization and truncation, these equations yield a system of nonlinear discretized state equations, which are more practical for numerical calculations and controller design. Linearization is carried out based on the assumption that the inertia of the rigid body is large relative to that of flexible body. The equations of motion for a two-dimensional model are also given. The feedback controls are designed in several ways. Disturbance-minimization control plus regulation is considered by using constant gains obtained on the basis of the premaneuver configuration of the otherwise time-varying system. In the case of unknown constant disturbance, proportional-plus-integral (PI) control has proven very effective. PI control is used to control the perturbed motions of the platform with multi-targeted flexible appendages. A new control law is obtained for the system with small time-varying configuration during a specified time period by applying a perturbation method to the Riccati equation obtained for PI control. According to the the proposed perturbation method, the control gains consist of zero-order time-invariant gains obtained from the solution of the matrix algebraic Riccati equation

(MARE) for the post-maneuver state and first-order time-varying gains obtained from the solution of the matrix differential Lyapunov equation (MDLE). The solution of the MDLE has an integral form, which can be approximated by a matrix difference equation. The adiabatic approximation, which freezes the matrix differential Riccati equation or Lyapunov equation is also discussed. Comparisons are made based on system stability by Lyapunov's second method. A spacecraft consisting of a rigid platform and a single flexible antenna is used to illustrate disturbance-minimization control, and a spacecraft consisting of a rigid platform and two flexible antennas reorienting into different directions is used to demonstrate the effectiveness of the disturbance-accommodating control. A time-varying spring-mass-damper and a two-dimensional model, representing a reduced version of the original spacecraft model, are considered to demonstrate the perturbation and adiabatic approximation methods. To illustrate the effect of nonlinearity on the dynamic response during reorientation, a numerical example of the spacecraft having a membrane-type antenna is presented.

Acknowledgements

I am deeply indebted to Professor Leonard Meirovitch for the many opportunities, guidance and support he has provided me in the course of my graduate studies at VPI &SU. All of his labor on my behalf is greatly appreciated.

I am grateful to Drs. C. W. Smith, H. F. Vanlandingham, S. L. Hendricks and D. P. Telionis for serving on my examining committee and for their review of this dissertation.

My thanks extend to my friends, especially Drs. M. A. Norris and M. E. B. France, for the beneficial discussions and pleasant times we shared.

I wish to express my deep appreciation to my parents for their continued encouragement during the course of my education.

To _____, my beloved wife, I cannot begin to express my appreciation for her patience and emotional support.

Table of Contents

1.0	Introduction	1
1.1	Preliminary Remarks	1
1.2	Literature Survey	4
1.3	Outline	7
2.0	Derivation of the Equations of Motion	9
2.1	Introduction	9
2.2	Equations of Motion of the Spacecraft	10
2.3	Hybrid Nonlinear State Equations of Motion	15
2.4	The Discretized Nonlinear State Equations of Motion	16
2.5	The Discretized Linear State Equations of Motion	19
2.6	Two-Dimensional Equations of Motion	27
3.0	Control Design	34
3.1	Maneuvering and Disturbances	34
3.2	Disturbance-Minimization Control	35
3.3	Disturbance-Accommodating Control	39

3.4	Perturbation Method	41
4.0	Numerical Results	51
4.1	Numerical Example 1	51
4.2	Numerical Example 2	54
4.3	Numerical Example 3	55
4.4	Numerical Example 4	59
4.5	Numerical Example 5	60
5.0	Summary and Conclusion	65
	References	67
	Figures	71
	Appendix A. Some Useful Properties	103
	Appendix B. Proof of Eq. (3-42)	105
	Appendix C. Derivation of Eq. (3-43)	108
	Appendix D. Expressions for Parameters	109
	Appendix E. Expressions for Matrices	110
	Appendix F. Expressions for Parameters	114
	Vita	120

List of Illustrations

Figure 1. The Rigid Platform with Flexible Appendages	72
Figure 2. Angular Displacements and Velocities of the Rigid Platform	73
Figure 3. The Spacecraft with a Single Maneuvering Flexible Appendage	74
Figure 4. Time History of the Appendage Maneuver	75
Figure 5. Time History of the Uncontrolled Tip Elastic Displacement	76
Figure 6. Time History of the Rigid-Body Translations	77
Figure 7. Time History of the Rigid-Body Rotation	78
Figure 8. Time History of the Tip Elastic Displacement	79
Figure 9. Rigid Platform with Two Flexible Beams	80
Figure 10. Time History of the Platform Translational Motions	81
Figure 11. Time History of the Platform Angular Motion	82
Figure 12. Tip Displacement of Beam 1	83
Figure 13. Tip Displacement of Beam 2	84
Figure 14. Gain corresponding to integral of x	85
Figure 15. Gain corresponding to x	86
Figure 16. Gain corresponding to derivative of x	87
Figure 17. Time Response	88
Figure 18. The Two-Dimensional Spacecraft	89
Figure 19. Time History of the Rigid-Body Translation	90
Figure 20. Time History of the Rigid-Body Translation	91
Figure 21. Time History of the Rigid-Body Rotation	92

Figure 22. Time History of the Tip Elastic Displacement	93
Figure 23. The Spacecraft with a Membrane Antennas	94
Figure 24. Time History of the Rigid-Body Translations	95
Figure 25. Time History of the Rigid-Body Rotations	96
Figure 26. Elastic Displacements at the Center	97
Figure 27. Elastic Displacements at the $r = 0.5 a$	98
Figure 28. Time History of the Rigid-Body Translations	99
Figure 29. Time History of the Rigid-Body Rotations	100
Figure 30. Elastic Displacements at the Center	101
Figure 31. Elastic Displacements at the $r = 0.5 a$	102

1.0 Introduction

1.1 *Preliminary Remarks*

In many space applications, it becomes necessary to reorient a certain line of sight in a spacecraft. Examples of this are the reorientation of a space telescope or of an antenna in a spacecraft. In some cases, such as in the space telescope, the line of sight can be regarded as being fixed relative to the undeformed structure, in which cases reorientation of the line of sight implies maneuvering of the whole spacecraft (Refs. 3-5,16,28-30,38,40-43,46 and 47). However, many spacecraft can be represented by mathematical models consisting of a rigid platform with one or more flexible appendages, such as flexible antennas, so that the mission involves the maneuvering of a hybrid (lumped and distributed flexible) system. Quite often, the line of sight coincides with an axis fixed in a small component of the spacecraft, such as an antenna, in which case it may be more advisable to retarget only the antenna and not the entire spacecraft. This is particularly true when the inertia of the antenna is much smaller than the inertia of the spacecraft. The argument becomes even stronger when several antennas must be retargeted independently in space. In such cases, it appears more sensible to conceive of a spacecraft consisting of a platform stabilized in an inertial space with several

appendages, rigid or flexible, hinged to the platform and capable of pivoting about two orthogonal axes relative to the platform (Refs. 31,33-36). In this case, reorientation relative to the stabilized platform is equivalent to retargeting in an inertial space. Note that such a maneuvering spacecraft is characterized by the fact that its configuration varies with time. This dissertation is concerned with the mission of independent retargeting of the line of sight of each antenna relative to the inertial space.

Figure 1 shows a spacecraft comprising a rigid platform with a given number of flexible appendages. Assuming that the flexible appendages represent antennas, the mission consists of maneuvering the antennas so as to coincide with preselected lines of sight. For given target directions of the antennas, the maneuvers can be designed as if the antennas were rigid. Of course, the antennas are flexible in actuality, so that the maneuvers are likely to cause elastic vibration of the antennas, which in turn also induce perturbations in the platform. Hence, the mission design can be regarded as involving several interdependent tasks. The first task is to select and implement policies for the maneuvering of the antennas relative to the inertial space. The second consists of stabilizing the attitude and position of the platform relative to the inertial space. The third task is simply to suppress any vibration of the flexible antennas caused by the maneuver. Of course, maneuvering of the antennas, stabilization of the platform and vibration suppression are to take place simultaneously.

The mathematical formulation consists of a hybrid set of equations of motion, in the sense that there are six ordinary differential equations for the rigid-body translations and rotations of the platform and partial differential equations for the elastic motion of each antenna. The equations of motion are not only hybrid, but the maneuvering of the antennas relative to the platform according to some prescribed function of time introduces time-dependent coefficients into the equations. Moreover, the equations contain terms reflecting persistent disturbances caused by inertial forces. If the mass of the antennas is small relative to the mass of the platform, then the equations of motion can be regarded as linear. Because control of the systems governed by sets of hybrid differential equations cannot be readily designed, even when the equations are linear, it is necessary to discretize

the partial differential equations in space, which can be carried out by the classical Rayleigh-Ritz method or the finite element method (Ref. 24).

Under certain circumstances, the time-varying terms are sufficiently small that they can be ignored in the control design. Even then, however, the full time-varying system must be considered in implementing the feedback controls designed on the basis of the time-invariant system.

This dissertation contains the derivation of the equation of motion for the spacecraft described above, as well as the procedure for designing the feedback controls. Hybrid state equation of motion for a spacecraft with retargeting flexible antennas are derived by a Lagrangian approach using quasi-coordinates (Refs. 23, 32 and 34). Upon discretization and linearization, a more manageable set of state equations is obtained. For future reference, state equations for the case of two-dimensional elastic members are also derived. In general, a time-varying gain matrix for the system is obtained by solving the matrix differential Riccati equation (MDRE), where the backward integration process must be carried out before the maneuver.

For a given maneuver, the control problem reduces to the minimization of the effect of the persistent disturbances caused by the maneuver and the annihilation of the elastic vibration and of the perturbations in the rigid-body maneuvers. To design the control minimizing the effect of the disturbances, the disturbances must be known a priori. This is, of course, a trivial matter if we can predict the disturbances accurately. However, the disturbances can be different for each maneuver, so that designer may not be always successful in accommodating the disturbances.

If the maneuver is to be carried out in minimum time, then the control law must be bang-bang (Ref. 25). Bang-bang control implies that the maneuver angular acceleration is constant over the first half of the maneuver, reverses sign at one half of the maneuver period and continues at the same level over the second half of the maneuver. Proportional-plus-integral (PI) control of the perturbations proves to be effective in the case of constant disturbances (Ref. 1 and 11). This approach is used in Chapter 3 to control the

vibration and rigid body perturbations in a spacecraft. Under the same assumption that the time-varying part in the coefficients is small, the control design is based on the constant part, which permits the use of constant control gains.

The PI control can be extended by considering control gains consisting of a large constant part and a small time-varying part. To this end, this dissertation presents a genuine perturbation approach to the optimal control problem for systems with time-varying coefficients, where the time-varying part is of one order magnitude smaller than the constant part. As in Ref. 33, we solve a steady-state matrix Riccati equation for the constant part. This represents the zero-order portion of the solution. On the other hand, for the first-order portion of the solution, we solve a differential (instead of an algebraic) matrix Lyapunov equation, thus permitting fast time variation in the time-varying part of the Riccati matrix.

1.2 Literature Survey

Beginning in the late 1950's, the dynamics of flexible spacecraft became a concern (Modi, Ref. 37). The maneuvering of flexible spacecraft has received considerable attention since flexibility makes the control design more complex, because the control objective is now to maneuver the spacecraft and suppress vibrations simultaneously.

Turner and Junkins (Ref. 45) addressed the problem of single-axis rotational maneuver of flexible spacecraft. They formulated the necessary conditions from Pontryagin's minimum principle and proposed a relaxation procedure for solving the associated nonlinear two-point boundary-value problem. The model considered in Ref. 45 consists of a rigid hub with four identical elastic appendages, in which a control torquer is located on the hub and is used for both rotational maneuver and vibration suppression. This places severe requirements on the controller, since the large-angle rotational maneuver and vibration suppression are performed simultaneously. In fact, numerical difficulties are encountered when solving the associated

two-point boundary problem with terminal constraints. Turner and Chun (Ref. 46) extended the results by adding extra torquers to the elastic appendages. Breakwell (Ref. 5) addressed the same problem in a similar manner and used standard fixed-time linear-quadratic-Gaussian regulator control theory and verified the proposed method experimentally. A common approach is to represent the elastic motion as a finite series of space-dependent admissible functions multiplied by generalized coordinates. This implies simultaneous discretization and truncation. Baruh and Silverberg (Ref. 3 and 4) suggested removing the terminal constraints, thereby permitting separation of the control problem into two problems, maneuver control and vibration suppression, where vibration suppression was carried out without considering rigid-body motions. Mostafa and Oz (Ref. 38) applied the variable structure control (VSC) technique to the model considered by Turner and Junkins (Ref. 45). They proposed ways of eliminating the chatter phenomenon, which occurs when implementing VSC.

Some projected NASA missions involve experiments consisting of the control of flexible bodies carried by a shuttle in Earth orbit. Wang, Lin and Ih (Ref. 48) presented a paper concerning the feasibility study of dynamics and control of shuttle-attached antenna experiments. They proposed a hardware design for isolation and decoupling between the shuttle and the antenna. A program initiated by NASA is referred to as the Spacecraft Control Laboratory Experiment (SCOLE) (Taylor and Balakrishnan, Ref. 44). The control objective of SCOLE is to reorient the line of sight in minimum time with limited control authority. Kakad (Ref. 16) presented a paper concerning the dynamics and control of the SCOLE model. He considered Euler parameters to define the rigid-body slewing. In this case, vibration suppression was performed at the end of the maneuver, where the feedback control law was derived from an infinite-time regulator problem. Juang, Horta and Robertshaw (Ref. 15) conducted hardware experiments involving the slewing control of a structure consisting of a steel beam and a solar panel. Although these experiments lacked some rigid-body motions, it was sufficient to demonstrate the hardware design concepts necessary for slewing flexible

structures. In their experiments, the linear optimal terminal control law was implemented by means of an analog computer.

Meirovitch and Quinn (Refs. 28 and 29), Quinn (Ref. 40) and Quinn and Meirovitch (Refs. 41 and 42) applied a perturbation method to control the motion of a SCOLE model undergoing large rigid-body motions and small elastic deformations. The perturbation method permits a maneuver strategy independent of the vibration control. Of course, there are small perturbed rigid-body motions resulting from the elastic vibrations. A minimum-time open-loop control was used for the large-angle slewing, and optimal control and pole placement techniques were used to suppress the vibration. First-order actuator dynamics, leading to a smoothed bang-bang, were considered to reduce the excitation. Meirovitch and Sharony (Ref. 30), Sharony and Meirovitch (Ref. 43) extended the previous studies (Ref. 42) by introducing integral control to accommodate the piecewise-constant disturbances caused by the internal forces resulting from the maneuver, and suggested a method of alleviating the effect of control spillover on the residual modes by introducing a Luenberger observer. Finite-time stability was achieved by means of an exponential convergence term included in the finite-time performance index.

The above papers were concerned with the reorientation of the entire spacecraft. Quite often, the line of sight coincides with an axis fixed in an antenna, in which case it may be more advisable to retarget only the antenna and not the entire spacecraft. Meirovitch and Kwak (Ref. 31) first addressed this situation. In Ref. 31, the elastic appendages are hinged to the platform and capable of pivoting about two-orthogonal axes relative to the platform and the maneuvering angles are assumed to be the known functions of time. A disturbance-minimization technique was used in Ref. 31, a proportional-plus-integral (PI) control was used in Ref. 33 and a perturbation method was applied to the time-varying system in Ref. 36. This dissertation contains the summary of these papers. Recently, Meirovitch and France (Ref. 35) introduced a discrete-time approach to the system considered in Ref. 31, and developed the substructure decentralized control method in which each substructure was controlled independently by either linear or bang-off-bang controllers.

The main difficulty encountered in addressing the dynamics of a system is how to derive the equations of motion easily. In general, the equations of motion for the spacecraft have very complicated expressions (Refs. 8, 18-20, 47), so that new methods of deriving equations of motion have been proposed (Refs. 9, 17 and 21). Kane and Levinson (Ref. 17) compared seven methods in their paper. Lagrange's equations of motion in terms of quasi-coordinates for a hybrid system were used first by Meirovitch (Ref. 26) and then by Williams (Ref. 49) and Brown (Ref. 6). Recently, Meirovitch (Ref. 32) and Meirovitch and Kwak (Ref. 34) showed that Lagrange's equations of motion in terms of quasi-coordinates are quite useful for deriving the equations of motion for the maneuvering and control of flexible spacecraft. Because the derived equations of motion are based on body-fixed coordinates, control design based on body-fixed coordinates is very convenient.

1.3 Outline

This dissertation is concerned with the dynamics and control of spacecraft with retargeting flexible antennas. The object of Chapter 2 is to produce equations capable of describing the motion of such a spacecraft. To this end, Lagrange's equations of motion using quasi-coordinates are first derived. In the derivation, the spacecraft is treated as a rigid body and the antennas as flexible appendages.

The equations describing the rigid-body motions of the spacecraft are nonlinear ordinary differential equations. On the other hand, the equations describing the small elastic displacements of a flexible appendage relative to a frame embedded in the undeformed appendage are partial differential equations. Hence, the complete equations describing a spacecraft during reorientation represent a set of nonlinear hybrid differential equations.

In general, hybrid systems of equations do not permit closed-form solution, so that one must consider an approximate solution, which implies spatial discretization and truncation.

Spatial discretization and truncation can be carried out by representing the motion as a finite set of admissible functions multiplied by time-dependent generalized coordinates; this is done in Section 2.4. The resulting discretized equations are nonlinear and can be cast in state form.

If the inertia of the platform is much larger than that of the flexible appendages, the equations can be linearized, so that the control design can be carried out as if the system were linear; this is done in Section 2.5. At times, especially when there is only one appendage and the motion takes place in a given plane, the equations of motion for the three-dimensional case are not really necessary. The equations are considerably simpler than those for the three-dimensional motion, as can be concluded from Section 2.6.

Chapter 3 deals with the implementation of control for the suppression of the perturbations caused by the maneuver and other disturbances. The maneuver strategy and the nature of the disturbances are discussed in Section 3.1. Disturbance-minimization control method is discussed in Section 3.2. Disturbance-accommodating control is discussed in Section 3.3, in which a proportional-plus-integral (PI) controller is introduced. A perturbation method is introduced in Section 3.4. and a new control law is obtained for systems with time-varying configuration.

Chapter 4 contains numerical examples illustrating the control strategies developed in Chapter 3.

Finally, Chapter 5 presents a summary of the solution techniques and of the numerical results, as well as conclusions. Recommendations for the future work are also included.

2.0 Derivation of the Equations of Motion

2.1 Introduction

In this chapter, the equations of motion for a spacecraft with retargeting flexible antennas are derived. The spacecraft is assumed to consist of a rigid body and flexible antennas, where the flexible appendages are regarded as distributed parameter members.

The equations describing the rigid-body motions of the spacecraft are nonlinear ordinary differential equations. On the other hand, the equations describing the small elastic displacements of a flexible appendage relative to a frame embedded in the undeformed appendage are partial differential equations. Hence, the complete equations describing a spacecraft during reorientation represent a set of nonlinear hybrid differential equations.

In general, hybrid systems of equations do not permit closed-form solution, so that one must consider an approximate solution, which implies spatial discretization and truncation. Spatial discretization and truncation can be carried out by representing the motion as a finite set of admissible functions multiplied by time-dependent generalized coordinates. Moreover, the equations are first linearized and then recast in compact state equations. However, the state equations still contain time-varying coefficients and persistent disturbances.

2.2 Equations of Motion of the Spacecraft

Let us consider a system consisting of a main rigid body, acting as a platform, and a certain number of flexible appendages hinged to the main rigid body. The interest lies in reorienting the flexible appendages independently so as to point in different preselected directions in the inertial space. The object is to derive the equations of motion capable of describing this task.

To describe the motion of the platform, we introduce a set of inertial axes XYZ and a set of body axes xyz attached to the rigid platform. Then, the motion of the platform can be defined in terms of three translations and three rotations of body axes xyz relative to the inertial axes XYZ. To describe the motion of the flexible appendages, we consider a typical appendage hinged at point e and regard e as the origin of a set of body axes x_e, y_e, z_e embedded in the appendage in its undeformed state. Then, the motion of a nominal point of the appendage consists of the motion of xyz, the motion of x_e, y_e, z_e relative to xyz and the elastic motion relative to x_e, y_e, z_e . The system and the various reference frames are shown in Fig. 1.

From Fig. 1., the position vector of a point in the rigid body and in the appendage can be written as

$$\underline{R}_r = \underline{R}_o + \underline{r} \quad (2 - 1a)$$

$$\underline{R}_e = \underline{R}_o + \underline{r}_{oe} + \underline{r}_e + \underline{u}_e \quad , \quad e = 1, 2, \dots, N \quad (2 - 1b)$$

where \underline{R}_o is the radius vector from O to o, \underline{r} is the position vector of a nominal point in the rigid body relative to xyz, \underline{r}_{oe} is the radius vector from o to e, \underline{r}_e is the position vector of a nominal point in undeformed appendage relative to x_e, y_e, z_e and \underline{u}_e is the elastic displacement of that point. Vector \underline{R}_o is given in terms of components along XYZ, \underline{r} and \underline{r}_{oe} in terms of components along xyz, and \underline{r}_e and \underline{u}_e in terms of components along x_e, y_e, z_e .

The velocity vector of o can be written in terms of components along xyz in the form

$$\underline{V}_o = C\dot{\underline{R}}_o \quad (2-2a)$$

where C is the matrix of direction cosines between xyz and XYZ and $\dot{\underline{R}}_o$ is the velocity vector of o in terms of components along XYZ. Matrix C depends on the angular displacements θ_i ($i=1,2,3$) defining the orientation of axes xyz relative to axes XYZ. Furthermore, the angular velocity vector of axes xyz in terms of components along xyz is given by

$$\underline{\omega} = D\dot{\underline{\theta}} \quad (2-2,b)$$

where $\dot{\underline{\theta}}$ is a vector of angular velocities $\dot{\theta}_i$ and D is a matrix depending on angular displacements θ_i ($i=1,2,3$). Figure 2 shows a set of such angular displacements. For this choice of angles, the matrices C and D are as follows:

$$C = \begin{bmatrix} c\theta_2c\theta_3 & c\theta_1s\theta_3 + s\theta_1s\theta_2c\theta_3 & s\theta_1s\theta_3 - c\theta_1s\theta_2c\theta_3 \\ -c\theta_2s\theta_3 & c\theta_1c\theta_3 - s\theta_1s\theta_2s\theta_3 & s\theta_1c\theta_3 + c\theta_1s\theta_2s\theta_3 \\ s\theta_2 & -s\theta_1c\theta_2 & c\theta_1c\theta_2 \end{bmatrix} \quad (2-3a)$$

$$D = \begin{bmatrix} c\theta_2c\theta_3 & s\theta_3 & 0 \\ -c\theta_2s\theta_3 & c\theta_3 & 0 \\ s\theta_2 & 0 & 1 \end{bmatrix} \quad (2-3b)$$

where $c\theta_i = \cos \theta_i$ and $s\theta_i = \sin \theta_i$. Note that this choice of angles helps us avoid singularities at the initial stage of the motion, $\theta_i = 0$.

In view of the above, the velocity vector of a point in the rigid body in terms of components along xyz is simply

$$\underline{V}_r = \underline{V}_o + \underline{\omega} \times \underline{r} \quad (2 - 4a)$$

and that of a point in the typical appendage e in terms of components along x_e, y_e, z_e is

$$\underline{V}_e = E_e(\underline{V}_o + \underline{\omega} \times \underline{r}_{oe}) + (E_e \underline{\omega} + \underline{\omega}_e) \times (\underline{r}_e + \underline{u}_e) + \underline{v}_e \quad , \quad e = 1, 2, \dots, N \quad (2 - 4b)$$

where $\underline{\omega}_e$ is the angular velocity vector of axes x_e, y_e, z_e , E_e is a matrix of direction cosines between the x_e, y_e, z_e and xyz and \underline{v}_e is the elastic velocity of the point in the appendage relative to x_e, y_e, z_e , $\underline{v}_e = \dot{\underline{u}}_e$. In the maneuver proposed, the angular velocity vectors $\underline{\omega}_e$ of x_e, y_e, z_e relative to xyz are given, so that the rotational motions of the appendages relative to the platform do not add degrees of freedom. The only degrees of freedom arises from the rigid-body translations and rotations of the platform and the elastic displacements of the appendages.

The equations of motion can be obtained by means of Lagrange's equations in terms of quasi-coordinates (Ref. 32 and 34).

$$\frac{\partial}{\partial t} \left(\frac{\partial L}{\partial \underline{V}_o} \right) + \tilde{\omega} \frac{\partial L}{\partial \underline{V}_o} - C \frac{\partial L}{\partial \underline{R}_o} = \underline{F} \quad (2 - 5a)$$

$$\frac{\partial}{\partial t} \left(\frac{\partial L}{\partial \underline{\omega}} \right) + \tilde{V}_o \frac{\partial L}{\partial \underline{V}_o} + \tilde{\omega} \frac{\partial L}{\partial \underline{\omega}} - (D^T)^{-1} \frac{\partial L}{\partial \underline{\theta}} = \underline{M} \quad (2 - 5b)$$

$$\frac{\partial}{\partial t} \left(\frac{\partial \hat{L}_e}{\partial \underline{v}_e} \right) - \frac{\partial \hat{T}_e}{\partial \underline{u}_e} + \mathcal{L}_e \underline{u}_e = \hat{\underline{U}}_e \quad (2 - 5c)$$

where

$$L = T - V \quad (2 - 6)$$

is the Lagrangian and \hat{T}_e is the kinetic energy density, in which T is the kinetic energy and V is the potential energy, \hat{L}_e is the Lagrangian density, both for appendage e , and \mathcal{L}_e is a matrix of homogenous differential operators. Equations (2-5) are hybrid in the sense that Eqs. (2-5a) and (2-5b) are ordinary differential equations and Eqs. (2-5c) are partial differential equations. It should be noted that the tilde over a symbol indicates a skew symmetric matrix with entries corresponding to the components of the associated vector (Ref. 31; see also Appendix A for vector and matrix operations). For the system of Fig. 1, we write the kinetic energy

$$\begin{aligned}
T &= \frac{1}{2} \int_{D_r} \rho_r \underline{v}_r^T \underline{v}_r dD_r + \sum_{e=1}^N \frac{1}{2} \int_{D_e} \rho_e \underline{v}_e^T \underline{v}_e dD_e \\
&= \frac{1}{2} m_t \underline{v}_o^T \underline{v}_o + \underline{v}_o^T \tilde{S}_t^T \underline{\omega} + \frac{1}{2} \underline{\omega}^T I_t \underline{\omega} + \sum_{e=1}^N \left[\frac{1}{2} \underline{\omega}_e^T I_e \underline{\omega}_e + \frac{1}{2} \int_{D_e} \rho_e \underline{v}_e^T \underline{v}_e dD_e \right. \\
&\quad \left. + (\underline{v}_o + \tilde{r}_{oe}^T \underline{\omega})^T E_e^T (\tilde{S}_e^T \underline{\omega}_e + \int_{D_e} \rho_e \underline{v}_e dD_e) + \underline{\omega}_e^T E_e^T I_e \underline{\omega}_e \right. \\
&\quad \left. + (E_e \underline{\omega} + \underline{\omega}_e)^T \int_{D_e} \rho_e (\tilde{r}_e + \tilde{u}_e) \underline{v}_e dD_e \right] \tag{2-7}
\end{aligned}$$

where

$$m_t = m_r + \sum_{e=1}^N m_e \quad , \quad m_r = \int_{D_r} \rho_r dD_r \quad , \quad m_e = \int_{D_e} \rho_e dD_e \tag{2-8a,b,c}$$

$$\tilde{S}_t = \tilde{S}_r + \sum_{e=1}^N (m_e \tilde{r}_{oe} + E_e^T \tilde{S}_e E_e) , \quad \tilde{S}_r = \int_{D_r} \rho_r \tilde{r} dD_r , \quad \tilde{S}_e = \int_{D_e} \rho_e (\tilde{r}_e + \tilde{u}_e) dD_e \quad (2-8d,e,f)$$

$$I_t = I_r + \sum_{e=1}^N (m_e \tilde{r}_{oe} \tilde{r}_{oe}^T + E_e^T I_e E_e - \tilde{r}_{oe} E_e^T \tilde{S}_e E_e - E_e^T \tilde{S}_e E_e \tilde{r}_{oe}) \quad (2-8g)$$

$$I_r = \int_{D_r} \rho_r \tilde{r} \tilde{r}^T dD_r , \quad I_e = \int_{D_e} \rho_e (\tilde{r}_e + \tilde{u}_e) (\tilde{r}_e + \tilde{u}_e)^T dD_e \quad (2-8i,j)$$

in which ρ_r and ρ_e are mass densities and D_r and D_e are the domain of the rigid platform and of a typical appendage, respectively, m_t is the total mass of the system, \tilde{S}_t is a skew symmetric matrix of first moments of inertia for the system and I_t is the inertia matrix. For simplicity, we assume that the potential energy is due entirely to elastic effects, in which case it can be written in the form

$$V = \frac{1}{2} \sum_{e=1}^N [\underline{u}_e , \underline{u}_e] = \sum_{e=1}^N \int_{D_e} \underline{u}_e^T \underline{\mathcal{L}}_e \underline{u}_e dD_e \quad (2-9)$$

where $[,]$ denotes an energy inner product (Ref. 24). The terms \underline{F} and \underline{M} on the right side of Eqs. (2-5a) and (2-5b), respectively, are the force and torque vectors on the platform, both in terms of components along axes xyz , and the term $\hat{\underline{U}}_e$ on the right side of Eq. (2-5c) is a distributed force vector on appendage e in terms of components along $x_e y_e z_e$.

2.3 Hybrid Nonlinear State Equations of Motion

Inserting Eqs. (2-7) and (2-9) into Eqs. (2-5) and considering Eqs. (2-2) and (2-3), we obtain the hybrid nonlinear Lagrange's equations

$$m_t \dot{V}_o + \tilde{S}_t^T \dot{\omega} + \sum_{e=1}^N E_e^T \int_{D_e} \rho_e \dot{V}_e dD_e = -m_t \tilde{\omega} V_o + \tilde{\omega} \tilde{S}_t \omega + \sum_{e=1}^N E_e^T \{ 2([\tilde{\omega}_e \tilde{S}_e] + \tilde{S}_{ev}) E_e \omega - 2\tilde{\omega}_e \int_{D_e} \rho_e V_e dD_e + \tilde{\omega}_e \tilde{S}_e \omega_e + \tilde{S}_e \dot{\omega}_e \} + \mathcal{L} \quad (2-10a)$$

$$\begin{aligned} \tilde{S}_t \dot{V}_o + I_t \dot{\omega} + \sum_{e=1}^N \int_{D_e} \rho_e [\tilde{r}_{oe} E_e^T + E_e^T (\tilde{r}_e + \tilde{u}_e)] \dot{V}_e dD_e &= \tilde{S}_t \tilde{V}_o \omega - \tilde{\omega} I_t \omega \\ + \sum_{e=1}^N \{ [-E_e^T (2\tilde{\omega}_e I_e - \text{tr} I_e \tilde{\omega}_e) + 2\tilde{r}_{oe} E_e^T ([\tilde{\omega}_e \tilde{S}_e] + \tilde{S}_{ev}) + 2E_e^T \int_{D_e} \rho_e (\tilde{r}_e \tilde{u}_e) \tilde{V}_e dD_e] E_e \omega V_e dD_e \\ - \int_{D_e} \rho_e [\tilde{r}_{oe} E_e^T \tilde{\omega} + E_e^T \tilde{\omega}_e (\tilde{r}_e + \tilde{u}_e)] + \tilde{r}_{oe} E_e^T (\tilde{\omega}_e \tilde{S}_e \omega_e + \tilde{S}_e \dot{\omega}_e + \tilde{S}_{ev} \omega_e) \\ - E_e^T (\tilde{\omega}_e I_e \omega_e + I_e \dot{\omega}_e + I_{ev} \omega_e) \} + \mathcal{M} \end{aligned} \quad (2-10b)$$

$$\begin{aligned} \rho_e \{ E_e \dot{V}_o + [E_e \tilde{r}_{oe} + (\tilde{r}_e + \tilde{u}_e)^T E_e] \dot{\omega} + \dot{V}_e \} \\ = \rho_e \{ -[E_e \omega] E_e (V_o - \tilde{r}_{oe} \omega) + 2[\tilde{V}_e E_e - (\tilde{r}_e + \tilde{u}_e) \tilde{\omega}_e E_e + \tilde{\omega}_e (\tilde{r}_e + \tilde{u}_e) E_e] \omega \\ - 2\tilde{\omega}_e V_e - ([E_e \omega]^2 + \tilde{\omega}_e^2 + \tilde{\omega}_e^2) (I_e + I_e) \} - \mathcal{L}_e \dot{u}_e + \hat{U}_e \end{aligned} \quad (2-10c)$$

where

$$\tilde{S}_{ev} = \int_{D_e} \rho_e \tilde{v}_e dD_e, \quad l_{ev} = \int_{D_e} \rho_e [\tilde{v}_e (\tilde{r}_e + \tilde{u}_e)^T + (\tilde{r}_e + \tilde{u}_e) \tilde{v}_e^T] dD_e \quad (2-11a,b)$$

The hybrid set of equations consist of Eqs. (2-10) and the kinematical relations

$$\dot{R}_o = C^T \underline{v}_o, \quad \dot{\theta} = D^{-1} \underline{\omega}, \quad \dot{u}_e = \underline{v}_e, \quad e = 1,2,\dots,N \quad (2-12a,b,c)$$

2.4 The Discretized Nonlinear State Equations of Motion

The equations of motion are hybrid, in the sense that the equations for the rigid-body translations and rotations of the platform are ordinary differential equations and those for the elastic motions of the appendages are partial differential equations. Moreover, because of the maneuver angular velocity vector $\underline{\omega}_o$, which is a given function of time, they possess time-dependent coefficients. Control design of systems described by hybrid equations is not feasible, so that we wish to discretize the partial differential equations in space, leaving us with only ordinary differential equations. To this end, we express the elastic displacements as linear combinations of space-dependent admissible functions multiplied by time-dependent generalized coordinates, or

$$u_e(r_e, t) = \Phi_e(r_e) q_e(t), \quad e = 1,2,\dots,N \quad (2-13)$$

where Φ_e is a matrix of admissible functions and q_e is a vector of generalized coordinates.

The Lagrangian equations in terms of quasi-coordinates for the rigid body motions of the platform remain in the form of Eqs. (2-5a) and (2-5b). On the other hand, inserting Eq. (2-13) into Eqs. (2-5c), we obtain the ordinary differential equations for the discretized elastic motions

$$\frac{d}{dt} \left(\frac{\partial L}{\partial \dot{p}_e} \right) - \frac{\partial L}{\partial q_e} = Q_e \quad , \quad e=1,2,\dots,N \quad (2-14)$$

where

$$\dot{p}_e = \dot{q}_e \quad (2-15)$$

$$Q_e = \int_{D_e} \Phi_e^T \hat{U}_e dD_e \quad , \quad e=1,2,\dots,N \quad (2-16)$$

are corresponding vectors of generalized forces.

The Lagrangian remains in the form (2-6) but the kinetic energy and potential energy change. Indeed, introducing Eq. (2-13) into Eqs. (2-7), we obtain the discretized kinetic energy

$$\begin{aligned} T = & \frac{1}{2} m_t \dot{V}_o^T V_o + \dot{V}_o^T \tilde{S}_t^T \omega + \frac{1}{2} \omega^T I_t \omega + \sum_{e=1}^N \left[\frac{1}{2} \omega_e^T I_e \omega_e + \frac{1}{2} \dot{p}_e^T \int_{D_e} \rho_e \Phi_e^T \Phi_e dD_e \dot{p}_e \right. \\ & + (\dot{V}_o + \tilde{r}_{oe}^T \omega)^T E_e^T (\tilde{S}_e^T \omega_e + \int_{D_e} \rho_e \Phi_e dD_e \dot{p}_e) + \omega^T E_e^T I_e \omega_e \\ & \left. + (E_e \omega + \omega_e)^T \int_{D_e} \rho_e (\tilde{r}_e + [\Phi_e \dot{q}_e]) \Phi_e dD_e \dot{p}_e \right] \end{aligned} \quad (2-17)$$

Many of the quantities in Eq. (2-17) are defined by Eqs. (2-8), with the exception of

$$\tilde{S}_e = \int_{D_e} \rho_e (\tilde{r}_e + [\Phi_e \dot{q}_e]) dD_e \quad , \quad I_e = \int_{D_e} \rho_e (\tilde{r}_e + [\Phi_e \dot{q}_e]) (\tilde{r}_e + [\Phi_e \dot{q}_e])^T dD_e \quad (2-18a,b)$$

Moreover, inserting Eq. (2-13) into Eq. (2-9), the discretized potential energy has the form

$$V = \frac{1}{2} \sum_{e=1}^N \dot{q}_e^T [\Phi_e \cdot \Phi_e] \dot{q}_e = \frac{1}{2} \sum_{e=1}^N \dot{q}_e^T K_e \dot{q}_e \quad (2-19)$$

where

$$K_e = [\Phi_e, \Phi_e] \quad (2-20)$$

Following the same procedure as used earlier, the discretized nonlinear state equations can be written as follows:

$$\begin{aligned} m\dot{V}_o + \tilde{S}_t^T \dot{\omega} + 2 \sum_{e=1}^N E_e^T ([\tilde{S}_e \omega_e]) E_e \omega - \tilde{S}_{ev} + \sum_{e=1}^N E_e^T \bar{\Phi}_e \dot{p}_e + 2 \sum_{e=1}^N E_e^T \tilde{\omega}_e \bar{\Phi}_e \tilde{p}_e \\ + m_t \tilde{\omega} V_o - \tilde{\omega} \tilde{S}_t \omega = \underline{F} + \sum_{e=1}^N E_e^T (\tilde{S}_e \dot{\omega}_e + \tilde{\omega}_e \tilde{S}_e \omega_e) \end{aligned} \quad (2-21a)$$

$$\begin{aligned} \tilde{S}_t \dot{V}_o + I_t \dot{\omega} + \sum_{e=1}^N \{ E_e^T (2\tilde{\omega}_e I_e - \text{tr} I_e \tilde{\omega}_e) + 2\tilde{r}_{oe} E_e^T ([\tilde{S}_e \omega_e]) - \tilde{S}_{ev} \} \\ - 2E_e^T \int_{D_e} \rho_e (\tilde{r}_e + [\Phi_e q_e]) [\Phi_e p_e] dD_e \} E_e \omega + \sum_{e=1}^N (E_e^T \bar{\Phi}_e + \tilde{r}_{oe} E_e^T \bar{\Phi}_e E_e^T \int_{D_e} \rho_e [\Phi_e p_e] \Phi_e dD_e) \dot{p}_e \\ + \sum_{e=1}^N [\tilde{r}_{oe} E_e^T \tilde{\omega}_e \bar{\Phi}_e + E_e^T \tilde{\omega}_e \tilde{\Phi}_e + E_e^T \tilde{\omega}_e \int_{D_e} \rho_e [\Phi_e q_e] \Phi_e dD_e] p_e + \tilde{S}_t \tilde{V}_o \omega + \tilde{\omega} I_t \omega \\ = \underline{M} + \sum_{e=1}^N [\tilde{r}_{oe} E_e^T (\tilde{S}_e \dot{\omega}_e + \tilde{\omega}_e \tilde{S}_e \omega_e) - E_e^T (I_e \dot{\omega}_e + \tilde{\omega}_e I_e \omega_e)] \end{aligned} \quad (2-21b)$$

$$\begin{aligned} \bar{\Phi}_e^T E_e \dot{V}_o + \bar{\Phi}_e^T E_e \tilde{\omega} V_o + (\bar{\Phi}_e^T E_e \tilde{r}_{oe}^T + \tilde{\Phi}_e^T E_e + \int_{D_e} \rho_e \Phi_e^T [\Phi_e q_e]^T dD_e E_e) \dot{\omega} \\ + 2[\tilde{\Phi}_e^T \tilde{\omega}_e^T + \int_{D_e} \rho_e \Phi_e^T ([\Phi_e q_e]) \tilde{\omega}_e - \tilde{\omega}_e \tilde{r}_e - [\Phi_e p_e] - \tilde{\omega}_e [\Phi_e q_e] dD_e] E_e \omega \\ + M_e \dot{p}_e + 2\tilde{H}_e(\omega_e) p_e + [K_e + \bar{H}_e(\omega_e) + \bar{H}_e(E_e \omega) + \tilde{H}_e(\dot{\omega}_e)] q_e \end{aligned}$$

$$= Q_e - \tilde{\Phi}_e^T \dot{\omega}_e + \int_{D_e} \rho_e \tilde{\Phi}_e \tilde{\omega}_e \tilde{r}_e \omega_e dD_e \quad (2-21c)$$

where

$$M_e = \int_{D_e} \rho_e \Phi_e^T \Phi_e dD_e, \quad \bar{\Phi}_e = \int_{D_e} \rho_e \Phi_e dD_e, \quad \tilde{\Phi}_e = \int_{D_e} \rho_e \tilde{r}_e \Phi_e dD_e \quad (2-22a,b,c)$$

$$\tilde{H}_e(\underline{a}) = \int_{D_e} \rho_e \Phi_e^T \tilde{a} \Phi_e dD_e, \quad \bar{H}_e(\underline{a}) = \int_{D_e} \rho_e \Phi_e^T \tilde{a}^2 \Phi_e dD_e \quad (2-22d,e)$$

2.5 The Discretized Linear State Equations of Motion

The object is to maintain the position and attitude of the platform fixed in a inertial space. Hence, we assumed that the rigid-body motions are small. Moreover, elastic displacements tend to be small. Expanding Eq. (2-17) and neglecting higher-order terms, the kinetic energy becomes

$$\begin{aligned} T = & \frac{1}{2} m_t \underline{V}_o^T \underline{V}_o + \underline{V}_o^T \tilde{S}_t^T \omega + \frac{1}{2} \omega^T I_t \omega + \sum_{e=1}^N \left[\frac{1}{2} \omega_e^T I_e \omega_e + \underline{V}_o^T E_e^T \tilde{S}_e^T \omega_e \right. \\ & + \omega^T (\tilde{r}_{oe} E_e^T \tilde{S}_e^T + E_e^T I_e) \omega_e + \frac{1}{2} \dot{q}_e^T M_e \dot{q}_e - \frac{1}{2} \dot{q}_e^T \bar{H}_e(\omega_e) \dot{q}_e + \underline{V}_o^T E_e^T \bar{\Phi}_e \dot{q}_e \\ & \left. + \underline{V}_o^T E_e^T \tilde{\omega}_e \bar{\Phi}_e \dot{q}_e + \omega^T \tilde{r}_{oe} E_e^T \bar{\Phi}_e \dot{q}_e + \omega^T \tilde{r}_{oe} E_e^T \bar{\Phi}_e \dot{q}_e + \dot{q}_e^T \tilde{\Phi}_e^T E_e \omega \right] \end{aligned}$$

$$+ \dot{q}_e^T \tilde{\Phi}_e^T \omega_e + \dot{q}_e^T \tilde{H}_e(\omega_e) \dot{q}_e + \omega_e^T E_e^T J_e(\omega_e) \dot{q}_e + \omega_e^T \int_{D_e} \rho_e \tilde{r}_e \tilde{\omega}_e \Phi_e dD_e \dot{q}_e] \quad (2-23)$$

In addition to the various quantities defined by Eqs. (2-22), we have

$$J_e(\underline{a}) = \int_{D_e} \rho_e (\tilde{r}_e \tilde{a} + [\tilde{r}_e \tilde{a}]) \Phi_e dD_e \quad (2-24)$$

in which \underline{a} is a vector representing ω_e or $\dot{\omega}_e$, and \underline{S}_e and \underline{I}_e are redefined for the linearized equation as follows:

$$\underline{S}_e = \int_{D_e} \rho_e \underline{r}_e dD_e, \quad \underline{I}_e = \int_{D_e} \rho_e \tilde{r}_e \tilde{r}_e^T dD_e \quad (2-25a,b)$$

Also note that a tilde over a symbol denotes a skew symmetric matrix obtained from the associated vector (Ref. 31).

Before deriving the linearized equations of motion, it is advisable to express the generalized forces appearing on the right side of Eqs. (2-21) in terms of actual forces. To this end, we denote by \underline{F}_e the actuator force and by \underline{M}_e the actuator torque acting on the platform. In addition, every appendage e is subjected to a distributed actuator force vector $\hat{\underline{U}}_e$. The vector \underline{F}_e and \underline{M}_e are in terms of components along xyz and the vectors $\hat{\underline{U}}_e$ are in terms of components along $x_e y_e z_e$. In writing the virtual work, we propose to express all vectors in terms of components along xyz. Consistent with this, we write the distributed force in the form

$$\underline{f}_e = E_e^T \hat{\underline{U}}_e, \quad e=1,2,\dots,N \quad (2-26)$$

where E_e is the matrix of direction cosines introduced earlier. Moreover, the virtual displacement associated with a point on appendage e can be written in terms of components along xyz as

$$\delta \underline{R}_e = \delta \underline{R}_o - (\tilde{r}_{oe} + [E_e^T \underline{r}_{e}]) \delta \theta + E_e^T \delta \underline{u}_e \quad (2-27)$$

Hence, considering Eqs. (2-26) and (2-27), the virtual work in terms of actual forces has the form

$$\begin{aligned} \delta W &= \underline{F}_o^T \delta \underline{R}_o + \underline{M}_o^T \delta \theta + \sum_{e=1}^N \int_{D_e} \underline{f}_e^T \delta \underline{R}_e dD_e \\ &= \underline{F}_o^T \delta \underline{R}_o + \underline{M}_o^T \delta \theta + \sum_{e=1}^N \int_{D_e} \hat{\underline{U}}_e^T E_e [\delta \underline{R}_o - (\tilde{r}_{oe} + [E_e^T \underline{r}_{e}]) \delta \theta + E_e^T \delta \underline{u}_e] dD_e \\ &= \underline{F}^T \delta \underline{R}_o + \underline{M}^T \delta \theta + \sum_{e=1}^N \int_{D_e} \hat{\underline{U}}_e^T \delta \underline{u}_e dD_e \end{aligned} \quad (2-28)$$

where

$$\underline{F} = \underline{F}_o + \sum_{e=1}^N \int_{D_e} E_e^T \hat{\underline{U}}_e dD_e, \quad \underline{M} = \underline{M}_o + \sum_{e=1}^N \int_{D_e} (\tilde{r}_{oe} + [E_e^T \underline{r}_{e}]) E_e^T \hat{\underline{U}}_e dD_e \quad (2-29a,b)$$

In practice, we use point actuators instead of distributed ones. But, discrete forces can be regarded as distributed by writing

$$\hat{\underline{U}}_e = \sum_{i=1}^{n_e} \underline{f}_{ei} \delta(\underline{r}_e - \underline{r}_{ei}) \quad (2-30)$$

where \underline{f}_{ei} time-dependent force amplitudes and $\delta(\underline{r}_e - \underline{r}_{ei})$ are spatial Dirac delta functions.

Inserting Eqs. (2-30) into Eqs. (2-29) and (2-16), we obtain

$$\underline{F} = \underline{F}_o + \sum_{e=1}^N \sum_{i=1}^{n_e} E_e^T \underline{f}_{ei}, \quad \underline{M} = \underline{M}_o + \sum_{e=1}^N \sum_{i=1}^{n_e} (\tilde{r}_{oe} E_e^T + E_e^T \tilde{r}_{ei}) \underline{f}_{ei} \quad (2-31a,b)$$

$$\underline{Q}_e = \sum_{i=1}^{n_e} \int_{D_e} \Phi_e^T \underline{f}_{ei} \delta(\underline{r}_e - \underline{r}_{ei}) dD_e = \sum_{i=1}^{n_e} \Phi_e^T(\underline{r}_{ei}) \underline{f}_{ei} \quad , \quad e=1,2,\dots,N \quad (2-31c)$$

Linearized state equation can be obtained either by inserting Eq. (2-23) and (2-19) into Eqs. (2-5a), (2-5b) and (2-14) or neglecting nonlinear terms in Eqs. (2-21). Recalling Eqs. (2-31), we obtain the following equations of motion

$$\begin{aligned} m \dot{\underline{V}}_o + \tilde{S}_t^T \dot{\underline{\omega}} + 2 \sum_{e=1}^N E_e^T [\tilde{S}_e \underline{\omega}_e] E_e \underline{\omega} + \sum_{e=1}^N E_e^T \bar{\Phi}_e \ddot{\underline{q}}_e + 2 \sum_{e=1}^N E_e^T \tilde{\omega}_e \bar{\Phi}_e \dot{\underline{q}}_e \\ + \sum_{e=1}^N E_e^T (\tilde{\omega}_e + \tilde{\omega}_e^2) \bar{\Phi}_e \underline{q}_e = \underline{F}_o + \sum_{e=1}^N \sum_{i=1}^{n_e} E_e^T \underline{f}_{ei} + \sum_{e=1}^N E_e^T (\tilde{S}_e \dot{\underline{\omega}}_e + \tilde{\omega}_e \underline{S}_e \underline{\omega}_e) \end{aligned} \quad (2-32a)$$

$$\begin{aligned} \tilde{S}_t \dot{\underline{V}}_o + I_t \dot{\underline{\omega}} + \sum_{e=1}^N (E_e^T (2\tilde{\omega}_e I_e - \text{tr} I_e \tilde{\omega}_e) E_e + 2\tilde{r}_{oe} E_e^T [\tilde{S}_e \underline{\omega}_e] E_e) \underline{\omega} \\ + \sum_{e=1}^N (E_e^T \tilde{\Phi}_e + \tilde{r}_{oe} E_e^T \bar{\Phi}_e) \ddot{\underline{q}}_e + \sum_{e=1}^N [2\tilde{r}_{oe} E_e^T \tilde{\omega}_e \bar{\Phi}_e + E_e^T \tilde{\omega}_e \tilde{\Phi}_e + E_e^T J_e(\underline{\omega}_e)] \dot{\underline{q}}_e \\ + \sum_{e=1}^N [\tilde{r}_{oe} E_e^T (\tilde{\omega}_e^2 + \tilde{\omega}_e) \bar{\Phi}_e + E_e^T (\tilde{\omega}_e J_e(\underline{\omega}_e) + J_e(\dot{\underline{\omega}}_e))] \underline{q}_e \\ = \underline{M}_o + \sum_{e=1}^N \sum_{i=1}^{n_e} (\tilde{r}_{oe} E_e^T + E_e^T \tilde{r}_{ei}) \underline{f}_{ei} + \sum_{e=1}^N [\tilde{r}_{oe} E_e^T (\tilde{S}_e \dot{\underline{\omega}}_e + \tilde{\omega}_e \underline{S}_e \underline{\omega}_e) - E_e^T (I_e \dot{\underline{\omega}}_e + \tilde{\omega}_e I_e \underline{\omega}_e)] \end{aligned} \quad (2-32b)$$

$$\bar{\Phi}_e^T E_e \dot{\underline{V}}_o + (\bar{\Phi}_e^T E_e \tilde{r}_{oe}^T + \bar{\Phi}_e^T E_e) \dot{\underline{\omega}} + [\bar{\Phi}_e^T \tilde{\omega}_e^T - J_e^T(\underline{\omega}_e)] E_e \underline{\omega} + M_e \ddot{\underline{q}}_e + 2\tilde{H}_e(\underline{\omega}_e) \dot{\underline{q}}_e$$

$$+ [K_e + \bar{H}_e(\underline{\omega}_e) + \tilde{H}_e(\dot{\underline{\omega}}_e)] \underline{q}_e = \sum_{i=1}^{n_e} \Phi_e^T(\underline{r}_{ei}) \underline{f}_{ei} - \tilde{\Phi}_e^T \dot{\underline{\omega}}_e + \int_{D_e} \rho_e \tilde{\Phi}_e \tilde{\omega}_e \tilde{r}_{e\omega_e} dD_e \quad (2-32c)$$

In addition to the above equations, if we assume small motions, Eqs. (2-12) become

$$\underline{V}_o = \dot{\underline{R}}_o, \quad \underline{\omega} = \dot{\underline{\theta}}, \quad \underline{p}_e = \dot{\underline{q}}_e \quad (2-33a,b,c)$$

If we express Eq. (2-32) and (2-33) in matrix form, then we obtain the linearized state equation

$$\dot{\underline{x}}(t) = \underline{A}(t)\underline{x}(t) + \underline{B}(t)\underline{f}(t) + \underline{D}(t)\underline{g}(t) \quad (2-34)$$

where

$$\underline{x}(t) = [\underline{R}_o^T \ \underline{\theta}^T \ \underline{q}_1^T \ \underline{q}_2^T \ \dots \ \underline{q}_N^T \ \underline{V}_o^T \ \underline{\omega}^T \ \underline{p}_1^T \ \underline{p}_2^T \ \dots \ \underline{p}_N^T]^T \quad (2-35)$$

is the state vector, in which $\underline{\theta}$ is a vector of angular displacements of the platform, \underline{V}_o is the translational velocity vector of the platform and \underline{p}_e ($e = 1,2,\dots,N$) are elastic velocity vectors,

$$\underline{A}(t) = \begin{bmatrix} \mathbf{0} & \mathbf{I} \\ -\underline{M}^{-1}(t) \underline{K}(t) & -\underline{M}^{-1}(t) \underline{G}(t) \end{bmatrix} \quad (2-36)$$

$$\underline{B}(t) = \begin{bmatrix} \mathbf{0} \\ \underline{M}^{-1}(t) \underline{B}^*(t) \end{bmatrix} \quad (2-37)$$

$$\underline{D}(t) = \begin{bmatrix} \mathbf{0} \\ \underline{M}^{-1}(t) \end{bmatrix} \quad (2-38)$$

are the matrices of coefficients,

$$\underline{d}(t) = \begin{bmatrix} \sum_{e=1}^N E_e^T (\tilde{S}_e \dot{\omega}_e + \tilde{\omega}_e \tilde{S}_e \omega_e) \\ \sum_{e=1}^N [\tilde{r}_{oe} E_e^T (\tilde{S}_e \dot{\omega}_e + \tilde{\omega}_e \tilde{S}_e \omega_e) - E_e^T (I_e \dot{\omega}_e + \tilde{\omega}_e I_e \omega_e)] \\ - \tilde{\Phi}_1^T \dot{\omega}_1 + \int_{D_1} \rho_1 \Phi_1^T \tilde{\omega}_1 \tilde{r}_1 \omega_1 dD_1 \\ \vdots \\ - \tilde{\Phi}_N^T \dot{\omega}_N + \int_{D_N} \rho_N \Phi_N^T \tilde{\omega}_N \tilde{r}_N \omega_N dD_N \end{bmatrix} \quad (2-39)$$

is the disturbance vector and

$$\underline{f}(t) = [F_o^T \quad M_o^T \quad \underline{f}_{11}^T \quad \underline{f}_{12}^T \quad \dots \quad \underline{f}_{1n_1}^T \quad \underline{f}_{21}^T \quad \underline{f}_{22}^T \quad \dots \quad \underline{f}_{2n_2}^T \quad \underline{f}_{31}^T \quad \dots \quad \underline{f}_{Nn_N}^T]^T \quad (2-40)$$

is the vector of control forces. Moreover, the mass matrix is given by

$$M(t) = \begin{bmatrix} mI & \tilde{S}_t^T & E_1^T \bar{\Phi}_1 & \dots & E_N^T \bar{\Phi}_N \\ \tilde{S}_t & I_t & E_1^T \tilde{\Phi}_1 + \tilde{r}_{o1} E_1^T \bar{\Phi}_1 & \dots & E_N^T \tilde{\Phi}_N + \tilde{r}_{oN} E_N^T \bar{\Phi}_N \\ \bar{\Phi}_1^T E_1 & \tilde{\Phi}_1^T E_1 + \bar{\Phi}_1^T E_1 \tilde{r}_{o1}^T & M_1 & \dots & 0 \\ \cdot & \cdot & \cdot & \cdot & \cdot \\ \cdot & \cdot & \cdot & \cdot & \cdot \\ \bar{\Phi}_N^T E_N & \tilde{\Phi}_N^T E_N + \bar{\Phi}_N^T E_N \tilde{r}_{oN}^T & 0 & \dots & M_N \end{bmatrix}$$

(2 - 41)

and

$$G(t) = \begin{bmatrix} 0 & 2 \sum_{e=1}^N E_e^T [\tilde{S}_e \omega_e] & 2E_1^T \tilde{\omega}_1 \bar{\Phi}_1 & \dots & 2E_N^T \tilde{\omega}_N \bar{\Phi}_N \\ 0 & G_{22} & G_{23}^1 & \dots & G_{23}^N \\ 0 & [\tilde{\Phi}_1^T \tilde{\omega}_1^T - J_1(\omega_1)] E_1 & 2\tilde{H}_1(\omega_1) & \dots & 0 \\ \cdot & \cdot & \cdot & \cdot & \cdot \\ \cdot & \cdot & \cdot & \cdot & \cdot \\ 0 & [\tilde{\Phi}_N^T \tilde{\omega}_N^T - J_N(\omega_N)] E_N & 0 & \dots & 2\tilde{H}_N(\omega_N) \end{bmatrix}$$

(2 - 42)

plays the role of a gyroscopic matrix, where

$$G_{22} = \sum_{e=1}^N (E_e^T (2\tilde{\omega}_e I_e - \text{tr} I_e \tilde{\omega}_e) E_e + 2\tilde{r}_{oe} E_e^T [\tilde{S}_e \tilde{\omega}_e] E_e) \quad (2-43a)$$

$$G_{23}^e = 2\tilde{r}_{oe} E_e^T \tilde{\omega}_e \bar{\Phi}_e + E_e^T \tilde{\omega}_e \tilde{\Phi}_e + E_e^T J_e(\omega_e) \quad (2-43b)$$

In addition,

$$K(t) = \begin{bmatrix} 0 & 0 & E_1^T (\tilde{\omega}_1 + \tilde{\omega}_1^2) \bar{\Phi}_1 & \dots & E_N^T (\tilde{\omega}_N + \tilde{\omega}_N^2) \bar{\Phi}_N \\ 0 & 0 & K_{23}^1 & \dots & K_{23}^N \\ 0 & 0 & K_1 + \bar{H}_1(\omega_1) + \tilde{H}_1(\dot{\omega}_1) & \dots & 0 \\ \dots & \dots & \dots & \dots & \dots \\ \dots & \dots & \dots & \dots & \dots \\ 0 & 0 & 0 & \dots & K_N + \bar{H}_N(\omega_N) + \tilde{H}_N(\dot{\omega}_N) \end{bmatrix} \quad (2-44)$$

is effectively the stiffness matrix, where

$$K_{23}^e = \tilde{r}_{oe} E_e^T (\tilde{\omega}_e^2 + \dot{\tilde{\omega}}_e) \bar{\Phi}_e + E_e^T (\tilde{\omega}_e J_e(\omega_e) + J_e(\dot{\omega}_e)) \quad (2-45)$$

$$B^*(t) = \begin{bmatrix} 1 & b^1 & b^2 & \dots & b^N \\ 0 & c^1 & 0 & \dots & 0 \\ 0 & 0 & c^2 & \dots & 0 \\ \dots & \dots & \dots & \dots & \dots \\ \dots & \dots & \dots & \dots & \dots \\ 0 & 0 & 0 & \dots & c^N \end{bmatrix} \quad (2-46)$$

relates the discrete force vectors to the modal force vectors, in which

$$b^e = \begin{bmatrix} E_e^T & E_e^T & \dots & E_e^T \\ \tilde{r}_{oe} E_e^T + E_e^T \tilde{r}_{e1} & \tilde{r}_{oe} E_e^T + E_e^T \tilde{r}_{e2} & \dots & \tilde{r}_{oe} E_e^T + E_e^T \tilde{r}_{en_e} \end{bmatrix} \quad (2-47)$$

$$c^e = [\Phi_e^T(r_{e1}) \quad \Phi_e^T(r_{e2}) \quad \dots \quad \Phi_e^T(r_{en_e})] \quad (2-48)$$

2.6 Two-Dimensional Equations of Motion

Let us consider the planar motion of a system consisting of a main rigid body and a flexible appendage hinged to the main rigid body (Fig. 18). The equations of motion for the two-dimensional motion of the system shown in Fig. 18 can be obtained from Eqs. (2-34) as follows:

$$[M_0 + M_1(t)] \ddot{\underline{\delta}} + G_1(t) \dot{\underline{\delta}} + [K_0 + K_1(t)] \underline{\delta} = \underline{f}(t) + \underline{d}(t) \quad (2-49)$$

where

$$\underline{\delta} = [R_y \quad R_z \quad \theta \quad \underline{q}_e^T]^T \quad (2-50)$$

is the configuration vector, in which R_y and R_z represent the translations in the y - and z -directions, θ represents the angular motion and \underline{q}_e are generalized coordinates. Moreover, $\underline{f}(t)$ and $\underline{d}(t)$ represent resultant control forces and disturbances, respectively, and they are given by

$$\underline{f} = [F_y \quad F_z \quad M_o \quad \underline{Q}_e^T]^T \quad (2-51)$$

and

$$\underline{d} = \begin{bmatrix} S_e(\dot{\beta}^2 c\beta + \ddot{\beta} s\beta) \\ S_e(\dot{\beta}^2 s\beta - \ddot{\beta} c\beta) \\ -l_e \ddot{\beta} + S_e r_{oe}(\dot{\beta}^2 s\beta - \ddot{\beta} c\beta) \\ -\tilde{\Phi}_e^T \ddot{\beta} \end{bmatrix} \quad (2-52)$$

In addition,

$$M_0 = \begin{bmatrix} m_t & 0 & 0 & 0 \\ 0 & m_t & S_t & \bar{\Phi}_e \\ 0 & S_t & l_t & \tilde{\Phi}_e + r_{oe} \bar{\Phi}_e \\ 0 & \bar{\Phi}_e^T & \tilde{\Phi}_e^T + r_{oe} \bar{\Phi}_e^T & M_e \end{bmatrix} \quad (2-53)$$

$$K_0 = \begin{bmatrix} 0 & 0 & 0 & 0 \\ 0 & 0 & 0 & 0 \\ 0 & 0 & 0 & 0 \\ 0 & 0 & 0 & K_e \end{bmatrix} \quad (2-54)$$

are the constant part of the coefficient matrices and

$$M_1 = s\beta M_s + (1 - c\beta) M_c \quad (2 - 55)$$

$$K_1 = (\dot{\beta}^2 s\beta - \ddot{\beta} c\beta) K_{b1} - (\dot{\beta}^2 c\beta + \ddot{\beta} s\beta) K_{b2} - \dot{\beta}^2 K_{b3} \quad (2 - 56)$$

$$G_1 = -2\dot{\beta} (s\beta G_s + c\beta G_c) \quad (2 - 57)$$

are the time-varying parts, in which

$$M_s = \begin{bmatrix} 0 & 0 & -S_e & -\bar{\Phi}_e \\ 0 & 0 & 0 & 0 \\ -S_e & 0 & 0 & 0 \\ -\bar{\Phi}_e^T & 0 & 0 & 0 \end{bmatrix} \quad (2 - 58a)$$

$$M_c = \begin{bmatrix} 0 & 0 & 0 & 0 \\ 0 & 0 & S_e & \bar{\Phi}_e \\ 0 & S_e & 2S_e r_{oe} & r_{oe} \bar{\Phi}_e \\ 0 & \bar{\Phi}_e^T & r_{oe} \bar{\Phi}_e^T & 0 \end{bmatrix} \quad (2 - 58b)$$

$$K_{b1} = \begin{bmatrix} 0 & 0 & S_e & \bar{\Phi}_e \\ 0 & 0 & 0 & 0 \\ 0 & 0 & 0 & 0 \\ 0 & 0 & 0 & 0 \end{bmatrix} \quad (2 - 58c)$$

$$K_{b2} = \begin{bmatrix} 0 & 0 & 0 & 0 \\ 0 & 0 & S_e & \bar{\Phi}_e \\ 0 & 0 & 0 & r_{oe}\bar{\Phi}_e \\ 0 & 0 & 0 & 0 \end{bmatrix} \quad (2 - 58d)$$

$$K_{b3} = \begin{bmatrix} 0 & 0 & 0 & 0 \\ 0 & 0 & 0 & 0 \\ 0 & 0 & 0 & 0 \\ 0 & 0 & 0 & M_e \end{bmatrix} \quad (2 - 58e)$$

$$G_s = \begin{bmatrix} 0 & 0 & 0 & 0 \\ 0 & 0 & S_e & -\bar{\Phi}_e \\ 0 & 0 & r_{oe}S_e & -r_{oe}\bar{\Phi}_e \\ 0 & 0 & 0 & 0 \end{bmatrix} \quad (2-58f)$$

$$G_c = \begin{bmatrix} 0 & 0 & S_e & -\bar{\Phi}_e \\ 0 & 0 & 0 & 0 \\ 0 & 0 & 0 & 0 \\ 0 & 0 & 0 & 0 \end{bmatrix} \quad (2-58g)$$

where β represents the angle between the flexible body and the rigid body, in which $s\beta$ and $c\beta$ denote $\sin \beta$ and $\cos \beta$, respectively. Finally,

$$m_t = m_r + m_e, \quad S_t = S_r + S_e + m_e r_{oe}, \quad I_t = I_r + I_e + m_e r_{oe}^2 + 2r_{oe}S_e \quad (2-59a,b,c)$$

$$S_r = \int_{D_r} \rho_r r dD_r, \quad S_e = \int_{D_e} \rho_e r_e dD_e \quad (2-59d,e)$$

$$I_r = \int_{D_r} \rho_r r^2 dD_r, \quad I_e = \int_{D_e} \rho_e r_e^2 dD_e \quad (2-59f,g)$$

$$\bar{\Phi}_e = \int_{D_e} \rho_e \Phi_e dD_e , \quad \tilde{\Phi}_e = \int_{D_e} \rho_e r_e \Phi_e dD_e \quad (2-59h,i)$$

$$M_e = \int_{D_e} \rho_e \Phi_e^T \Phi_e dD_e , \quad K_e = [\Phi_e , \Phi_e] \quad (2-59j,k)$$

in which ρ_r and ρ_e represent the mass density for the rigid body and flexible body, m_r and m_e represent the mass of the rigid and flexible bodies, respectively, S_r and S_e represent the first mass moments about the point o for the rigid body, about the point e for the flexible body, I_r and I_e are the mass moments of inertia of the rigid body and flexible body, respectively, and $[,]$ represents the energy inner product (Ref. 24). It can be seen that time-varying matrices depend on the maneuver angle, angular velocity and acceleration of the flexible body. Let us consider a pseudo-modal approach whereby the eigenvectors of the premaneuver spacecraft are used to simplify the equations. The eigenvalue problem for the premaneuver spacecraft has the form

$$K_0 \underline{\xi} = \lambda M_0 \underline{\xi} \quad (2-60)$$

Solving Eq. (2-60), we obtain the matrix U_0 of eigenvectors. Then, introducing the linear transformation

$$\underline{\xi} = U_0 \underline{\eta} \quad (2-61)$$

into Eq. (2-49) and using the orthonormality relations

$$U_0^T M_0 U_0 = I , \quad U_0^T K_0 U_0 = \Lambda_0 \quad (2-62a,b)$$

Eq. (2-49) can be rewritten as follows:

$$(I + \bar{M}_1) \ddot{\underline{\eta}} + \bar{G}_1 \dot{\underline{\eta}} + (\Lambda_0 + \bar{K}_1) \underline{\eta} = \underline{F} + \underline{D} \quad (2-63)$$

where

$$\bar{M}_1 = U_0^T M_1 U_0 = s\beta \bar{M}_s + (1 - c\beta) \bar{M}_c \quad (2 - 64a)$$

$$\bar{G}_1 = U_0^T G_1 U_0 = -2\dot{\beta}(s\beta \bar{G}_s + c\beta \bar{G}_c) \quad (2 - 64b)$$

$$\bar{K}_1 = U_0^T K_1 U_0 = (\dot{\beta}^2 s\beta - \ddot{\beta} c\beta) \bar{K}_{b1} - (\dot{\beta}^2 c\beta + \ddot{\beta} s\beta) \bar{K}_{b2} - \dot{\beta}^2 \bar{K}_{b3} \quad (2 - 64c)$$

$$\bar{M}_s = U_0^T M_s U_0, \quad \bar{M}_c = U_0^T M_c U_0 \quad (2 - 64d,e)$$

$$\bar{G}_s = U_0^T G_s U_0, \quad \bar{G}_c = U_0^T G_c U_0 \quad (2 - 64f,g)$$

$$\bar{K}_{b1} = U_0^T K_{b1} U_0, \quad \bar{K}_{b2} = U_0^T K_{b2} U_0, \quad \bar{K}_{b3} = U_0^T K_{b3} U_0 \quad (2 - 64h,i,j)$$

$$\bar{F} = U_0^T f, \quad \bar{D} = U_0^T d \quad (2 - 64k,l)$$

Equation (2-63) is said to be in pseudo-modal form. The equation can be used for the simulation and testing of new control laws, because it has the same dynamic characteristics as Eq. (2-34) and it is easier to work with.

3.0 Control Design

3.1 *Maneuvering and Disturbances*

The maneuver considered consists of retargeting antennas so as to point in given directions in the inertial space. By stabilizing the platform in an inertial space, the task reduces to reorienting the antennas relative to the platform. For a minimum-time maneuver, the control law is bang-bang, which implies that the angular acceleration of an antenna relative to the platform is constant, with the sign changing at half the maneuver period. Ideally, the maneuver should not cause elastic deformations in the flexible appendages. This is not possible in theory. Even, infinitesimally small deformations are likely to require a long maneuver time, which is in conflict with the minimum-time requirement. Hence, elastic deformations are likely to occur, which in turn implies perturbation of the platform from a fixed position in the inertial space.

The motion of the system is governed by Eq. (2-34). The system is characterized by two factors that distinguish it from most commonly encountered systems: it is time-varying and it is subjected to persistent disturbances. Both factors arise from the retargeting

maneuver angular velocities ω_e , angular accelerations $\dot{\omega}_e$, and the matrices E_e of direction cosines ($e = 1, 2, \dots, N$), all quantities being known functions of time.

Disturbances acting persistently on the system during reorientation arise from known sources. Indeed, these disturbances arise from the inertial loading due to the motion of the flexible appendages. This information depends on the policy of reorienting flexible appendages and should be regarded as qualitative in nature. In practical applications, disturbances appear as given functions of time, so that conventional design methods for time-varying systems can be used. Disturbances tend to have undesirable effects on the pointing accuracy of spacecraft. As a result, it is necessary to design counteracting controls to mitigate any adverse effects. Moreover, discretization and truncation of the distributed-parameter system results in reduced-order realization for the disturbances. Hence, the a priori information concerning $d(t)$ is usually not complete enough to permit accurate description of the nature of the disturbance, so that we are faced with the problem of designing disturbance-accommodating control with only an incomplete knowledge of this disturbance.

In this chapter, we consider first a disturbance-minimization control. To cope with unknown disturbances, proportional plus integral (PI) control will be explored. PI control will be extended by applying a perturbation method to the optimal control problem for systems with time-varying coefficients, where the time-varying part is of one order magnitude smaller than the constant part.

3.2 Disturbance-Minimization Control

The action of disturbances on the system tends to produce undesirable effects on the pointing accuracy. In view of this, it is customary to view the ideal control situation as one in

which the effects of the disturbances on the system performance can be completely eliminated by proper choice of counteracting controls.

Consistent with the nature of the system, we consider a control consisting of two parts: one part counteracting the persistent disturbances and a second part driving the state to zero. The control counteracting the persistent disturbances is open loop and the regulator is closed-loop. Hence, we assume a control vector in the form

$$\underline{f}(t) = \underline{f}_o(t) + \underline{f}_c(t) \quad (3-1)$$

where $\underline{f}_o(t)$ is responsible for the disturbance-minimization and $\underline{f}_c(t)$ is responsible for regulating the perturbed motions in the system. Substitution of Eq. (3-1) into Eq. (2-34) yields

$$\dot{\underline{x}} = A(t)\underline{x}(t) + B(t)(\underline{f}_o(t) + \underline{f}_c(t)) + D(t)\underline{d}(t) \quad (3-2)$$

The strategy of disturbance-accommodation consists of designing the control \underline{f}_o to cancel out the effects of the disturbances on the system completely. Hence, the open-loop control is assumed to satisfy

$$B(t)\underline{f}_o + D(t)\underline{d}(t) = 0 \quad (3-3)$$

or, recalling Eqs. (2-37) and (2-38),

$$B^*(t)\underline{f}_o(t) + \underline{d}(t) = 0 \quad (3-4)$$

In general, there are fewer actuators than the number of degrees of freedom of the discretized model, so that $B^*(t)$ is a rectangular matrix, which does not possess an exact inverse. Hence, when the number of actuators is smaller than the number of degrees of freedom, it is impossible to eliminate completely the effect of disturbances. In such a case, one can minimize the effect of the disturbance in a least-squares sense by choosing $\underline{f}_o(t)$ so as to satisfy

$$\underline{f}_o(t) = -[B^*(t)]^\dagger \underline{d}(t) \quad (3-5)$$

where $[B^*]^{\dagger} = (B^{*\top} B^*)^{-1} B^{*\top}$ is the pseudo-inverse of B^* .

On the assumption that the effect of the disturbances is virtually eliminated by the control $f_c(t)$, the remaining control problem can be regarded as an ordinary regulator problem. In view of Eqs. (3-2) and (3-3), the regulator is governed by

$$\dot{\underline{x}} = A(t)\underline{x}(t) + B(t)\underline{f}_c(t) \quad (3-6)$$

so that one can now proceed to design $f_c(t)$ by conventional methods. It should be noted that the technique of dividing the control design into two parts, as shown in Eq. (3-1), is a simple but effective idea, which appears to be unique to disturbance-accommodating control (DAC) theory (Refs. 12-14).

The closed-loop control is assumed to be optimal, in the sense that it minimizes the performance index

$$J = \frac{1}{2} \underline{x}^{\top}(t_f) H \underline{x}(t_f) + \frac{1}{2} \int_{t_0}^{t_f} (\underline{x}^{\top} Q \underline{x} + \underline{f}_c^{\top} R \underline{f}_c) dt \quad (3-7)$$

where t_0 and t_f are the initial and final time, respectively, and H , Q and R are penalty coefficient matrices to be selected by the analyst (Ref. 2). Minimization of J yields the optimal control law

$$\underline{f}_c = -R^{-1}(t) B^{\top}(t) P(t) \underline{x} \quad (3-8)$$

where P is an optimal control gain matrix satisfying the matrix Riccati equation

$$\dot{P} = -PA - A^{\top}P - Q + PBR^{-1}B^{\top}P \quad (3-9a)$$

subject to the boundary condition

$$P(t_f) = H \quad (3-9b)$$

The closed-loop state equation is obtained by inserting Eqs. (3-4) and (3-8) into Eq. (3-2), with the result

$$\dot{\underline{x}}(t) = A_c(t)\underline{x}(t) + D_c(t)\underline{d}(t) \quad (3-10)$$

where

$$A_c = A - BR^{-1}B^T P$$

$$= \begin{bmatrix} 0 & I \\ -M^{-1}[K + B^*R^{-1}(M^{-1}B^*)^T P_{21}] & -M^{-1}[G + B^*R^{-1}(M^{-1}B^*)^T P_{22}] \end{bmatrix} \quad (3-11a)$$

in which P_{21} and P_{22} are submatrices of P , as given by

$$P = \begin{bmatrix} P_{11} & P_{12} \\ P_{21} & P_{22} \end{bmatrix} \quad (3-11b)$$

and

$$D_c = D - B(B^*)^\dagger = \begin{bmatrix} 0 \\ M^{-1}\{I - B^*[(B^*)^T B^*]^{-1}(B^*)^T\} \end{bmatrix} \quad (3-11c)$$

Clearly, how well the controller is able to reduce the elastic vibration and deviations of the platform from equilibrium relative to the inertial space depends to a large extent on how close D_c is to the null matrix, which in turn depends on how close the matrix B^* is to a square matrix. The latter depends on the number of actuators.

3.3 Disturbance-Accommodating Control

In the previous section, we designed counteracting controls and optimal controls based on the assumption that the disturbances are known functions of time. Clearly, the disturbance term $D(t)\underline{d}(t)$ in Eq. (2-34) depends on the maneuver policy. In the case of minimum-time maneuver, the policy is bang-bang, which implies that the maneuver angular acceleration is constant over both halves of the maneuver period. If the maneuver is relatively slow, so that M^{-1} is virtually constant, then the disturbance is constant over both halves of the maneuver period. In this case, we can use proportional-plus-integral (PI) feedback control.

Introducing the notation

$$B(t)\underline{u}(t) = B(t)\underline{f}(t) + D(t)\underline{d}(t) \quad (3 - 12)$$

Eq. (2-34) can be rewritten as

$$\dot{\underline{x}}(t) = A(t)\underline{x}(t) + B(t)\underline{u}(t) \quad (3 - 13)$$

Assuming that $D(t)$ and $\underline{d}(t)$ vary slowly, so that $D(t)\underline{d}(t)$ is almost constant during the control interval, we can write

$$\underline{u}(t) = \underline{f}(t) = \underline{f}_d(t) \quad (3 - 14)$$

Introducing a new state vector defined by

$$\underline{z} = [\underline{x}^T \quad \underline{u}^T]^T \quad (3 - 15)$$

Eqs. (3-13) and (3-14) can be combined into the expanded state equation

$$\dot{\underline{z}}(t) = \hat{A}(t)\underline{z}(t) + \hat{B}(t)\underline{f}_d(t) \quad (3 - 16)$$

where

$$\hat{A}(t) = \begin{bmatrix} A(t) & B(t) \\ 0 & 0 \end{bmatrix}, \quad \hat{B}(t) = \begin{bmatrix} 0 \\ I \end{bmatrix} \quad (3-17a,b)$$

are coefficient matrices. Note that if $A(t)$ and $B(t)$ are a controllable pair, then $\hat{A}(t)$ and $\hat{B}(t)$ are also a controllable pair (Ref. 1).

We consider an optimal control policy in the sense that $\underline{f}_d(t)$ minimizes the performance measure

$$J = \frac{1}{2} \underline{z}^T(t_f) \hat{H} \underline{z}(t_f) + \frac{1}{2} \int_{t_0}^{t_f} (\underline{z}^T(t) \hat{Q}(t) \underline{z}(t) + \underline{f}_d^T(t) \hat{R}(t) \underline{f}_d(t)) dt \quad (3-18)$$

The optimal control law is

$$\underline{f}_d(t) = -\hat{R}^{-1}(t) \hat{B}^T(t) P(t) \underline{z}(t) = G(t) \underline{z}(t) \quad (3-19)$$

where $G(t) = -\hat{R}^{-1}(t) \hat{B}^T(t) P(t)$ represents a control gain matrix, in which $P(t)$ satisfies the matrix Riccati equation

$$\dot{P} = -P\hat{A} - \hat{A}^T P - \hat{Q} + P\hat{B}\hat{R}^{-1}\hat{B}^T P \quad (3-20)$$

Solving Eq. (3-20), we essentially obtain the optimal control law. Using Eqs. (3-13) - (3-15) and (3-19), it can be shown

$$\frac{d\underline{f}}{dt} = (G_1 - G_2 B^\dagger A) \underline{x} + G_2 B^\dagger \dot{\underline{x}} \quad (3-21)$$

where G_1 and G_2 represent the submatrices of G corresponding \underline{x} and \underline{u} , correspondingly, and $B^\dagger = (B^T B)^{-1} B^T$ is the pseudo-inverse of B . Integrating Eq. (3-21), we obtain the optimal control law

$$\underline{f}(t) = \underline{f}(0) + \int_0^t (G_1 - G_2 B^\dagger A) \underline{x} d\tau + \int_0^t G_2 B^\dagger \underline{\dot{x}} d\tau \quad (3 - 22)$$

If t , is sufficiently large and A and B can be assumed to be constant, then the gain matrix is constant. Moreover, if $\underline{x}(0)$ and $\underline{f}(0)$ are zero, then Eq. (3-22) yields

$$\underline{f}(t) = G_p \underline{x} + G_i \int_0^t \underline{x} d\tau \quad (3 - 23)$$

where

$$G_p = G_2 B^\dagger, \quad G_i = G_1 - G_2 B^\dagger A \quad (3 - 24a,b)$$

Equation (3-23) represents the optimal control law for the time-invariant system subjected to unknown constant disturbances, and is known as proportional-plus-integral (PI) control.

In general, the above control law cannot be used for the type of problem considered here. When the maneuver is relatively slow, however, so that the matrices A and B are nearly constant, the control law (3-23) can be used with satisfactory results. In this case, the control must be regarded suboptimal.

3.4 Perturbation Method

We are concerned here with the case in which the time-varying part of the coefficients is of one order of magnitude smaller than the constant part. In this case, we can use a perturbation approach to compute the control gains. To this end, we rewrite Eq. (2-63) in the form

$$\dot{\underline{\zeta}}(t) \cong [A_0 + A_1(t)]\underline{\zeta}(t) + [B_0 + B_1(t)](\underline{E}(t) + \underline{D}(t)) \quad (3-25)$$

where

$$\underline{\zeta} = [\underline{\eta}^T \quad \dot{\underline{\eta}}^T]^T \quad (3-26)$$

$$A_0 = \begin{bmatrix} 0 & I \\ -\Lambda_0 & 0 \end{bmatrix}, \quad B_0 = \begin{bmatrix} 0 \\ I \end{bmatrix} \quad (3-27a,b)$$

$$A_1 = \begin{bmatrix} 0 & 0 \\ \bar{M}_1\Lambda_0 - \bar{K}_1 & -\bar{G}_1 \end{bmatrix}, \quad B_1 = \begin{bmatrix} 0 \\ -\bar{M}_1 \end{bmatrix} \quad (3-27c,d)$$

in which quantities with the subscript 1 are of one order of magnitude smaller than quantities with the subscript 0.

Introducing the notation

$$\underline{g} = \underline{E} + \underline{D} \quad (3-28)$$

and assuming that the disturbance vector \underline{D} is constant during each half interval of the maneuver, we can write

$$\dot{\underline{g}} = \dot{\underline{E}} \quad (3-29)$$

Inserting Eq. (3-28) into Eq. (3-25) and combining with Eq. (3-29), we obtain the new state equation

$$\dot{\underline{w}} = \hat{A}\underline{w} + \hat{B}\dot{\underline{E}} \quad (3-30)$$

where

$$\underline{w} = [\underline{\zeta}^T \underline{g}^T]^T, \quad \hat{A} = \hat{A}_0 + \hat{A}_1(t) \quad (3-31a,b)$$

$$\hat{A}_0 = \begin{bmatrix} A_0 & B_0 \\ 0 & 0 \end{bmatrix}, \quad \hat{A}_1(t) = \begin{bmatrix} A_1(t) & B_1(t) \\ 0 & 0 \end{bmatrix}, \quad \hat{B} = \begin{bmatrix} 0 \\ I \end{bmatrix} \quad (3-31c,d,e)$$

Next, we consider the performance index

$$J = \frac{1}{2} \int_0^T (\underline{w}^T Q \underline{w} + \dot{\underline{E}}^T R \dot{\underline{E}}) dt \quad (3-32)$$

so that the optimal control law is given by

$$\dot{\underline{F}} = -R^{-1} \hat{B}^T P \underline{w} \quad (3-33)$$

where P is the solution of matrix differential Riccati equation (MDRE)

$$-\dot{P} = P \hat{A} + \hat{A}^T P + Q - P \hat{B} R^{-1} \hat{B}^T P \quad (3-34a)$$

and is subject to the boundary condition

$$P(T) = 0 \quad (3-34b)$$

note that T represent the terminal time of control action.

Consistent with the perturbation approach, we divide P into a zero-order term and a small perturbing term, or

$$P = P_0 + P_1 \quad (3-35)$$

Inserting Eq. (3-35) into Eqs. (3-34), we obtain a zero-order matrix differential Riccati equation (MDRE)

$$-\dot{P}_0 = P_0 \hat{A}_0 + \hat{A}_0^T P_0 + Q - P_0 \hat{B} R^{-1} \hat{B}^T P_0 \quad (3-36)$$

and a first-order matrix differential Lyapunov equation (MDLE)

$$-\dot{P}_1 = P_1 \hat{A}_{0C} + \hat{A}_{0C}^T P_1 + P_0 \hat{A}_1 + \hat{A}_1^T P_0 \quad (3-37)$$

where

$$\hat{A}_{0C} = \hat{A}_0 - \hat{B} R^{-1} \hat{B}^T P_0 \quad (3-38)$$

denotes a closed-loop matrix. From Eq. (3-34b), the boundary conditions are

$$P_0(T) = 0 \quad , \quad P_1(T) = 0 \quad (3-39a,b)$$

If the final time T approaches infinity and the maneuver ends at time t_r , $t_r < T$, we can use the steady-state solution of the zero-order MDRE for the post maneuver period because time-varying coefficients no longer exist after the termination of the maneuver. Then, the zero-order MDRE, Eq. (3-36), becomes the MARE

$$P_0 \hat{A}_0 + \hat{A}_0^T P_0 + Q - P_0 \hat{B} R^{-1} \hat{B}^T P_0 = 0 \quad (3-40)$$

The MDLE, Eq. (3-37), is effective only during the maneuver, so that the boundary condition (3-39b) should be rewritten as

$$P_1(t_r) = 0 \quad (3-41)$$

where t_r indicates the final time of the maneuver. The solution of Eq. (3-37) subject to the boundary condition (3-41) can be expressed as

$$P_1(t) = \int_t^{t_f} e^{\hat{A}_{0c}(\tau-t)} [\hat{A}_1^T(\tau)P_0 + P_0\hat{A}_1(\tau)] e^{\hat{A}_{0c}(\tau-t)} d\tau \quad (3-42)$$

as shown in Appendix B.

To obtain a discrete-time solution, we discretize Eq. (3-42) in time. To this end, we let $t_{k+1} = t_k + \Delta t$, so that Eq. (3-42) yields

$$P_1(t_{k+1}) = e^{-\hat{A}_{0c}\Delta t} [P(t_k) - \int_0^{\Delta t} e^{\hat{A}_{0c}\xi} \Gamma(t_k + \xi) e^{\hat{A}_{0c}\xi} d\xi] e^{-\hat{A}_{0c}\Delta t} \quad (3-43)$$

where $\Gamma(t_k + \xi) = [\hat{A}_1^T(t_k + \xi)P_0 + P_0\hat{A}_1(t_k + \xi)]$. Derivation of Eq. (3-43) is given in Appendix C. Equation (3-43) represents a matrix difference equation for the first-order solution. The initial condition is given as

$$P_1(0) = \int_0^{t_f} e^{-\hat{A}_{0c}\tau} \Gamma(\tau) e^{-\hat{A}_{0c}\tau} d\tau \quad (3-44)$$

It is common to assume that the time-varying terms are constant over the small time interval $0 < t < \Delta t$, so that Eq. (3-43) gives

$$P_1(t_{k+1}) \cong e^{-\hat{A}_{0c}\Delta t} [P(t_k) - e^{\hat{A}_{0c} \frac{\Delta t}{2}} \Gamma(t_k + \frac{\Delta t}{2}) e^{\hat{A}_{0c} \frac{\Delta t}{2}} \Delta t] e^{-\hat{A}_{0c}\Delta t} \quad (3-45)$$

The control law given by Eq. (3-33) is not ready for implementation. The next task is to use the equation to generate the final control law. To this end, we consider the following partitioning of the matrix $P(t)$

$$P(t) = \begin{bmatrix} P_{11} & P_{12} & P_{13} \\ P_{21} & P_{22} & P_{23} \\ P_{31} & P_{32} & P_{33} \end{bmatrix} \quad (3-46)$$

Then, recalling Eq. (3-31e) and the nature of the state vector \underline{w} , Eq. (3-33) can be rewritten as

$$\dot{\underline{\zeta}} = -R^{-1}P_{31}\underline{\eta} - R^{-1}P_{32}\dot{\underline{\eta}} - R^{-1}P_{33}\underline{g} \quad (3-47)$$

so that, using Eqs. (3-28) and (2-63), \underline{g} can be expressed as

$$\underline{g} = (I + \bar{M}_1)\ddot{\underline{\eta}} + \bar{G}_1\dot{\underline{\eta}} + (\Lambda_0 + \bar{K}_1)\underline{\eta} \quad (3-48)$$

Inserting Eq. (3-48) into Eq. (3-47), we obtain

$$\dot{\underline{\zeta}} \cong - [G_1^0 + G_1^1(t)]\underline{\eta}(t) - [G_p^0 + G_p^1(t)]\dot{\underline{\eta}}(t) - [G_d^0 + G_d^1(t)]\ddot{\underline{\eta}}(t) \quad (3-49)$$

where

$$G_1^0 = R^{-1}[P_{31}^0 + P_{33}^0\Lambda_0] \quad , \quad G_1^1 = R^{-1}[P_{31}^1 + P_{33}^1\Lambda_0 + P_{33}^0\bar{K}_1] \quad (3-50a,b)$$

$$G_p^0 = R^{-1}P_{32}^0 \quad , \quad G_p^1 = R^{-1}[P_{32}^1 + P_{32}^0\bar{G}_1] \quad (3-50c,d)$$

$$G_d^0 = R^{-1}P_{33}^0 \quad , \quad G_d^1 = R^{-1}[P_{33}^1 + P_{33}^0\bar{M}_1] \quad (3-50e,f)$$

Superscripts 0 and 1 denote zero- and first-order, respectively. Integrating Eq. (3-47), we obtain

$$\underline{E}(t) = \underline{E}(0) - \int_0^t [\underline{G}_i^0 + \underline{G}_i^1(\tau)] \underline{\eta}(\tau) d\tau - \int_0^t [\underline{G}_p^0 + \underline{G}_p^1(\tau)] \underline{\dot{\eta}}(\tau) d\tau - \int_0^t [\underline{G}_d^0 + \underline{G}_d^1(\tau)] \underline{\ddot{\eta}}(\tau) d\tau \quad (3-51)$$

Assuming that the time-varying first-order gain matrices change slowly, $\underline{E}(t)$ can be approximated by taking the gain matrices outside the integral sign. Moreover, although initial conditions appear in Eq. (3-51), arbitrary values can be assigned to the initial control force $\underline{E}(0)$; we choose this value as zero. In addition, the maneuver starts from the rest, so that $\underline{\eta}(0)$ and $\underline{\dot{\eta}}(0)$ are zero as well. Hence, Eq. (3-51) can be rewritten as

$$\underline{E}(t) \cong -[\underline{G}_i^0 + \underline{G}_i^1(t)] \int_0^t \underline{\eta}(\tau) d\tau - [\underline{G}_p^0 + \underline{G}_p^1(t)] \underline{\eta}(t) - [\underline{G}_d^0 + \underline{G}_d^1(t)] \underline{\dot{\eta}}(t) \quad (3-52)$$

Inserting Eq. (3-52) into Eq. (2-63), we obtain the following closed-loop equation:

$$\begin{aligned} (1 + \bar{M}_1) \underline{\ddot{\eta}} + (\underline{G}_d^0 + \underline{G}_d^1 + \bar{G}_1) \underline{\dot{\eta}} + (\underline{\Lambda}_0 + \underline{G}_p^0 + \underline{G}_p^1 + \bar{K}_1) \underline{\eta} \\ + (\underline{G}_i^0 + \underline{G}_i^1) \int_0^t \underline{\eta}(\tau) d\tau = \underline{D} \end{aligned} \quad (3-53)$$

Equation (3-53) can be written in the state form

$$\dot{\underline{y}} = \underline{A} \underline{y} + \underline{B} \underline{D} \quad (3-54)$$

where

$$\underline{y}(t) = \left[\int_0^t \underline{\eta}(\tau) d\tau \quad \underline{\eta}(t) \quad \underline{\dot{\eta}}(t) \right] \quad (3-55a)$$

$$A^* = \begin{bmatrix} 0 & I & 0 \\ 0 & 0 & I \\ A_1^* & A_2^* & A_3^* \end{bmatrix}, \quad B^* = \begin{bmatrix} 0 \\ 0 \\ I \end{bmatrix} \quad (3 - 55b,c)$$

$$A_1^* = -(I + \bar{M}_1)^{-1}(G_1^0 + G_1^1) \quad (3 - 55d)$$

$$A_2^* = -(I + \bar{M}_1)^{-1}(\Lambda_0 + G_p^0 + G_p^1 + \bar{K}_1) \quad (3 - 55e)$$

$$A_3^* = -(I + \bar{M}_1)^{-1}(G_d^0 + G_d^1 + \bar{G}_1) \quad (3 - 55f)$$

Equation (3-54) is in a standard form and its solution can be obtained by the transition matrix approach.

The procedure for designing the control can be summarized as follows:

- Obtain the steady-state zero-order solution by solving the MARE, Eq. (3-40).
- Calculate the zero-order gains by means of Eqs. (3-50a,c,e).
- Obtain the time-varying first-order Riccati solution by evaluating the integral in Eq. (3-42).
- Calculate the first-order gains by means of Eq. (3-50b,d,f).
- Compute the closed-loop response by solving the state equation (3-54).

If the rate of time-variation of the parameters is slow relative to the closed-loop response, one approach is to design the control gains under the assumption that the process is time-invariant, and then schedule the gains as a function of parameters that varies with time (Ref. 7). The idea of an adiabatic approximation used in Ref. 7 is to use the solution of the

matrix algebraic Riccati equation (MARE) at each instant of time instead of solving the matrix differential Riccati equation (MDRE). If we use the concept of adiabatic approximation to the perturbed Riccati equation, the adiabatic solution for the time-varying part can be obtained by solving the MDLE, Eq. (3-13) by letting $\dot{P}_1 = 0$ for each instant of time. The resulting matrix algebraic Lyapunov equation (MALE) is

$$P_1(t)\hat{A}_{0c} + \hat{A}_{0c}^T P_1(t) + P_0\hat{A}_1(t) + \hat{A}_1^T(t)P_0 = 0 \quad (3 - 56)$$

The solution of the MALE should satisfy the stability criteria by the second method of Lyapunov. Its feasibility is decided by the asymptotic stability of the system, not by optimality. The advantage of this solution is that the time-varying gain matrix can be calculated at each instant time without solving the differential equation. However, stability must be checked a priori. All of this can also be precalculated prior to any maneuver, thus saving real-time computations.

The closed loop equation can be written as

$$\dot{w} = [\hat{A} - \hat{B}R^{-1}\hat{B}^T P] w = \hat{A}_c w \quad (3 - 57)$$

The second stability theorem of Lyapunov is concerned with the asymptotic stability of a system in the neighborhood of the origin and it reads as follows:

Theorem: If there exists for the system (3-57) a positive definite function $V(w)$ whose total time derivative $\dot{V}(w)$ is negative definite along every trajectory of (3-57), then the trivial solution is asymptotically stable.

By assumption, the matrix $P(t)$ that satisfies Eq.(3-34) is positive definite. Thus,

$$V = \underline{w}^T P \underline{w} > 0 \quad \text{for all } \underline{w} \neq 0 \text{ and } t \quad (3 - 58)$$

The scalar function V defined by Eq. (3-58) is a candidate Lyapunov function. Now consider dV/dt , or

$$\dot{V} = \underline{w}^T(\dot{P} + P\hat{A}_c + \hat{A}_c^T P)\underline{w} = \underline{w}^T F \underline{w} \quad (3-59)$$

where

$$F = \dot{P} + \hat{A}_c^T P + P\hat{A}_c \quad (3-60)$$

For the control law developed by applying a perturbation method in this section,

$$F_{\text{pert}} = -Q - (P_0 + P_1(t))\hat{B}R^{-1}\hat{B}^T(P_0 + P_1(t)) + O(\varepsilon^2) \quad (3-61)$$

For the adiabatic approximation case,

$$F_{\text{adia}} = \dot{P}_1(t) - Q - (P_0 + P_1(t))\hat{B}R^{-1}\hat{B}^T(P_0 + P_1(t)) + O(\varepsilon^2) \quad (3-62)$$

The stability of the system depends on negative definiteness of F . If the eigenvalues of F are all negative, the system is guaranteed to be stable. As can be seen from Eq. (3-61), the negative definiteness of F_{pert} can be easily justified. On the other hand, the negative definiteness of F_{adia} depends on the contribution of \dot{P}_1 to F_{adia} . Although P_1 is $O(\varepsilon)$, the time-derivative can be larger if the time-varying system parameters change abruptly. This can happen during maneuvering because there is a rapid change from the acceleration to deceleration at half the maneuver period due to the bang-bang control. Therefore, the use of the adiabatic approximation for the control of the maneuvering spacecraft is not indicated, even though the first-order solution can be obtained with relative ease when compared to the evaluation of the integral in Eq. (3-42).

4.0 Numerical Results

4.1 Numerical Example 1

The preceding developments for disturbance-minimization control have been applied to a spacecraft consisting of a rigid platform with a single flexible appendage in the form of a beam (Fig. 3). The maneuver consists of slewing the beam relative to the platform through a 45° angle about the x-axis, so that $\omega_o = [\dot{\beta}_x \ 0 \ 0]^T$. The time history of the angular acceleration $\ddot{\beta}_x$ is a smoothed bang-bang, where the smoothing was used to reduce the excitation of the elastic appendage. Plots of the angular acceleration $\ddot{\beta}_x$, angular velocity $\dot{\beta}_x$ and angular displacement β_x as functions of time are shown in Fig. 4. The elastic motion consists of bending vibration in the x- and y-directions, with the vibration in the z-direction being identically equal to zero. The vibration was represented by five admissible functions in each direction, so that the matrix Φ_o in Eq. (2-13) is 3×10 and the vector q_o is a ten-dimensional vector. The admissible functions have the expressions

$$\phi_{xj} = -(\cos \beta_j z - \cosh \beta_j z) + C_j(\sin \beta_j z - \sinh \beta_j z), \quad j = 1, 2, \dots, 5 \quad (4-1)$$

which are recognized as cantilever modes (Ref. 24). The admissible functions ϕ_{yj} ($j=6,7,\dots,10$) have exactly the same expressions. The coefficients in Eq. (4-1) have the values $C_j = 0.7341, 1.0185, 0.9992, 1, 1$ and the arguments of the trigonometric and hyperbolic functions can be obtained from $\beta_j l_e = 1.8751, 4.6941, 7.8548, 10.9955, 14.1732$, where l_e is the length of the beam. The mass matrix, Eq. (2-22a), and the stiffness matrix, Eq. (2-20), are 10×10 and have the block diagonal form

$$M_e = \begin{bmatrix} M_{e11} & 0 \\ 0 & M_{e22} \end{bmatrix}, \quad K_e = \begin{bmatrix} K_{e11} & 0 \\ 0 & K_{e22} \end{bmatrix} \quad (4-2a,b)$$

$$M_{e11} = M_{e22} = [m_e \delta_{ij}], \quad i,j = 1,2,\dots,5 \quad (4-3a)$$

$$K_{e11} = K_{e22} = \frac{EI_e}{l_e^3} (\beta_j l_e)^2 (\beta_j l_e)^2 \delta_{ij}, \quad i,j = 1,2,\dots,5 \quad (4-3b)$$

Moreover, the matrices $\bar{\Phi}_e$ and $\tilde{\Phi}_e$ given by Eqs. (2-22b) and (2-22c), respectively, are 3×10 and have the form

$$\bar{\Phi}_e = \begin{bmatrix} \bar{\phi}_e & 0 \\ 0 & \bar{\phi}_e \\ 0 & 0 \end{bmatrix}, \quad \tilde{\Phi}_e = \begin{bmatrix} 0 & -\tilde{\phi}_e \\ \tilde{\phi}_e & 0 \\ 0 & 0 \end{bmatrix} \quad (4-4a,b)$$

where $\bar{\phi}_e$ and $\tilde{\phi}_e$ are given in Appendix D. Other numerical values used are as follows:

$$m_r = 15.6 \text{ slugs}, \quad m_e = 0.30 \text{ slugs}$$

$$\underline{S}_r = (0., 0., 0.)^T \text{ slugs} \cdot \text{ft}, \quad \underline{S}_e = (0., 0., 1.65)^T \text{ slugs} \cdot \text{ft}$$

$$I_r = \begin{bmatrix} 13.0 & 0.0 & 0.0 \\ 0.0 & 48.0 & 0.0 \\ 0.0 & 0.0 & 59.0 \end{bmatrix} \text{ slugs} \cdot \text{ft}^2, \quad I_e = \begin{bmatrix} 1.25 & 0.0 & 0.0 \\ 0.0 & 1.25 & 0.0 \\ 0.0 & 0.0 & 0.0 \end{bmatrix} \text{ slugs} \cdot \text{ft}^2$$

$$l_e = 5 \text{ ft}, \quad EI = 500 \text{ lb} \cdot \text{ft}^2, \quad r_{oe} = (0., 0., 0.4)^T \text{ ft}$$

Figure 5 shows the time history of the tip elastic displacement of the appendage in the absence of control. Although five admissible functions were used to represent the elastic displacements, sufficient accuracy can be obtained with a single admissible function alone. Indeed, there is no discernible difference in the open-loop response using one or five admissible functions, as can be verified by examining Fig. 5.

Figures 6 and 7 show time histories of the rigid-body translations and rotation of the platform during the maneuver, respectively, without and with control. Finally, Figure 8 shows the tip elastic displacement of the appendage during the maneuver, without and with control. The controls were implemented by six actuators mounted on the rigid platform and two actuators each for the x- and y-directions and located on the appendage at $z_e = l_e/2$ and $z_e = l_e$.

For the values of the parameters chosen, the time-varying terms in the coefficient matrices turned out to be small compared to the constant terms. In view of this, the control gains were computed as if the system were time-invariant. They were obtained by solving the steady-state Riccati equation in conjunction with Potter's method (Ref. 39). The coefficient matrices A and B used in the solution were according to the premaneuver state. Moreover, we chose the performance index coefficient matrices $H = 0$, $Q = 100 I$ and $R = 0.001 I$ where I is the identity matrix. This assumes large final time t_f . It should be stressed once again that the time-invariant system was used only for computing the control gains, and the closed-loop response plots were obtained by considering the actual time-varying system, as described by Eq. (2-34).

4.2 Numerical Example 2

The mathematical model consists of a flat rigid platform and two flexible beams, each one having one end hinged to the platform and the other end free (Fig. 9), where the beams are originally parallel to the z-axis of the platform. The maneuver consists of slewing each of the beams through a 45° angle, one about the x-axis and the other about the y-axis of the platform. The beams are discretized in space by using three admissible functions for each component of displacement. Six actuators are used for the rigid platform and three actuators are used for each displacement component of both beams. The latter actuators are located at 4 ft, 7 ft and 10 ft from the pivot point, the third coinciding with the tip of the beam. Maneuver time histories are the same as those given in Numerical Example 1. Figures 10 and 11 display both the uncontrolled and controlled translational and angular displacements of the platform, respectively, and Figs. 12 and 13 show the tip displacements of the two beams. As can be verified, the maneuver and control of the spacecraft are quite satisfactory. The disturbance-accommodating control is carried out by the proportional-plus-integral control approach. In obtaining the numerical results, the following data was used:

$$m_r = 134.15 \text{ slugs}, \quad m_e = 0.1873 \text{ slugs}$$

$$\underline{S}_r = (0., 0., 0.)^T \text{ slugs} \cdot \text{ft}, \quad \underline{S}_e = (0., 0., 0.9365)^T \text{ slugs} \cdot \text{ft}$$

$$I_r = \begin{bmatrix} 186.021 & 0.0 & 0.0 \\ 0.0 & 186.021 & 0.0 \\ 0.0 & 0.0 & 357.733 \end{bmatrix} \text{ slugs} \cdot \text{ft}^2, \quad I_e = \begin{bmatrix} 6.243 & 0.0 & 0.0 \\ 0.0 & 6.243 & 0.0 \\ 0.0 & 0.0 & 0.0 \end{bmatrix} \text{ slugs} \cdot \text{ft}^2$$

$$l_1 = l_2 = 10 \text{ ft}, \quad EI = 3028.9 \text{ lb} \cdot \text{ft}^2$$

$$\underline{r}_{o1} = (0., -1.0, 0.5)^T \text{ ft}, \quad \underline{r}_{o2} = (0., 1.0, 0.5)^T \text{ ft}$$

Moreover, the weighting matrices appearing in the performance index, Eq. (3-18), are as follows:

$$\hat{Q} = \begin{bmatrix} 100I & 0.0 \\ 0.0 & I \end{bmatrix}, \quad \hat{R} = 0.001I$$

where I is the identity matrix. Of course, consistent with a steady-state solution of the matrix Riccati equation, \hat{H} was taken as zero. Finally, for control design purposes, the coefficient matrices A and B were taken as constant and corresponding to the premaneuver configuration of the spacecraft. Of course, in implementing the control, the time-varying matrices $A(t)$ and $B(t)$ were used.

4.3 Numerical Example 3

As an example of the control design by the perturbation method developed in Sec. 3.4, the following second-order differential equation is considered

$$\ddot{u} + (\omega^2 + \varepsilon)u = f + d \quad (4-5)$$

where f and d represent modal control force and disturbance respectively and ε is the small time-varying coefficient that exists only for some period. Recalling Eq. (3-31), we have

$$\hat{A}_0 = \begin{bmatrix} 0 & 1 & 0 \\ -\omega^2 & 0 & 1 \\ 0 & 0 & 0 \end{bmatrix} \quad \hat{A}_1 = \begin{bmatrix} 0 & 0 & 0 \\ -\varepsilon & 0 & 0 \\ 0 & 0 & 0 \end{bmatrix} \quad \hat{B} = \begin{bmatrix} 0 \\ 0 \\ 1 \end{bmatrix} \quad (4-6a,b,c)$$

We use the performance index

$$J = \int_0^{\infty} (x^T Q x + R \dot{x}^2) dt \quad (4-7)$$

with

$$Q = \begin{bmatrix} Q_1 & 0 & 0 \\ 0 & Q_2 & 0 \\ 0 & 0 & Q_3 \end{bmatrix} \quad (4-8)$$

The MARE, Eq. (3-40), yields the six nonlinear equations

$$Q_1 - 2P_{12}^0 \omega^2 - \frac{(P_{13}^0)^2}{R} = 0 \quad , \quad Q_2 + 2P_{12}^0 - \frac{(P_{23}^0)^2}{R} = 0 \quad (4-9a,b)$$

$$Q_3 + 2P_{23}^0 - \frac{(P_{33}^0)^2}{R} = 0 \quad , \quad P_{11}^0 - P_{22}^0 \omega^2 - \frac{P_{13}^0 P_{23}^0}{R} = 0 \quad (4-9c,d)$$

$$P_{12}^0 - P_{23}^0 \omega^2 - \frac{P_{13}^0 P_{33}^0}{R} = 0 \quad , \quad P_{13}^0 + P_{22}^0 - \frac{P_{23}^0 P_{33}^0}{R} = 0 \quad (4-9e,f)$$

The above equations can be reduced to the following 4th-order equation for P_{23}^0 :

$$(P_{23}^0)^4 + 4\omega^2 R (P_{23}^0)^3 + 2R(2\omega^4 R - Q_2 + 2\omega^2 Q_3) (P_{23}^0)^2 - 4R^2(\omega^2 Q_2 + 2Q_1) P_{23}^0 + Q_2^2 R^2 - 4R^2(Q_1 + \omega^2 Q_2) Q_3 = 0 \quad (4-10)$$

Solving Eq. (4-10) for P_{23}^0 , the remaining entries of P_0 can be obtained from Eqs. (4-9) as follows:

$$P_{12}^0 = \frac{1}{2} \left[\frac{(P_{23}^0)^2}{R} - Q_2 \right] \quad , \quad P_{13}^0 = -\sqrt{R(Q_1 - 2\omega^2 P_{12}^0)} \quad (4-11a,b)$$

$$P_{33}^0 = \sqrt{R(Q_3 + 2P_{23}^0)} \quad , \quad P_{22}^0 = \frac{P_{23}^0 P_{33}^0}{R} - P_{13}^0 \quad (4-11c,d)$$

$$P_{11}^0 = \omega^2 P_{22}^0 + \frac{P_{13}^0 P_{23}^0}{R} \quad (4-11e)$$

Instead of evaluating the integral in Eq. (3-42), because Eq. (3-37) is only of order six, we can write it explicitly as follows:

$$\begin{bmatrix} \dot{P}_{11}^1 \\ \dot{P}_{12}^1 \\ \dot{P}_{13}^1 \\ \dot{P}_{22}^1 \\ \dot{P}_{23}^1 \\ \dot{P}_{33}^1 \end{bmatrix} = \begin{bmatrix} 0 & 2\omega^2 & \frac{2P_{13}^0}{R} & 0 & 0 & 0 \\ -1 & 0 & \frac{P_{23}^0}{R} & \omega^2 & \frac{P_{13}^0}{R} & 0 \\ 0 & -1 & \frac{P_{33}^0}{R} & 0 & \omega^2 & \frac{P_{13}^0}{R} \\ 0 & -2 & 0 & 0 & \frac{2P_{23}^0}{R} & 0 \\ 0 & 0 & -1 & -1 & \frac{P_{33}^0}{R} & \frac{P_{23}^0}{R} \\ 0 & 0 & 0 & 0 & -2 & \frac{2P_{33}^0}{R} \end{bmatrix} \begin{bmatrix} P_{11}^1 \\ P_{12}^1 \\ P_{13}^1 \\ P_{22}^1 \\ P_{23}^1 \\ P_{33}^1 \end{bmatrix} + \begin{bmatrix} 2P_{12}^0 \\ P_{22}^0 \\ P_{23}^0 \\ 0 \\ 0 \\ 0 \end{bmatrix} \varepsilon \quad (4-12)$$

so that the first-order perturbation to the Riccati matrix can be obtained by integrating Eq. (4-12). Hence, using Eq. (3-52) and recalling Eqs. (3-50), we obtain the control law

$$f = -g_i \int_0^t u d\tau - g_p u - g_d \dot{u} \quad (4-13)$$

where

$$g_i = \frac{1}{R} [P_{13}^0 + P_{13}^1 + (\omega^2 + \varepsilon)P_{33}^0 + \omega^2 P_{33}^1] \quad (4 - 14a)$$

$$g_p = \frac{1}{R} [P_{23}^0 + P_{23}^1] \quad , \quad g_d = \frac{1}{R} [P_{33}^0 + P_{33}^1] \quad (4 - 14b,c)$$

For the example at hand, we use the numerical data

$$\varepsilon = \begin{cases} 10 \sin(2\pi t), & 0 \leq t \leq 3 \\ 0, & t < 0; t > 3 \end{cases} \quad , \quad d = \begin{cases} 100, & 0 \leq t \leq 3 \\ 0, & t < 0; t > 3 \end{cases}$$

$$\omega = 10 \quad , \quad Q_1 = Q_2 = 10 \quad , \quad Q_3 = 1 \quad , \quad R = 0.01$$

Zero-order solutions are obtained by solving Eqs. (4-10) and (4-11). Figures 14 through 16 show the gains obtained by backward integration, perturbation method and adiabatic approximation. It can be seen that the solution by the perturbation method is closer to the exact solution than the solution by the adiabatic approximation. Figure 17 shows the uncontrolled and controlled responses. For the comparison, the Independent Modal-Space Control (IMSC) method (Ref. 27) is applied to the same system. The IMSC control law is

$$f = \omega(\omega - \sqrt{\omega^2 + R^{-1}})u - \sqrt{[2\omega(-\omega + \sqrt{\omega^2 + R^{-1}}) + R^{-1}]} \dot{u} \quad (4 - 15)$$

where $R = 0.01$ is used. Note that IMSC had to be modified to account for the presence of unknown constant disturbances. As can be seen in Fig 17, IMSC is not effective for controlling the system under persistent disturbance. This comes as no surprise, as IMSC was not designed for this type of problems. The theory used in this dissertation can be extended to the case of any arbitrary disturbances.

4.4 Numerical Example 4

This example is concerned with the planar model shown in Fig. 18. The maneuver of the appendage relative to the platform was carried out by means of a bang-bang for the angular acceleration. Hence, we have

$$\ddot{\beta} = c, \quad \dot{\beta} = ct, \quad \beta = \frac{1}{2}ct^2 \quad \text{for } t \leq \frac{t_f}{2}$$

$$\ddot{\beta} = -c, \quad \dot{\beta} = -(ct - t_f), \quad \beta = \frac{-1}{2}c(t - t_f)^2 + \frac{1}{4}ct_f^2 \quad \text{for } \frac{t_f}{2} \leq t \leq t_f$$

where $c = \frac{4\theta_f}{t_f^2}$ and θ_f and t_f represent final maneuver angle and time.

Data for numerical model are as follows:

$$m_r = 15.6 \text{ slugs}, \quad m_e = 0.15 \text{ slugs}$$

$$S_r = 0.0 \text{ slugs} \cdot \text{ft}, \quad S_e = 0.375 \text{ slugs} \cdot \text{ft}$$

$$I_r = 13.0 \text{ slugs} \cdot \text{ft}^2, \quad I_e = 1.25 \text{ slugs} \cdot \text{ft}^2$$

$$r_{oe} = 0.4 \text{ ft}, \quad \bar{\Phi}_e = 0.117, \quad \tilde{\Phi}_e = 0.427$$

$$l_e = 5 \text{ ft}, \quad E I_e = 500, \quad K_e = 49.449, \quad M_e = 0.15$$

For simplicity, we used only one admissible function. Other parameters entering into Eq. (2-64) are given in Appendix E.

Figures 19 through 21 show uncontrolled and controlled responses for the solutions obtained by the perturbation method and adiabatic approximation, where $Q = I$, $R = 0.01 I$, $\theta_f = 90^\circ$ and $t_f = 3 \text{ s}$ are used. For the first-order solution, The approximation given by Eq. (3-45) is used.

4.5 Numerical Example 5

The effect of nonlinearity on the system response is illustrated by means of a spacecraft consisting of a rigid platform with a single membrane-type flexible appendage (Fig. 22). The maneuver of the appendage relative to the platform was carried out by means of a smoothed bang-bang (Ref. 40) for the angular acceleration, where the smoothing of the bang-bang was done to reduce the elastic deformations of the appendage. The elastic vibration of the appendage was represented by ten degrees of freedom in the z-direction, i.e., by ten admissible functions in the discretization(-in-space) process, so that the matrix Φ_e in Eq. (2-13) is 3×10 , or

$$\Phi_e = \begin{bmatrix} 0 & 0 & \dots & 0 \\ 0 & 0 & \dots & 0 \\ \phi_1 & \phi_2 & \dots & \phi_{10} \end{bmatrix} \quad (4-16)$$

in which

$$\phi_1 = \frac{1}{\sqrt{\pi \bar{\rho}_e} a} \frac{J_0(\beta_{01} r)}{J_1(\beta_{01} a)} , \quad \phi_2 = \frac{1}{\sqrt{\pi \bar{\rho}_e} a} \frac{J_0(\beta_{02} r)}{J_1(\beta_{02} a)} \quad (4-17a,b)$$

$$\phi_3 = \frac{\sqrt{2}}{\sqrt{\pi \bar{\rho}_e} a} \frac{J_1(\beta_{11} r)}{J_2(\beta_{11} a)} \cos \theta , \quad \phi_4 = \frac{\sqrt{2}}{\sqrt{\pi \bar{\rho}_e} a} \frac{J_1(\beta_{12} r)}{J_2(\beta_{12} a)} \cos \theta \quad (4-17c,d)$$

$$\phi_5 = \frac{\sqrt{2}}{\sqrt{\pi \bar{\rho}_e} a} \frac{J_2(\beta_{21} r)}{J_3(\beta_{21} a)} \cos 2\theta , \quad \phi_6 = \frac{\sqrt{2}}{\sqrt{\pi \bar{\rho}_e} a} \frac{J_2(\beta_{22} r)}{J_3(\beta_{22} a)} \cos 2\theta \quad (4-17e,f)$$

$$\phi_7 = \frac{\sqrt{2}}{\sqrt{\pi \bar{\rho}_e} a} \frac{J_1(\beta_{11} r)}{J_2(\beta_{11} a)} \sin \theta , \quad \phi_8 = \frac{\sqrt{2}}{\sqrt{\pi \bar{\rho}_e} a} \frac{J_1(\beta_{12} r)}{J_2(\beta_{12} a)} \sin \theta \quad (4-17g,h)$$

$$\phi_9 = \frac{\sqrt{2}}{\sqrt{\pi \bar{\rho}_e} a} \frac{J_2(\beta_{21}r)}{J_3(\beta_{21}a)} \sin 2\theta, \quad \phi_{10} = \frac{\sqrt{2}}{\sqrt{\pi \bar{\rho}_e} a} \frac{J_2(\beta_{22}r)}{J_3(\beta_{22}a)} \sin 2\theta \quad (4-17i,j)$$

in which ϕ_1 and ϕ_2 are recognized as axisymmetric modes, and the other as antisymmetric modes respectively (Ref. 22). The vector q_e is ten-dimensional. The arguments of the Bessel functions of the first kind can be obtained from $\beta_{01}a = 2.405$, $\beta_{02}a = 5.520$, $\beta_{11}a = 3.832$, $\beta_{12}a = 7.016$, $\beta_{21}a = 5.136$ and $\beta_{22}a = 8.417$. The mass matrix, Eq. (2-22a), and the stiffness matrix, Eq. (2-20), are 10×10 and have the block diagonal form

$$M_e = I, \quad K_e = \Lambda \quad (4-18a,b)$$

where I is the 10×10 identity matrix and Λ is a diagonal matrix with the diagonal entries

$$\Lambda(1,1) = \frac{c^2}{a^2} (\beta_{01}a)^2, \quad \Lambda(2,2) = \frac{c^2}{a^2} (\beta_{02}a)^2 \quad (4-19a,b)$$

$$\Lambda(3,3) = \Lambda(7,7) = \frac{c^2}{a^2} (\beta_{11}a)^2, \quad \Lambda(4,4) = \Lambda(8,8) = \frac{c^2}{a^2} (\beta_{12}a)^2 \quad (4-19c,d)$$

$$\Lambda(5,5) = \Lambda(9,9) = \frac{c^2}{a^2} (\beta_{21}a)^2, \quad \Lambda(6,6) = \Lambda(10,10) = \frac{c^2}{a^2} (\beta_{22}a)^2 \quad (4-19e,f)$$

where a is the radius of the membrane and $c = \sqrt{T_m/\bar{\rho}_e}$, in which T_m is the tension applied to the membrane and $\bar{\rho}_e$ represents the mass per unit area of the membrane. Moreover, the other matrices given by Eqs. (2-18) and (2-22) are given in Appendix F.

Two cases with the same numerical data for the elastic appendage but with different inertia terms for the rigid body are tested. The data for the elastic appendage is as follows:

$$m_e = 0.283 \text{ slugs}, \quad \underline{S}_e = (0., 0., 1.415) \text{ slugs} \cdot \text{ft}$$

$$I_e = \begin{bmatrix} 7.712 & 0.0 & 0.0 \\ 0.0 & 7.712 & 0.0 \\ 0.0 & 0.0 & 1.274 \end{bmatrix} \text{ slugs} \cdot \text{ft}^2$$

$$\bar{\rho}_e = 0.01 \text{ slugs/ft}^2, \quad a = 3 \text{ ft}, \quad c = 20 \text{ ft/sec}, \quad \underline{r}_{oe} = (0., 0., 1.0) \text{ ft}$$

For the rigid body, we consider:

Case 1

$$m_r = 134.15 \text{ slugs}, \quad \underline{S}_r = (0., 0., 0.) \text{ slugs} \cdot \text{ft}$$

$$I_r = \begin{bmatrix} 186.021 & 0.0 & 0.0 \\ 0.0 & 186.021 & 0.0 \\ 0.0 & 0.0 & 357.733 \end{bmatrix} \text{ slugs} \cdot \text{ft}^2,$$

and Case 2

$$m_r = 21.464 \text{ slugs}, \quad \underline{S}_r = (0., 0., 0.) \text{ slugs} \cdot \text{ft}$$

$$I_r = \begin{bmatrix} 8.943 & 0.0 & 0.0 \\ 0.0 & 8.943 & 0.0 \\ 0.0 & 0.0 & 14.309 \end{bmatrix} \text{ slugs} \cdot \text{ft}^2,$$

As seen above, the rigid-body model of Case 1 has large inertias relative to those of the flexible body. On the other hand, the mass moment of inertia of the rigid body of Case 2 is almost the same as that of the flexible body, although the mass of the rigid body is sufficiently large. This is due to the fact that the mass moment of inertia of rigid body is about the center of mass and the mass moment of inertia of flexible body is about the hinge, which is far removed from the mass center of the flexible body.

Two cases are compared with the results obtained by using linearized state equation. Figures 23 through 26 show time histories of the rigid-body translations and rotation and the elastic displacements of the membrane at the center and the point defined by $x_0 = 0$ and $r = 1.5$ ft for Case 1. The figures contain responses for the uncontrolled nonlinear system and linearized system, as well as for the controlled case. Figures 27 through 30 show the responses for Case 2.

A simple controller is considered for the nonlinear system control. Controllers for the rigid body translations and rotation are uniform damping control. The control laws are:

$$\underline{F}_0 = -\alpha m_t \underline{V}_0, \quad \underline{M}_0 = -\alpha I_t \underline{\omega} \quad (4-20a,b)$$

where $\alpha = 10$ is used for this example. Controllers for the elastic motions are IMSC controllers (Ref. 27), or

$$Q_i = \omega_i(\omega_i - \sqrt{\omega_i^2 + R^{-1}})q_i - \sqrt{[2\omega_i(-\omega_i + \sqrt{\omega_i^2 + R^{-1}}) + R^{-1}]} p_i$$

$$i = 1,2,\dots,10 \quad (4-20c)$$

where $\omega_i = \sqrt{\Lambda(i,i)}$ and $R = 0.0002$ are used. It can be shown that the control of the nonlinear system is possible, but the control gains are too high because of the presence of disturbances. Hence, control design for the nonlinear system should be carried out in a different way.

The elastic displacements at the center and at $r = 0.5 a, \theta = 90^\circ$ are calculated by using the following formulas:

$$w_{r=0} = \frac{1}{\sqrt{\rho_e}} (1.08684 q_1 - 1.65807 q_2) \quad (4-21a)$$

$$w_{r=0.5a, \theta=90^\circ} = \frac{1}{\sqrt{\rho_e}} (0.72806 q_1 + 0.27919 q_2$$

$$- 1.06924 q_5 + 0.90574 q_6 + 1.15061 q_7 - 0.35635 q_8) \quad (4-21b)$$

A nonlinear state equation is solved by using IMSL routine DIVPAG (Ref. 10).

5.0 Summary and Conclusion

The equations describing the motion of a spacecraft consisting of a rigid platform and retargeting flexible antennas can be derived most conveniently by means of a Lagrangian approach in terms of quasi-coordinates. The strategy used consists of stabilizing the platform relative to an inertial space and maneuvering the antennas relative to the platform. In general, the equations are nonlinear and time-varying. In the case in which the inertia of the antennas is small relative to the spacecraft, the equations can be linearized, although they remain time-varying. In addition, the equations contain persistent disturbances due to inertial loading. Because control design for the hybrid system is not feasible, discretization and truncation are carried out.

The control can be divided into two parts, the first counteracting the persistent disturbances and the second providing regulation of the perturbed system. The state subject to regulation consists of the deviations of the platform from equilibrium relative to the inertial space and the elastic motions of the appendages. The feedback control gains for the regulator can be made optimal by minimizing a certain performance measure. Numerical Example 1 shows the application of this control method.

Bang-bang control implies that the maneuver angular acceleration is constant over each half the maneuver period and disturbances depend largely on acceleration (by way of

inertial loading). This permits the use of proportional-plus-integral feedback control for disturbance accommodation. In the case in which the time-varying terms are relatively small, which means the maneuver is not very fast compared to the lowest natural frequencies of the nonmaneuvering antennas, the control gains can be computed on the basis of the time-invariant system obtained by ignoring the time-varying terms. Of course, in the computer simulation of the maneuver and control, the full time-varying system must be considered. A numerical example, in which a spacecraft consisting of a rigid platform and two flexible antennas undergoes reorientation in different planes, is presented.

To treat with the control problem of a system with small time-varying terms, and one subject to disturbances acting persistently on the system during reorientation, a new control method based on a perturbation technique is developed. The solution of the time-varying matrix differential Riccati equation (MDRE) for the case of infinite final time can be divided into two parts: time-invariant solution of matrix algebraic Riccati equation (MARE) and time-varying solution of matrix differential Lyapunov equation (MDLE). The time-varying solution takes an integral form, which enables us to compute the time-varying gains more easily. This method is superior in optimality and stability compared to the adiabatic approximation.

References

1. Anderson, B. D. O. and Moore, J. B., *Linear Optimal Control*, Prentice-Hall, Inc., Englewood Cliffs, NJ, 1971.
2. Athans, M. and Falb, P. L., *Optimal Control*, McGraw-Hill Book Co., New York, 1966.
3. Baruh, H. and Silverberg, L., "Maneuver of Distributed Spacecraft," *Proceedings of the AIAA Guidance and Control Conference*, Seattle, WA., Aug. 20-22, 1984, pp. 637-647.
4. Baruh, H. and Silverberg, L., "Implementation Problems Associated with Simultaneous Maneuver and Vibration Suppression of Flexible Spacecraft," *Proceedings of the Fifth VPI&SU/AIAA Symposium on Dynamics and Control Large Structures*, Blacksburg, Va, June 1985, pp. 585-599.
5. Breakwell, J. A., "Optimal Feedback Slewing of Flexible Spacecraft," *Journal of Guidance and Control*, Vol. 4, No. 5, 1981, pp. 472-479.
6. Brown, F. T., "Energy-Based Modeling and Quasi-Coordinates," *Journal of Dynamic Systems, Measurement, and Control*, Vol. 103, March 1981, pp.5-13.
7. Friedland, B., Richman, J. and Williams, D. E., "On the "Adiabatic Approximation" for Design of Control Laws for Linear, Time-Varying Systems," *IEEE Transactions on Automatic Control*, Vol. AC-32, No. 1, Jan. 1987, pp.62-63.
8. Grote, P. B., McMunn, J. C., and Gluck, R., "Equations of Motion of Flexible Spacecraft," *AIAA 8th Aerospace Science Meeting*, New York, New York, Jan. 1970.
9. Ho, J. Y. L., "Direct Path Method for Flexible Multibody Spacecraft Dynamics," *J. Spacecraft*, Vol. 14, Feb. 1977, pp. 102-110.
10. IMSL MATH/Library User's Manual, V. 10, *Fortran Subroutines for Mathematical Applications*, IMSL Inc.

11. Johnson, C. D., "Optimal Control of the Linear Regulator with Constant Disturbances," *IEEE Transactions on Automatic Control*, Vol. AC-13, No. 4, Aug. 1968, pp. 416-421.
12. Johnson, C. D., "Accommodation of External Disturbances in Linear Regulator and Servomechanism Problems," *IEEE Transactions on Automatic Control*, Vol. AC-16, No. 6, Dec. 1971, pp. 635-644.
13. Johnson, C. D., "Accommodation of Disturbances in Optimal Control Problems," *International Journal of Control*, Vol. 15, No. 2, 1972, pp. 209-231.
14. Johnson, C. D., "Theory of Disturbance-Accommodating Controller," *Control and Dynamic Systems, Advances in Theory and Application*, Ed. by C. T. Leondes, Vol.12, Academic Press, New York, 1976, pp. 387-489.
15. Juang, J.-N., Horta, L. G., and Robertshaw, W. H., "A Stewing Control Experiment for Flexible Structures," *Journal of Guidance and Control*, Vol. 9, No. 5, Sept.-Oct. 1986, pp. 599-607.
16. Kakad, Y. D., "Dynamics and Control of Slew Maneuver of Large Flexible Spacecraft," *Proceedings of AIAA Guidance, Navigation and Control Conference*, Williamsburg, Va, Aug. 1986, paper 86-2192, pp. 629-634.
17. Kane, T. R. and Levinson, D. A., "Formulation of Equations of Motion for Complex Spacecraft," *Journal of Guidance and Control*, Vol. 3, No. 2, March-April 1980, pp. 99-112.
18. Levinson, D. A. and Kane, T. R., "Simulation of Large Motions of Nonuniform Beams in Orbit, Part I - the Cantilever Beam," *Journal of the Astronautical Sciences*, Vol. XXIX, No. 3, July-Sept. 1981, pp. 213-244.
19. Likins, P. W., "Finite Element Appendage Equations for Hybrid Coordinate Dynamic Analysis," *Int. J. Solids Structures*, Vol.8, 1972, pp. 709-731.
20. Likins, P. W., "Dynamic Analysis of a System of Hinge-Connected Rigid Bodies with Nonrigid Appendages," *Int. J. Solids Structures*, Vol. 9, 1973, pp. 1473-1487.
21. McDonough, T. B., "Formulation of the Global Equations of Motion of a Deformable Body," *AIAA J.*, Vol. 14, No. 5, May 1976,
22. Meirovitch, L., *Analytical Methods in Vibrations*, The Macmillan Co., New York, 1967.
23. Meirovitch, L., *Methods of Analytical Dynamics*, McGraw-Hill Book Company, New York, 1970.
24. Meirovitch, L., *Computational Methods in Structural Dynamics*, Sijthoff & Noordhoff Co., the Netherlands, 1980.
25. Meirovitch, L., *Dynamics and Control of Structures*, Wiley Interscience, 1989 (to appear).
26. Meirovitch, L., "On the High-Spin Motion of a Satellite Containing Elastic Parts," *Journal of Spacecraft and Rocket*, Vol. 3, No. 11, 1966, pp. 1597-1602.
27. Meirovitch, L. and Baruh, H., "Control of Self-Adjoint Distributed-Parameter Systems," *Journal of Guidance and Control*, Vol. 5, Jan.-Feb. 1982, pp. 60-66.

28. Meirovitch, L. and Quinn, R. D., "Maneuvering and Vibration Control of Flexible Spacecraft," *The Journal of Astronautical Sciences*, Vol. 35, No. 3, 1987, pp.301-328.
29. Meirovitch, L. and Quinn, R. D., "Equations of Motion for Maneuvering Flexible Spacecraft," *Journal of Guidance and Control and Dynamics*, Vol. 10, No. 5, 1987, pp. 453-465.
30. Meirovitch, L. and Sharony Y., "Optimal Vibration Control of a Flexible Spacecraft During a Minimum-Time Maneuver," *Proceedings of the 6th VPI&SU/AIAA Symposium on Dynamics and Control of Large Structures*, Blacksburg, Va., 1987, pp.579-601.
31. Meirovitch, L. and Kwak, M. K., "Dynamics and Control of a Spacecraft with Retargeting Flexible Antennas," presented at AIAA/ASME/ASCE/AHS/ASC 29th Structures, Structural Dynamics and Materials Conference, Williamsburg, Va, April 18-20, 1988, pp.1584-1592, also *Journal of Guidance and Control and Dynamics*(to appear).
32. Meirovitch, L., "State Equations of Motion for Flexible Bodies in Terms of Quasi-Coordinates," *IUTAM/IFAC Symposium on Dynamics of Controlled Mechanical Systems*, ETH Zurich, Switzerland, May 30-June 3, 1988.
33. Meirovitch, L. and Kwak, M. K., "Control of a Spacecraft with Multi-Targeted Flexible Antennas," presented at AIAA/AAS Astrodynamics Conference, Minneapolis, Minnesota, Aug. 15-17, 1988.
34. Meirovitch, L. and Kwak, M. K., "State Equations for a Spacecraft with Maneuvering Flexible Appendages in terms of Quasi-Coordinates," presented at the Pan-American Congress of Applied Mechanics, Rio de Janeiro, Brazil, Jan. 1989.
35. Meirovitch, L. and France, M. E. B., "Discrete-Time Control of a Spacecraft with Retargetable Flexible Antennas," presented at 12th Annual AAS Guidance and Control Conference, Keystone, Colorado, Feb. 4-8, 1989.
36. Meirovitch, L. and Kwak, M. K., "Control of Flexible Spacecraft with Time-Varying Configuration," submitted to AAS/AIAA Astrodynamics Specialist Conference.
37. Modi, V. J., "Attitude Dynamics of Satellites with Flexible Appendages - A Brief Review," *Journal of Spacecraft and Rockets*, Vol. 11, Nov. 1974, pp. 743-751.
38. Mostafa, O. and Oz, H. "Maneuvering of Flexible Spacecraft via VSC," *Proceedings of AIAA Guidance, Navigation and Control Conference*, Williamsburg, Va, Aug. 1986, paper 86-2193.
39. Potter, J. E., "Matrix Quadratic Solutions," *SIAM Journal of Applied Mathematics*, Vol. 14, No. 3, Aug. 1966, pp. 496-501.
40. Quinn, R. D., "Maneuver and Control of Flexible Spacecraft," Ph. D. Dissertation, VPI&SU 1985.
41. Quinn, R. D. and Meirovitch, L., "Equations for the Vibration of Slewing Flexible Spacecraft," *AIAA/ASME/AHS 26th Structures, Structural Dynamics, and Materials Conference*, San Antonio, Texas, May 1986.
42. Quinn, R. D. and Meirovitch, L., "Maneuver and Vibration Control of Sacle," *Journal of Guidance, Control and Dynamics*, Vol. 11, No.6, 1988, pp.542-553.

43. Sharony Y. and Meirovitch, L., "Accommodation of Kinematic Disturbances During a Minimum-Time Maneuver of a Flexible Spacecraft," presented at AIAA/AAS Astrodynamics Conference, Minneapolis, Minnesota, Aug. 15-17, 1988.
44. Taylor, L. W. Jr. and Balakrishnan, A. V., "A Laboratory Experiment used to evaluate Control Laws for Flexible Spacecraft. NASA/IEEE Design Challenge," *Proceedings of the 4th VPI&SU/AIAA Symposium on Dynamics and Control of Large Structures*, Blacksburg, Va., 1983.
45. Turner, J. D. and Junkins, J. L., "Optimal Large-Angle Single-Axis Rotational Maneuvers of Flexible Spacecraft," *Journal of Guidance and Control*, Vol. 3, No. 6, 1980, pp. 578-585.
46. Turner, J. D. and Junkins, J. L., "Optimal Distributed Control of a Flexible Spacecraft During a Large-Angle Maneuver," *Journal of Guidance and Control*, Vol. 7, May-June 1984, pp. 257-264.
47. Vu-Quoc, L. and Simo, J. C., "Dynamics of Earth-Orbiting Flexible Satellites with Multibody Components," *Journal of Guidance and Control and Dynamics*, Vol. 10, No. 6, Nov.-Dec. 1987, pp. 549-558.
48. Wang, S. J., Lin, Y. H., and Ih, C. C., "Dynamics and Control of a Shuttle-Attached Antenna Experiment," *Journal of Guidance and Control and Dynamics*, Vol. 8, May-June 1985, pp. 344-353.
49. Williams, C. J. N., "Dynamics Modelling and Formulation Techniques for Non-Rigid Spacecraft," *Proceedings of a Symposium on Dynamics and Control of Non-Rigid Spacecraft*, Frascati, Italy, May 24-26, 1976, pp.53-70.

Figures

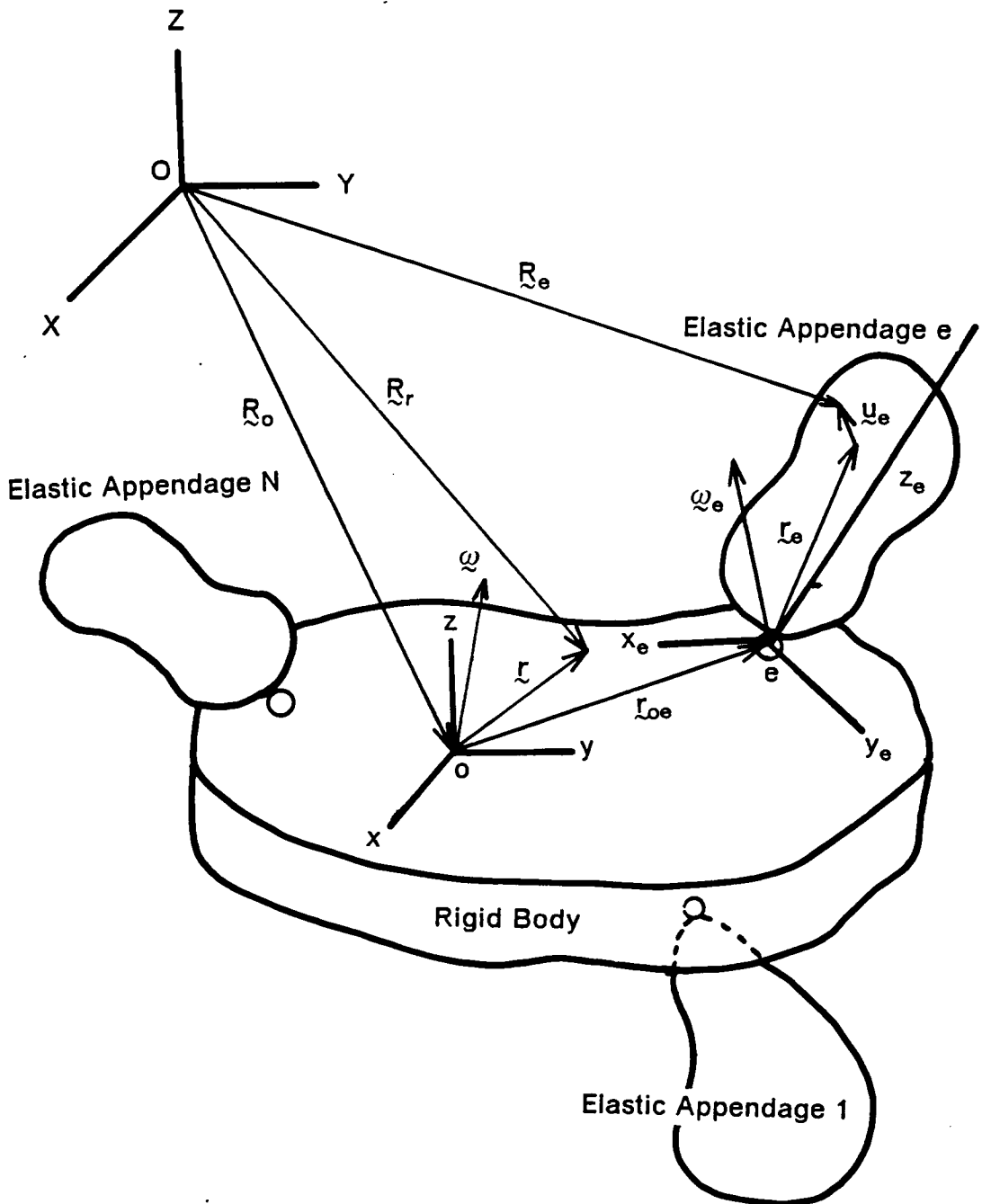


Figure 1. The Rigid Platform with Flexible Appendages

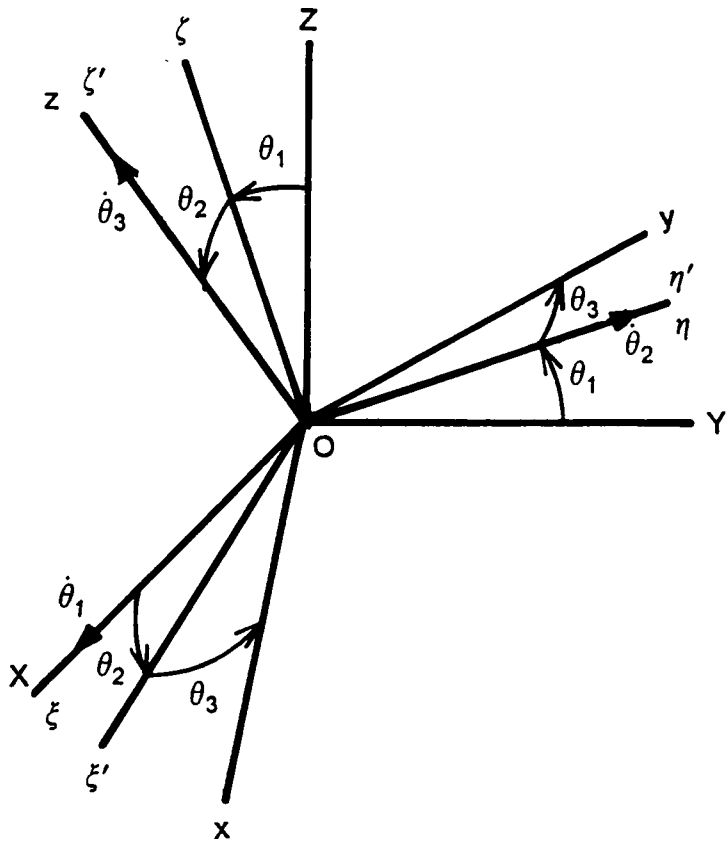


Figure 2. Angular Displacements and Velocities of the Rigid Platform

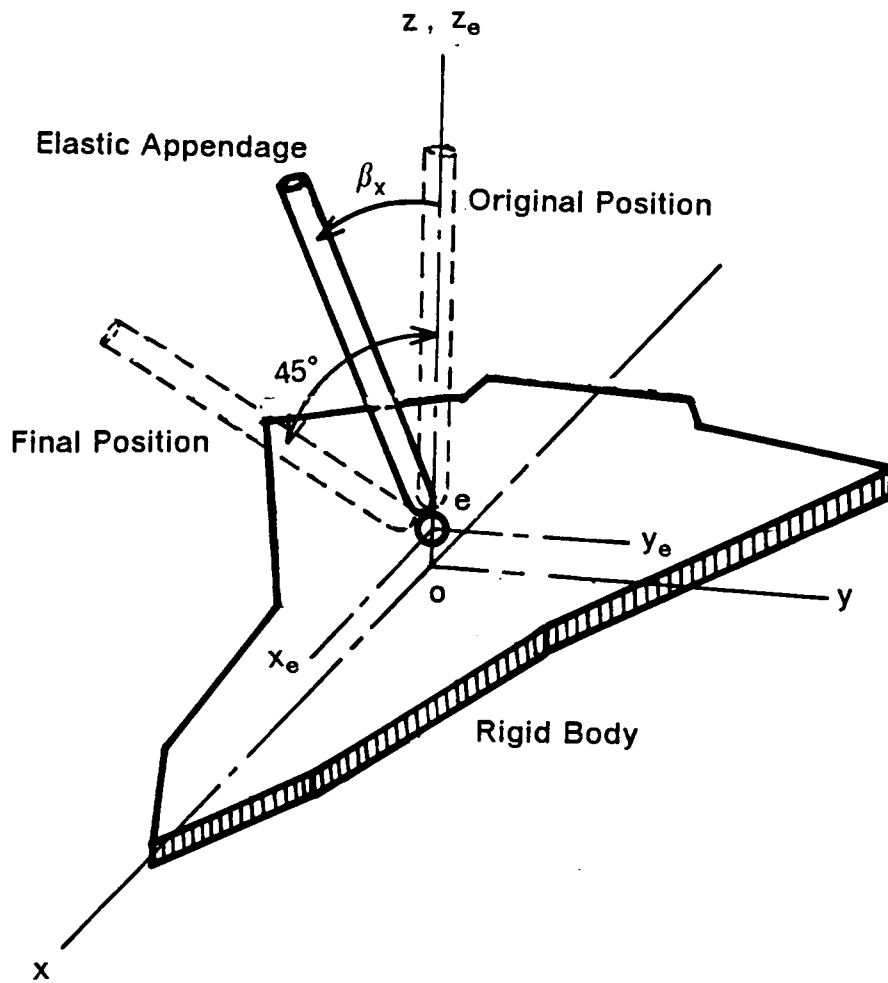


Figure 3. The Spacecraft with a Single Maneuvering Flexible Appendage

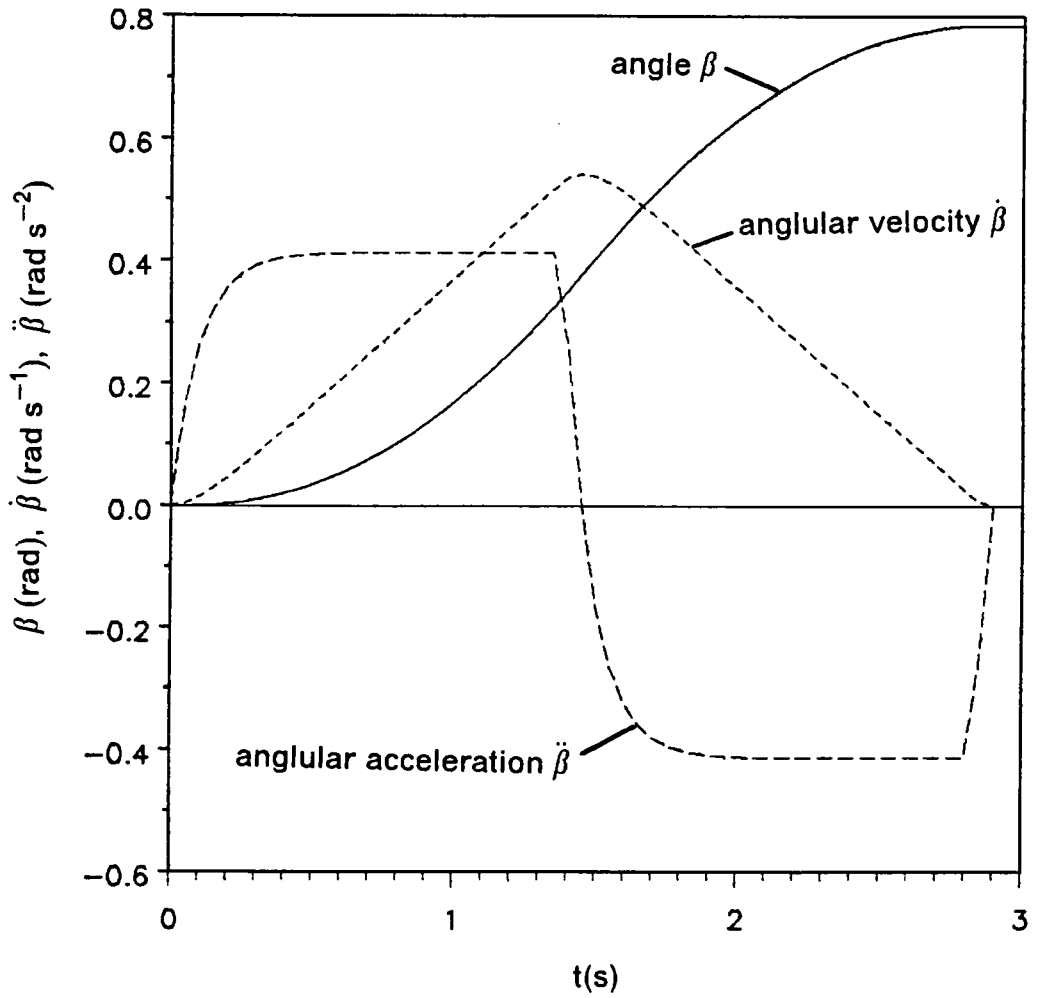


Figure 4. Time History of the Appendage Maneuver

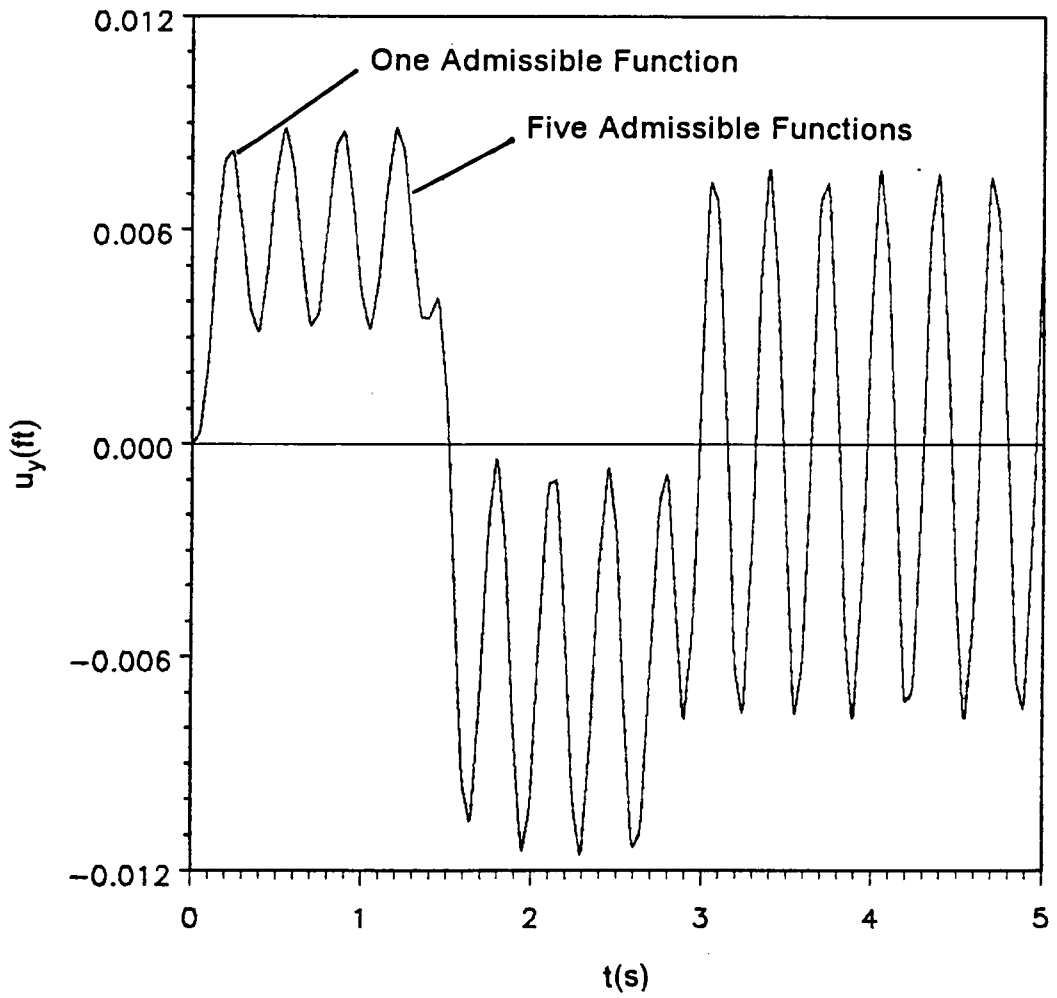


Figure 5. Time History of the Uncontrolled Tip Elastic Displacement

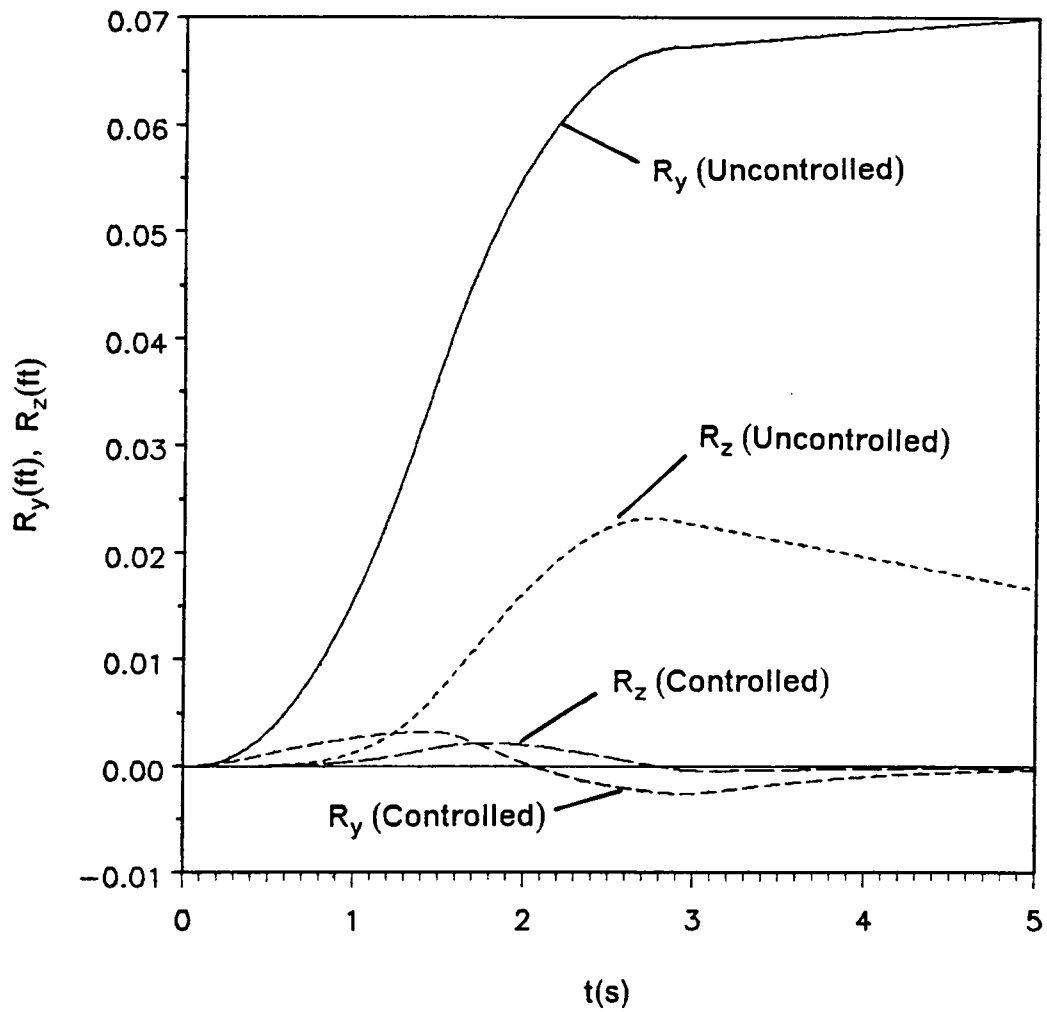


Figure 6. Time History of the Rigid-Body Translations

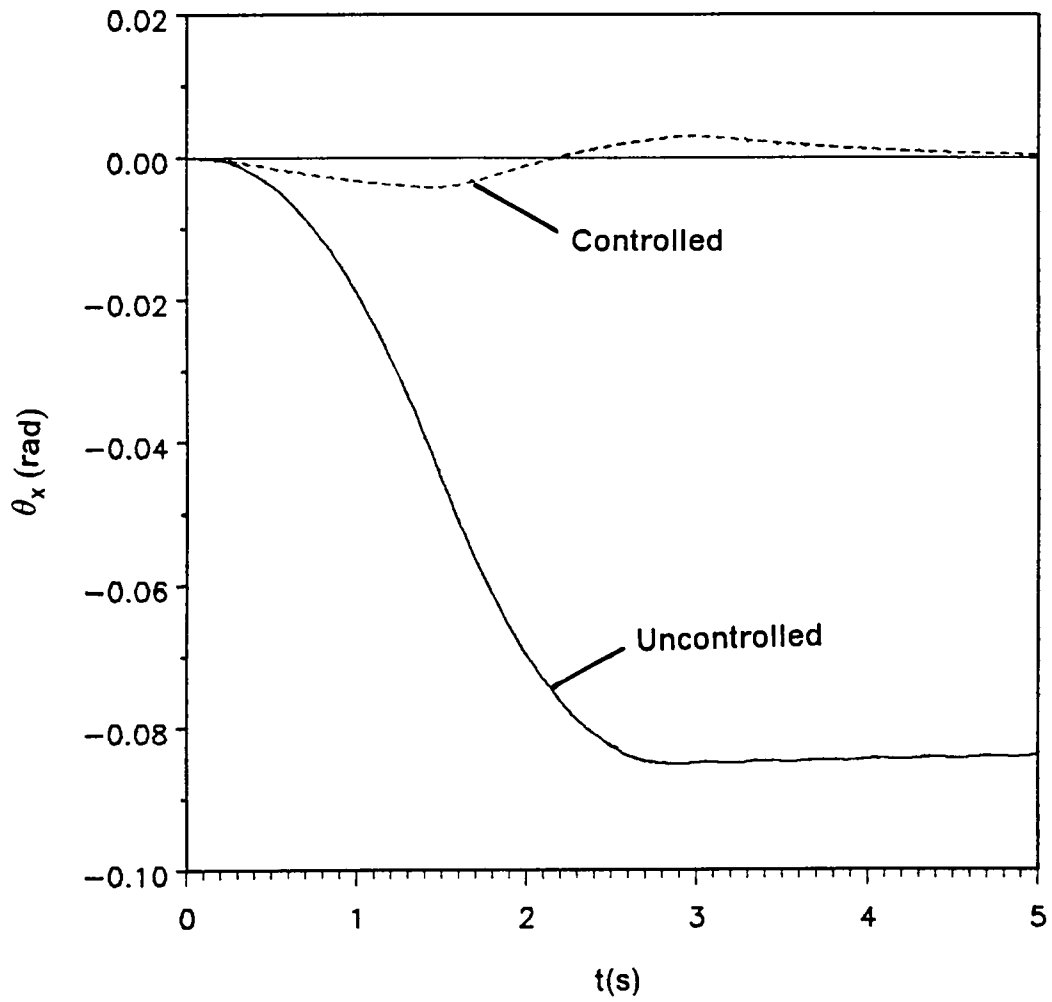


Figure 7. Time History of the Rigid-Body Rotation

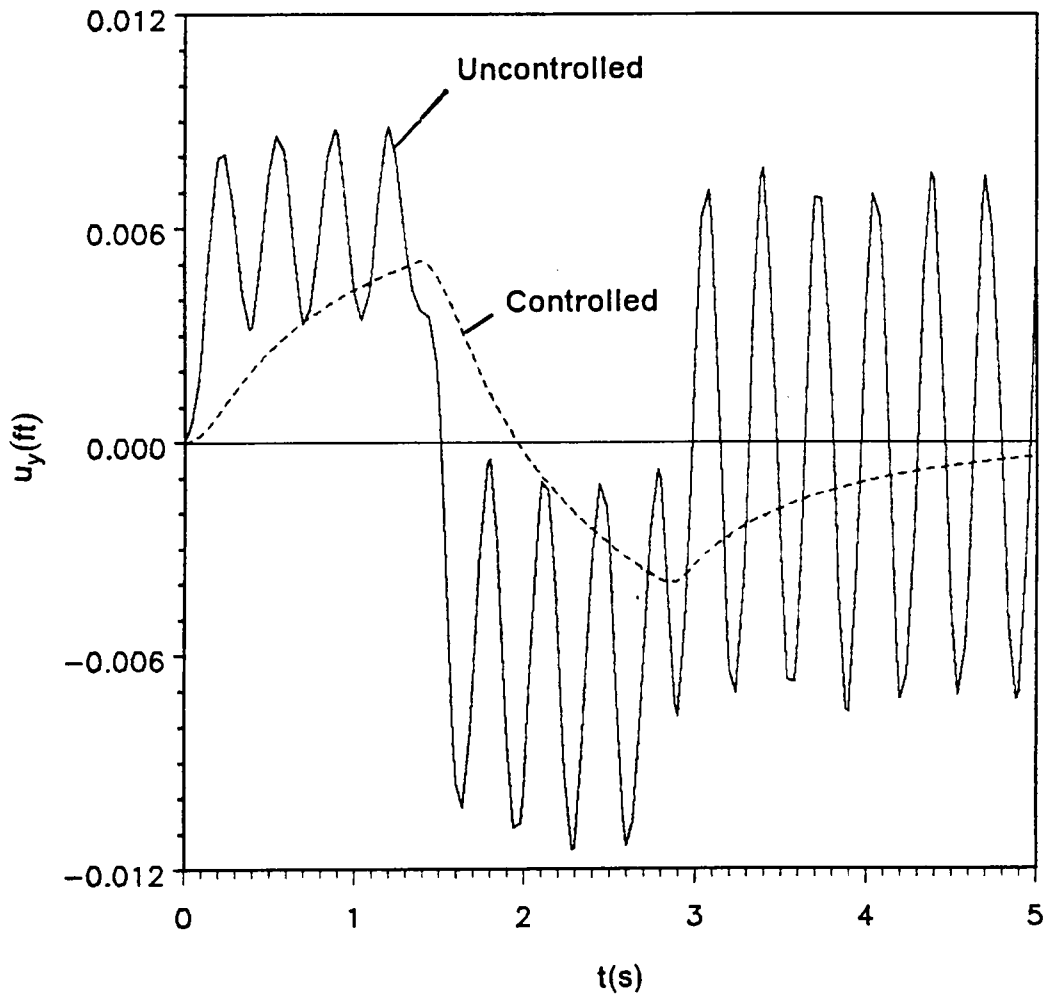


Figure 8. Time History of the Tip Elastic Displacement

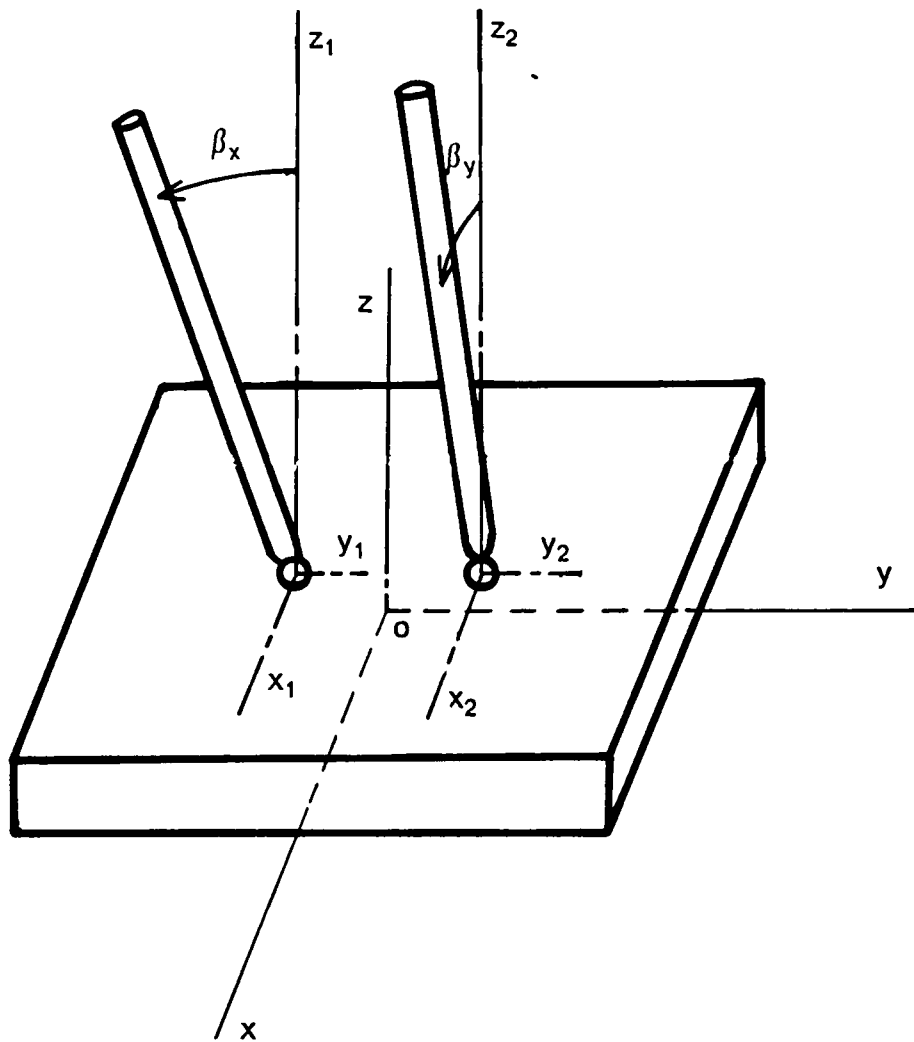


Figure 9. Rigid Platform with Two Flexible Beams

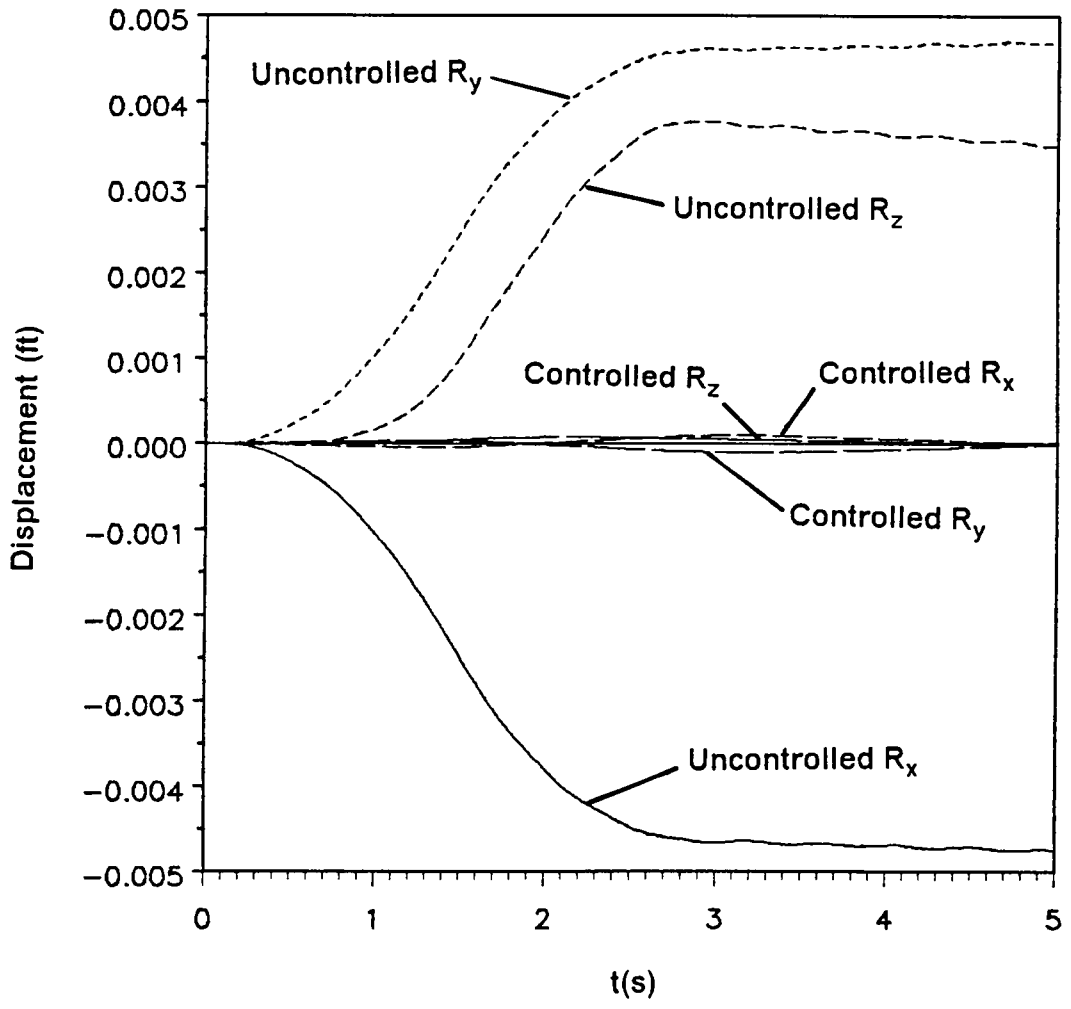


Figure 10. Time History of the Platform Translational Motions

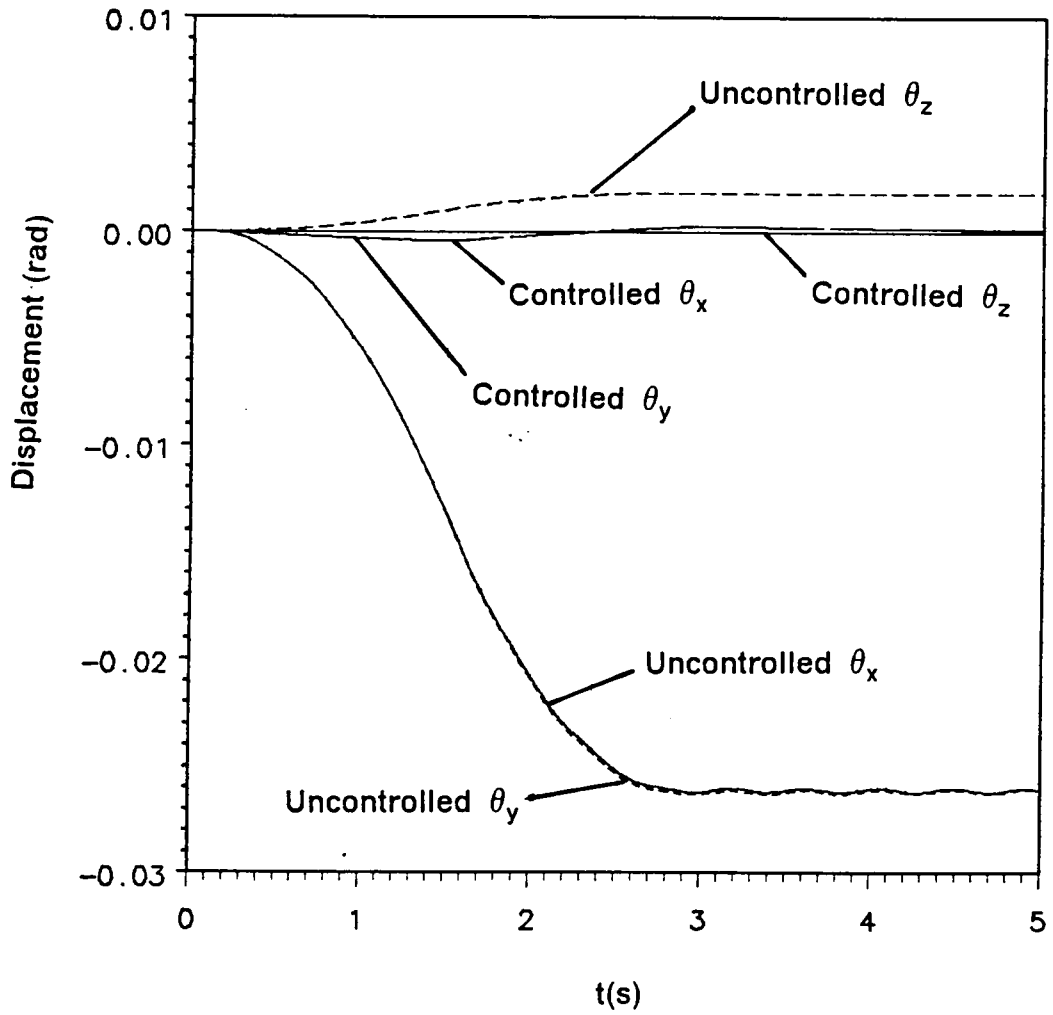


Figure 11. Time History of the Platform Angular Motion

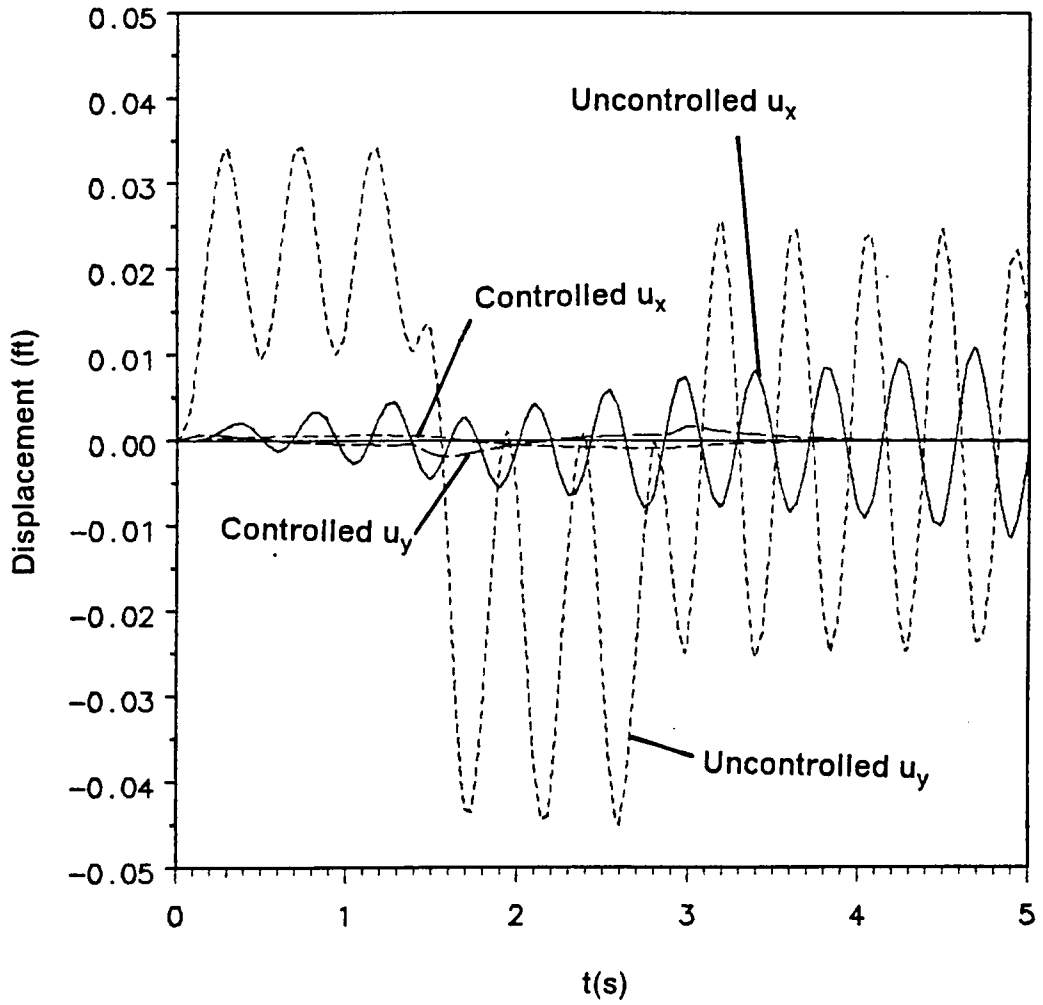


Figure 12. Tip Displacement of Beam 1

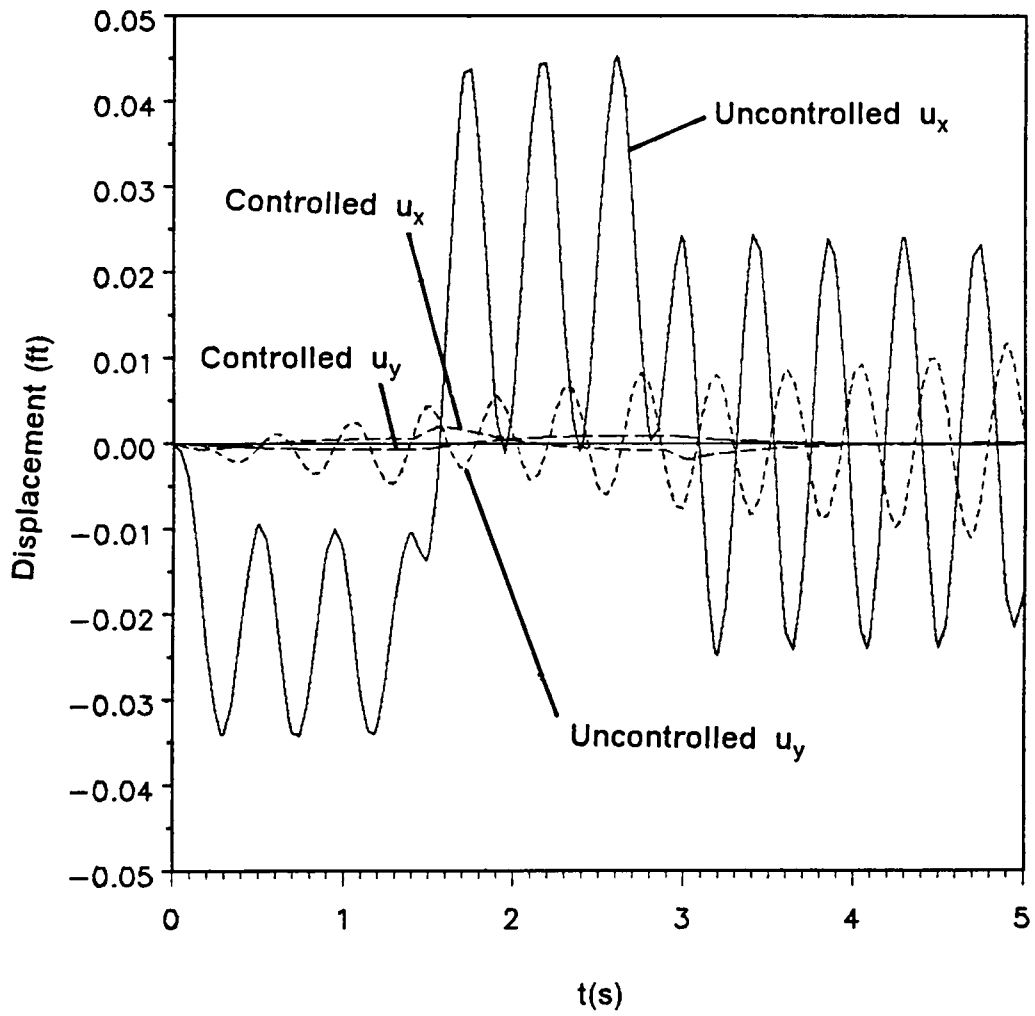


Figure 13. Tip Displacement of Beam 2

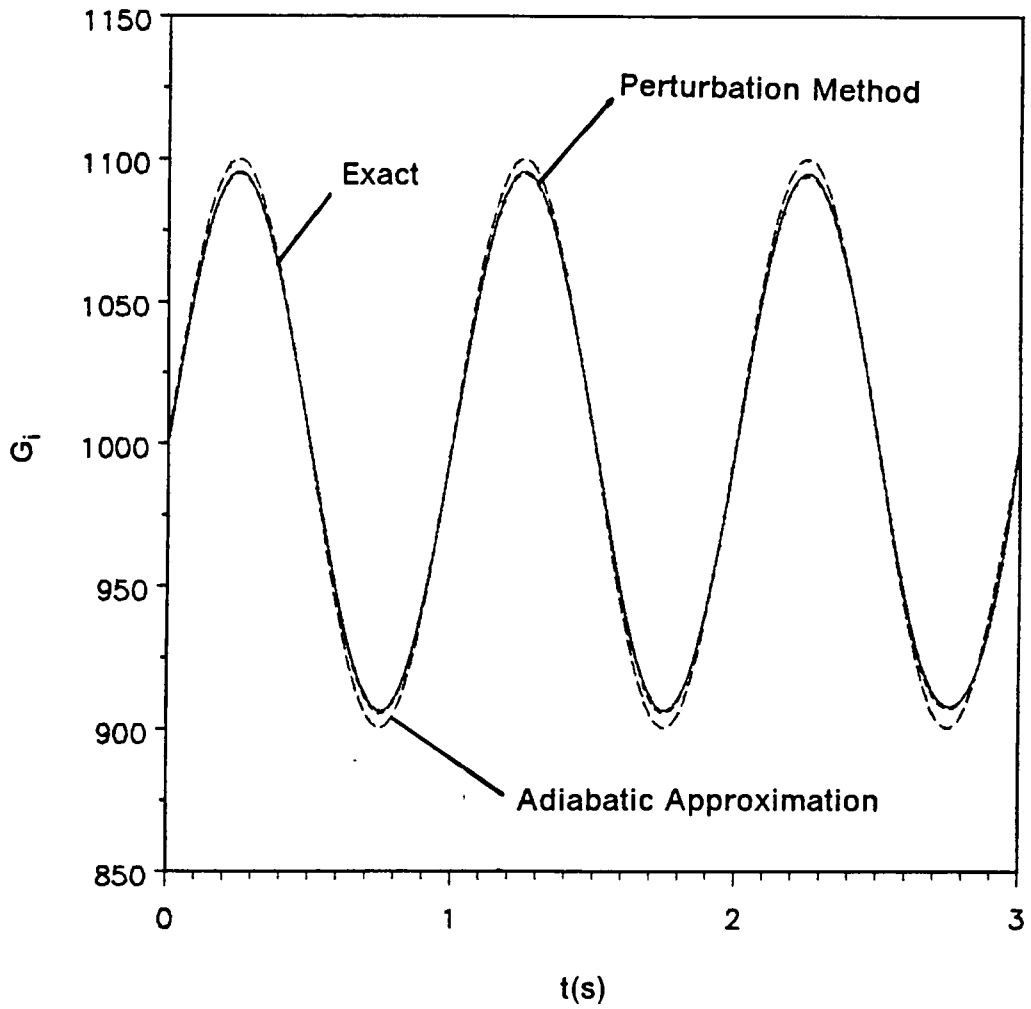


Figure 14. Gain corresponding to integral of x

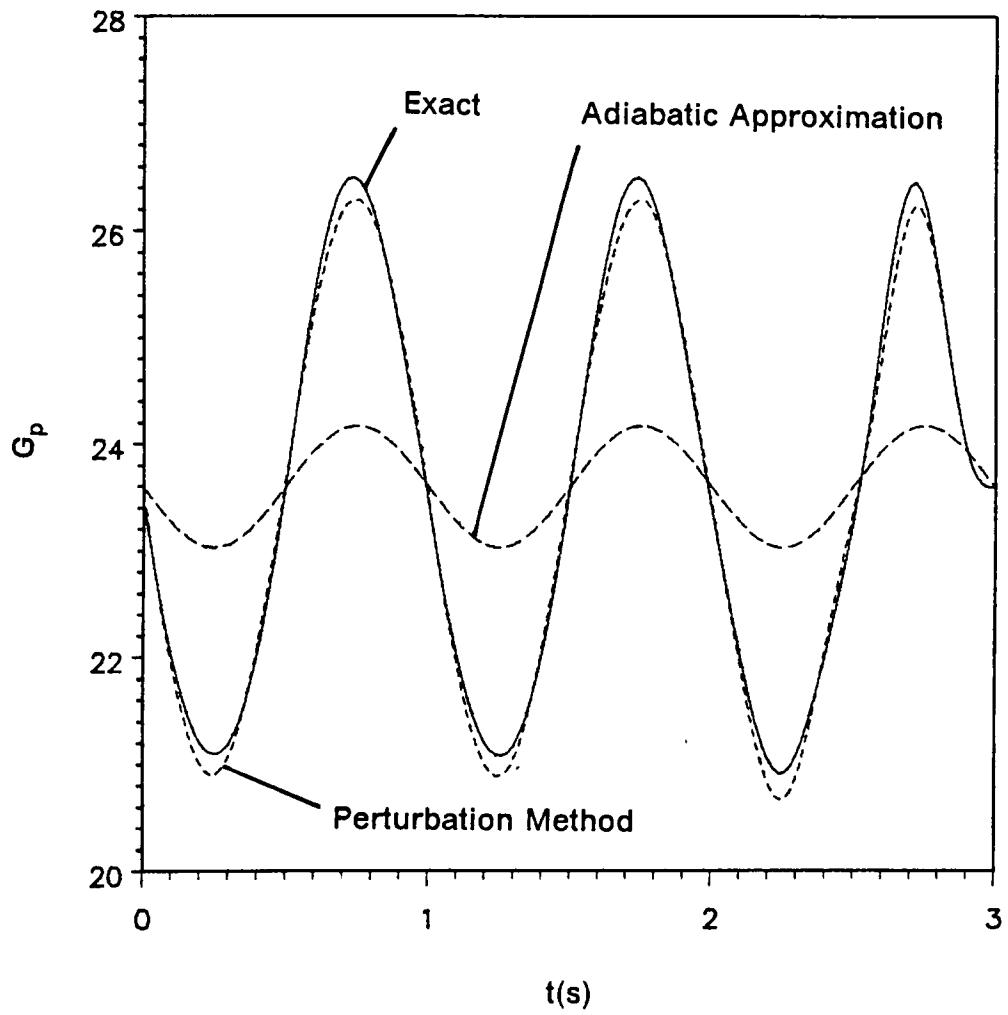


Figure 15. Gain corresponding to x

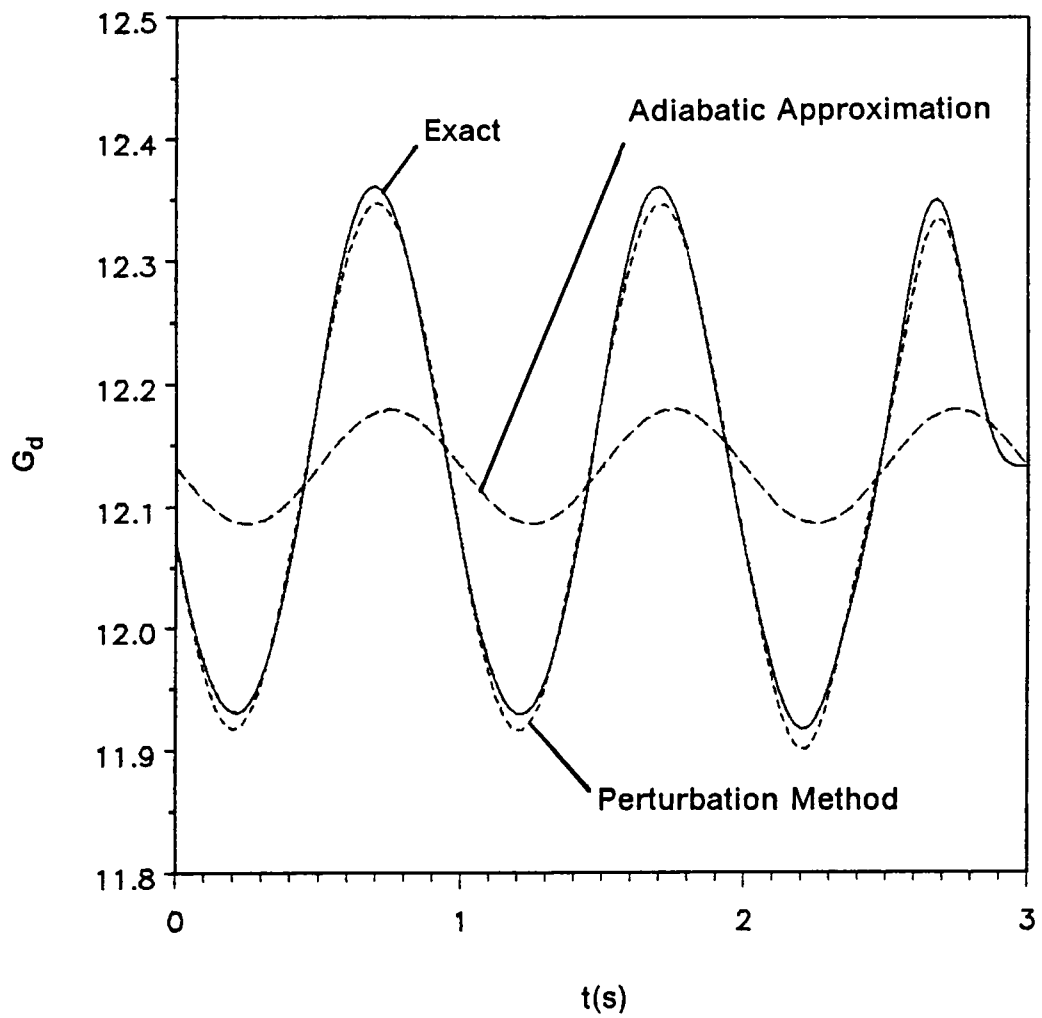


Figure 16. Gain corresponding to derivative of x

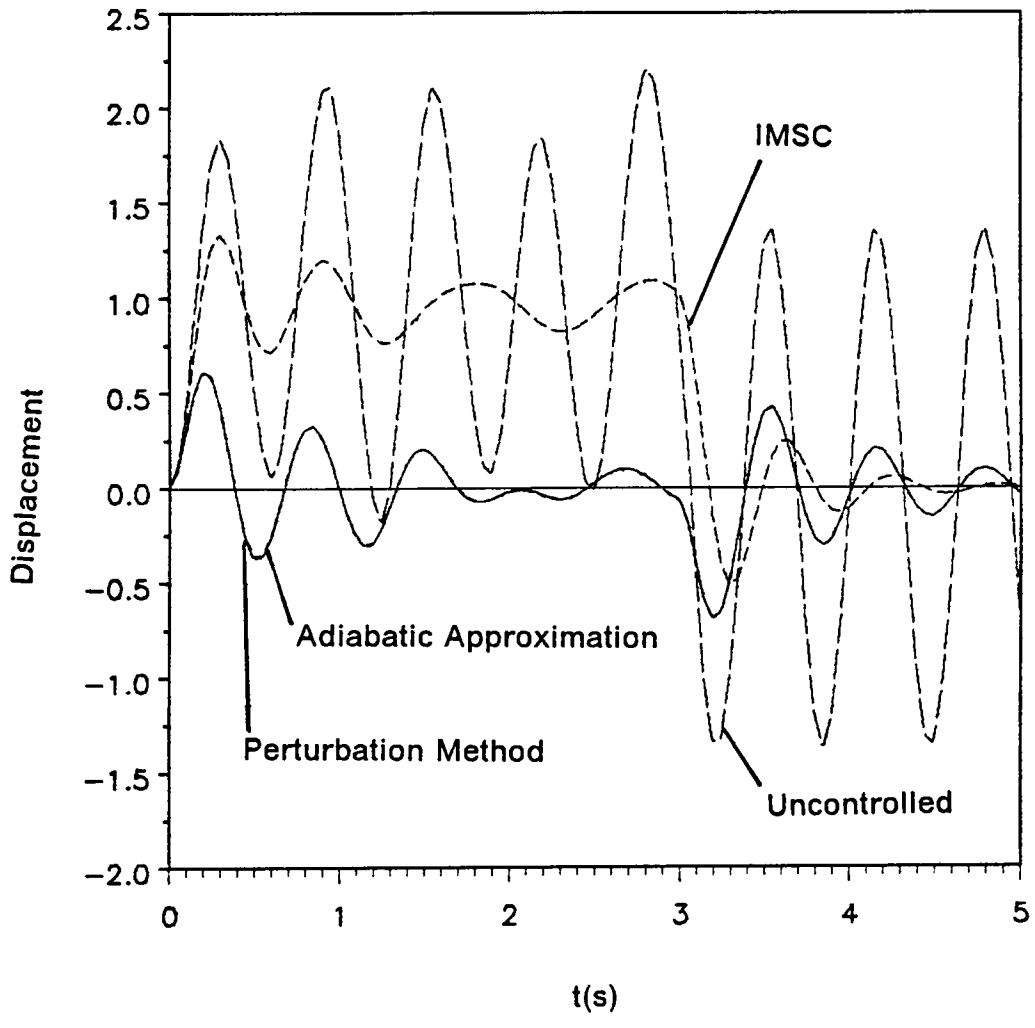


Figure 17. Time Response

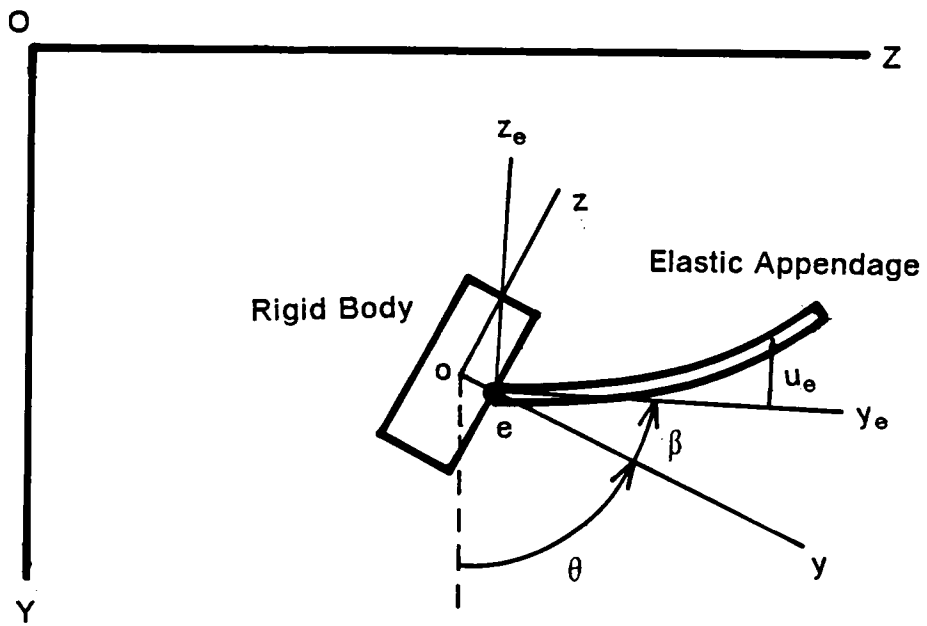


Figure 18. The Two-Dimensional Spacecraft

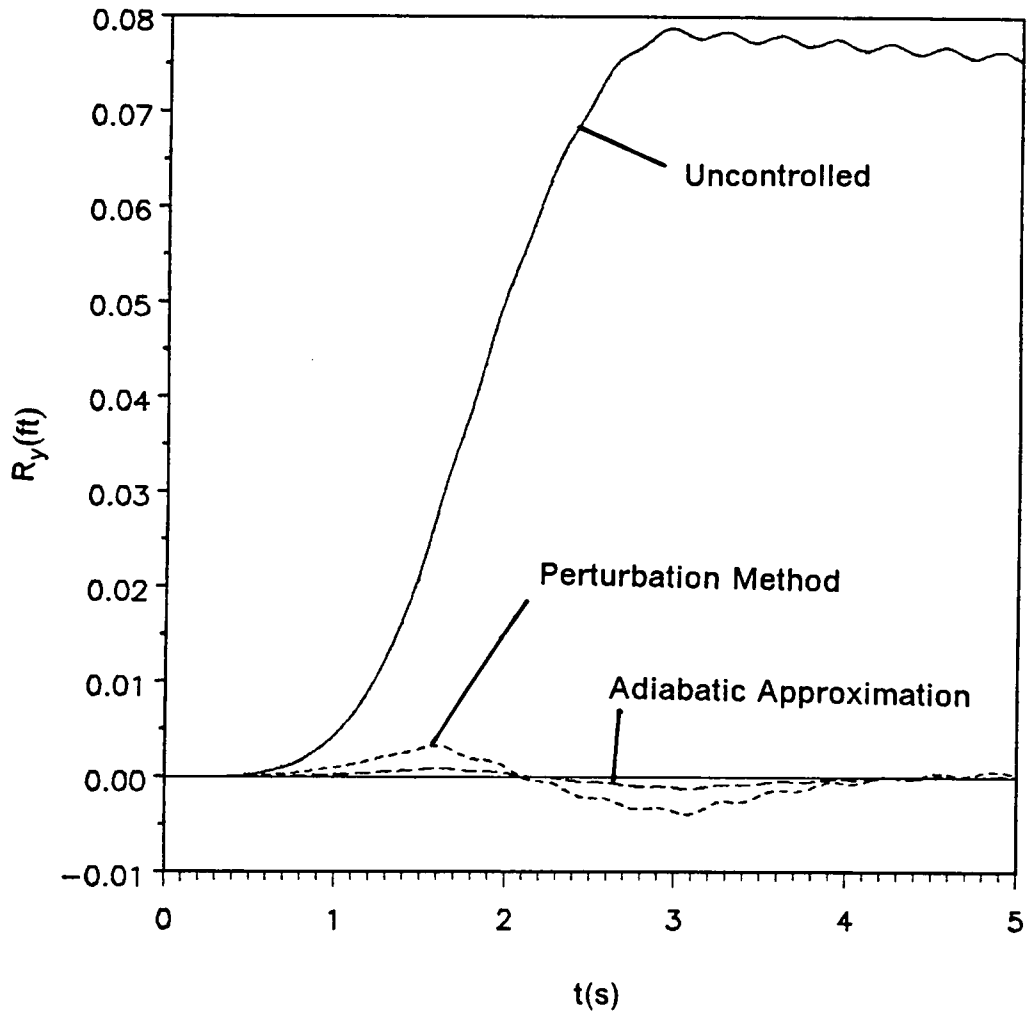


Figure 19. Time History of the Rigid-Body Translation

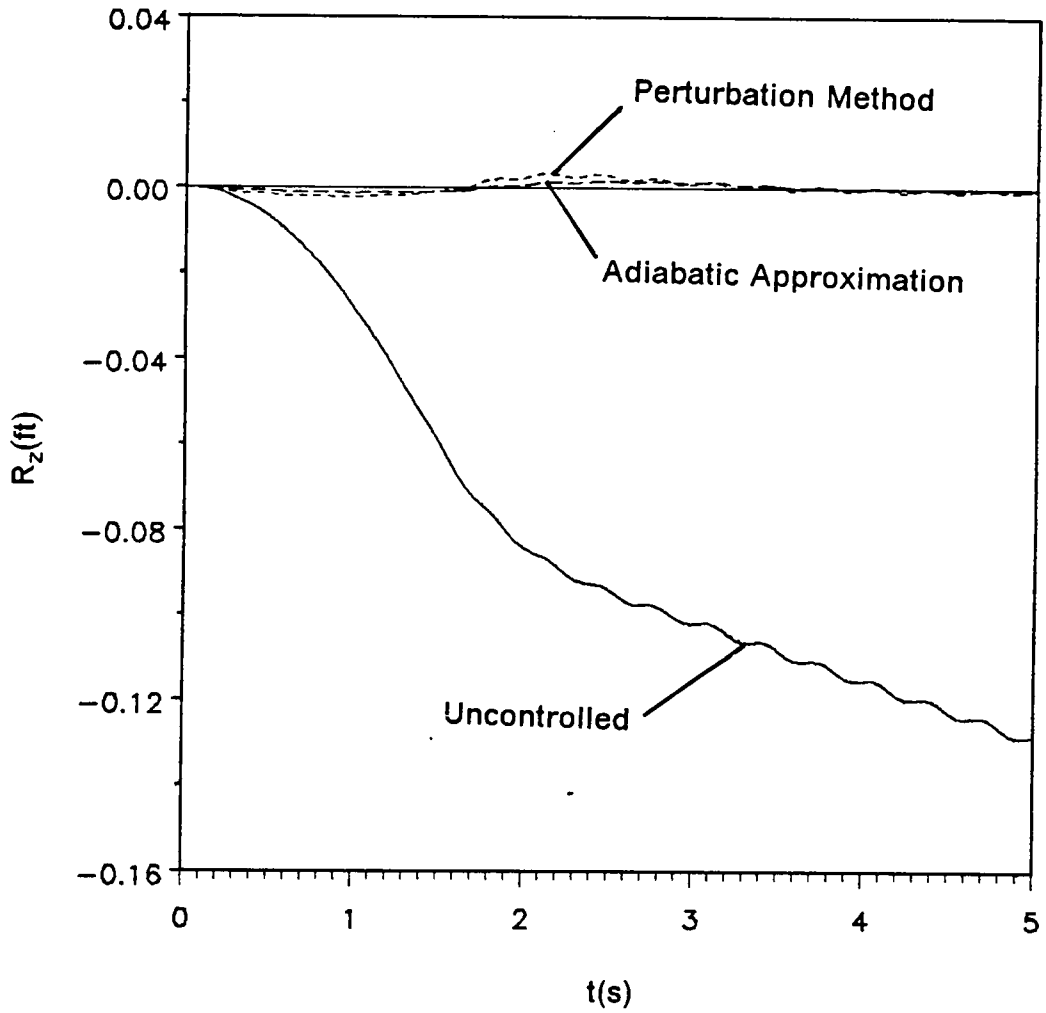


Figure 20. Time History of the Rigid-Body Translation

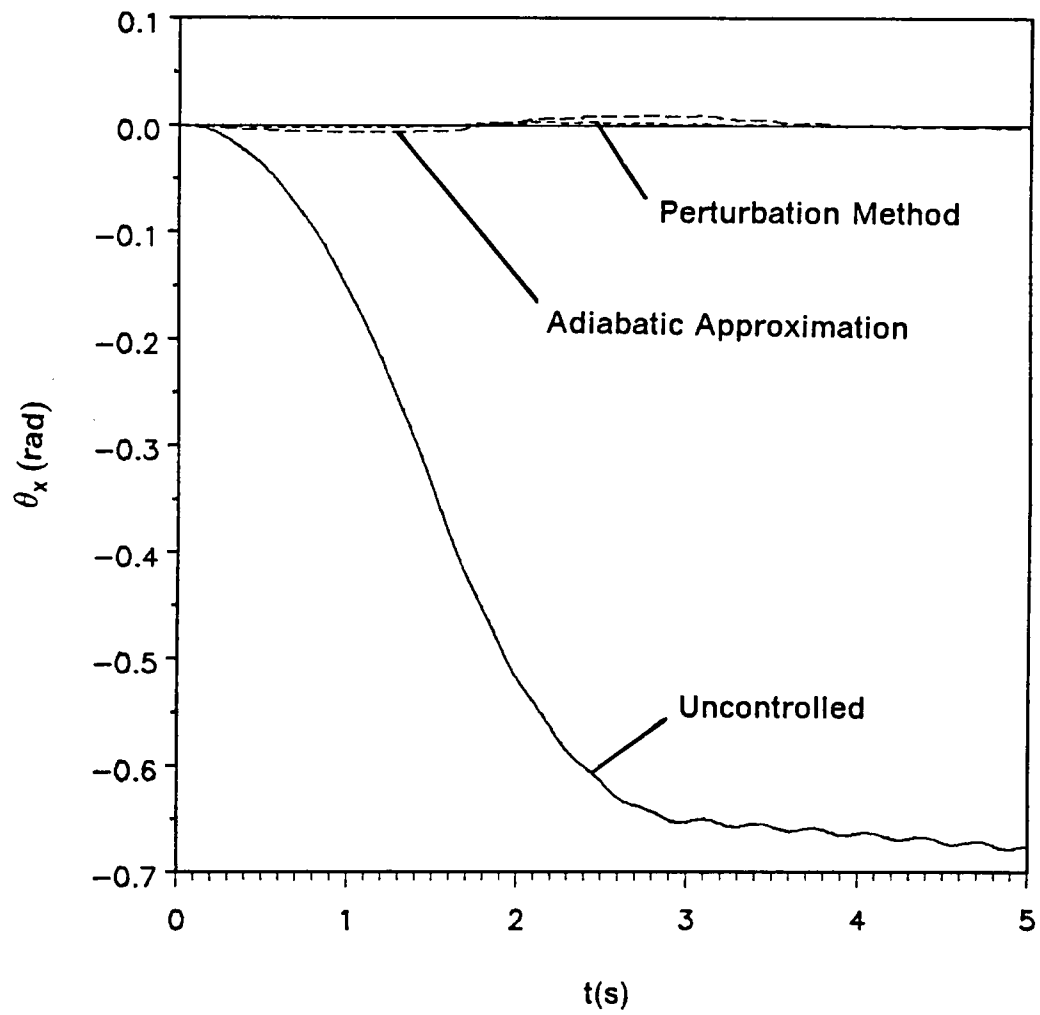


Figure 21. Time History of the Rigid-Body Rotation

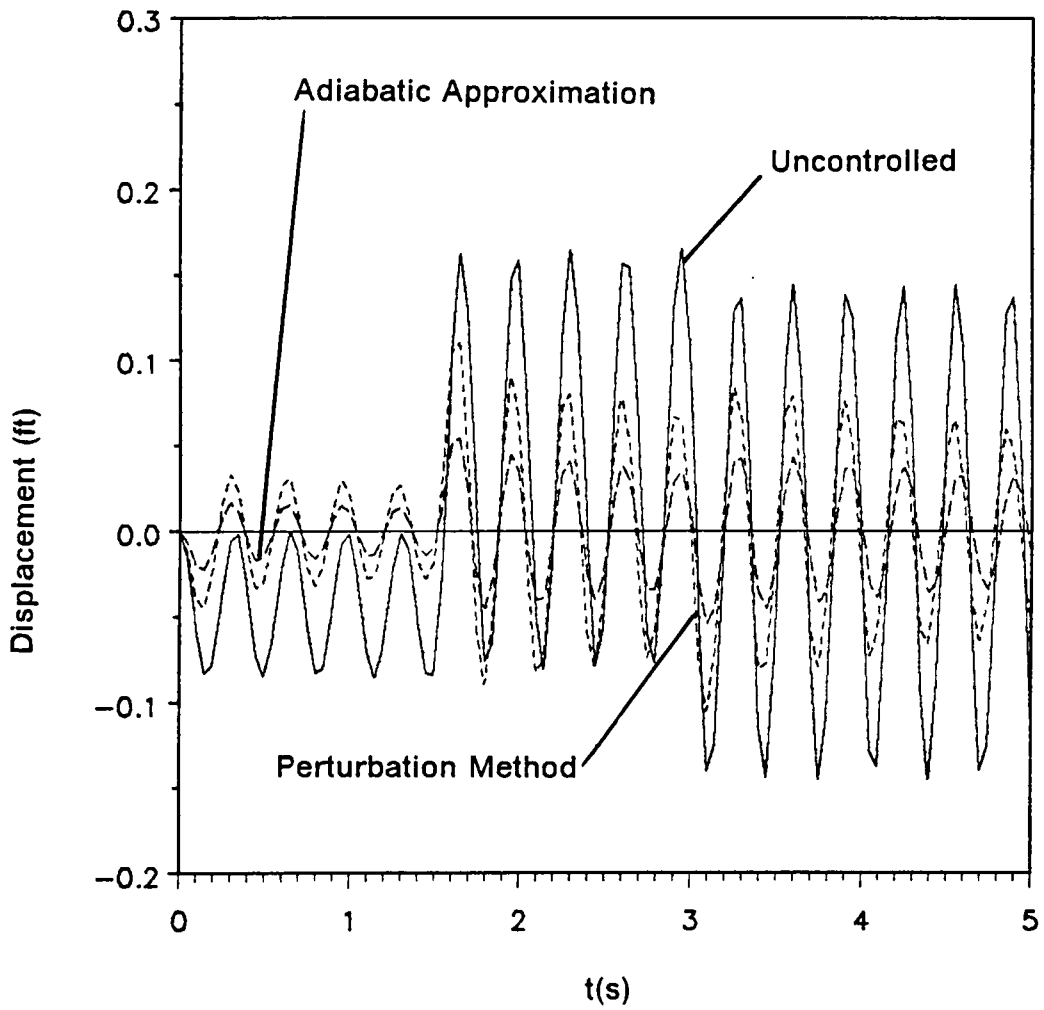


Figure 22. Time History of the Tip Elastic Displacement

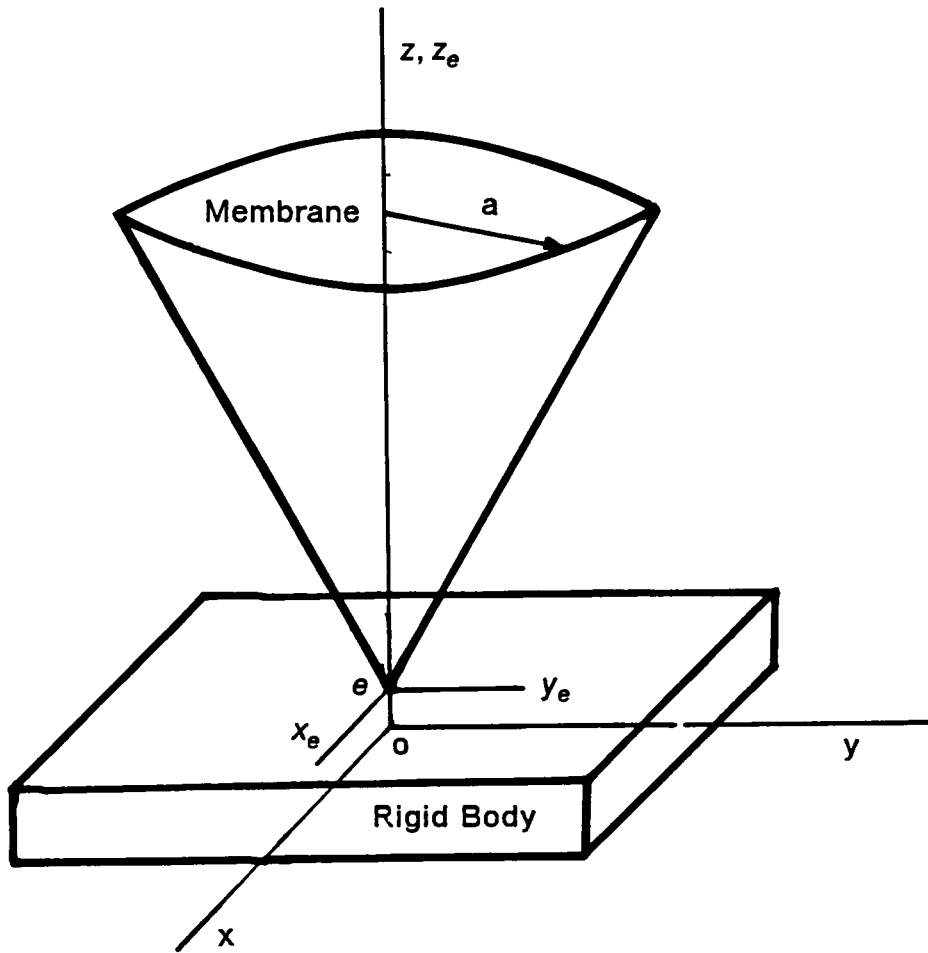


Figure 23. The Spacecraft with a Membrane Antennas

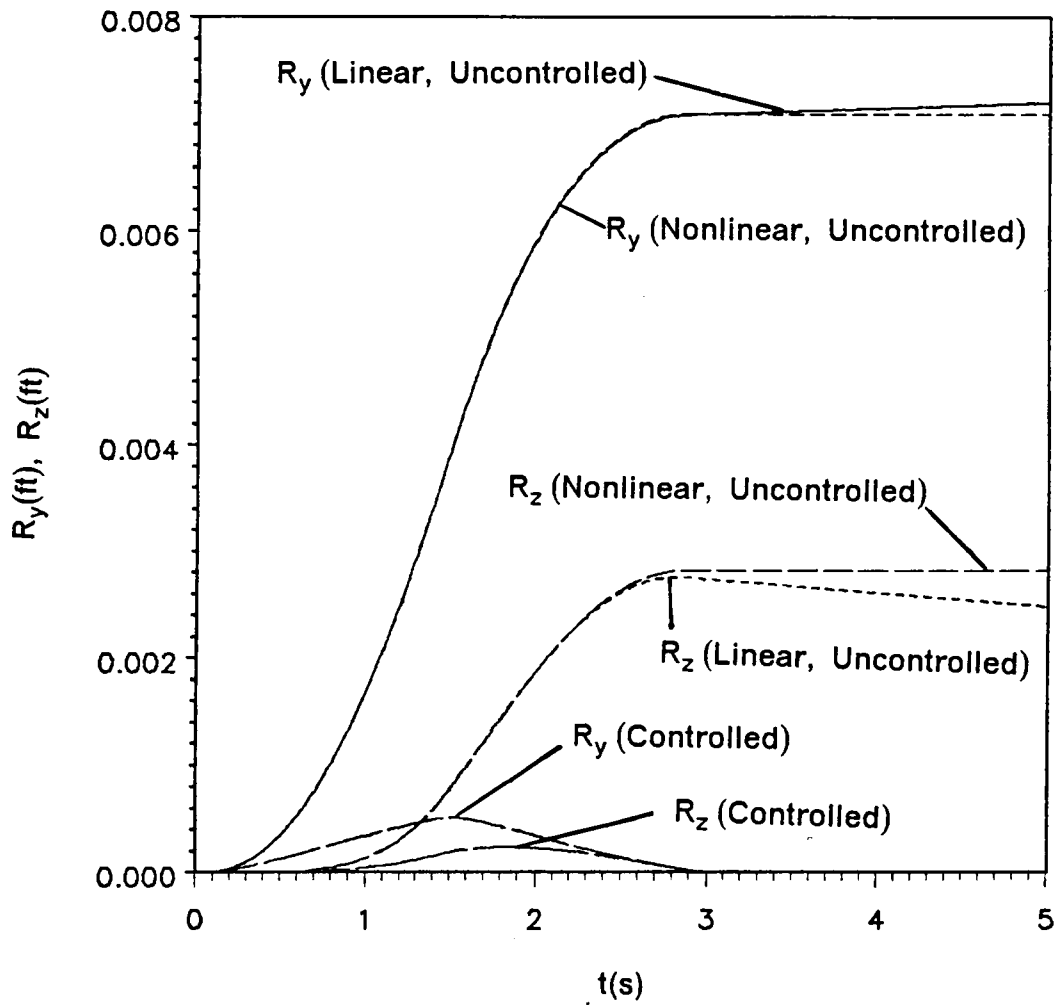


Figure 24. Time History of the Rigid-Body Translations

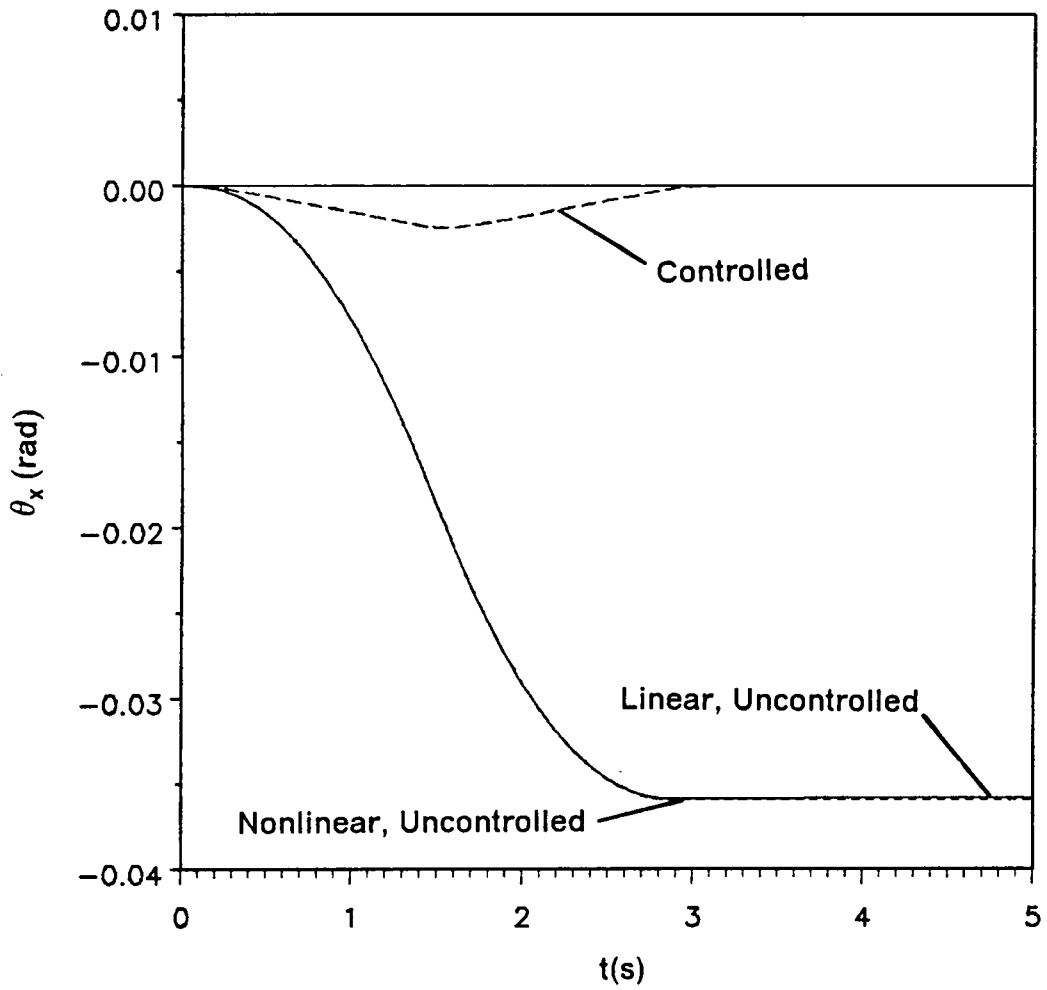


Figure 25. Time History of the Rigid-Body Rotations

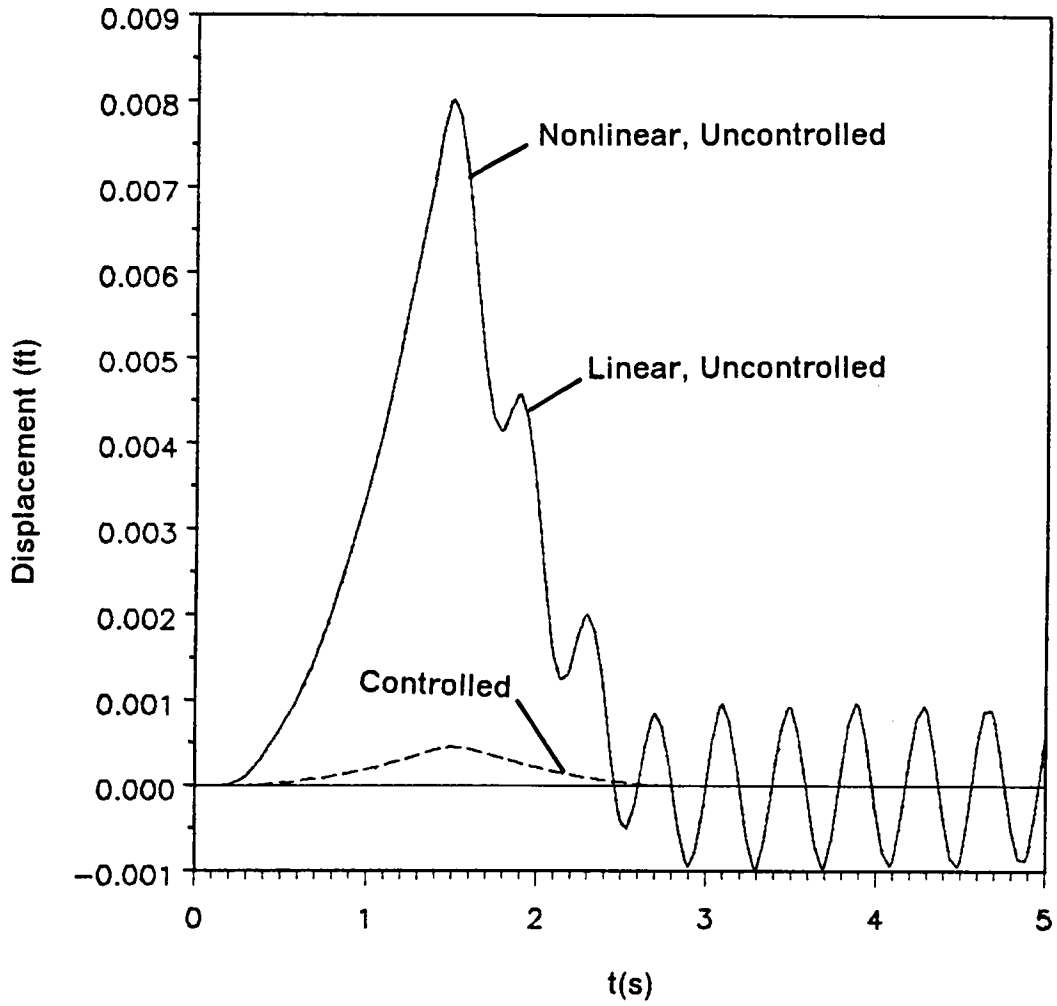


Figure 26. Elastic Displacements at the Center

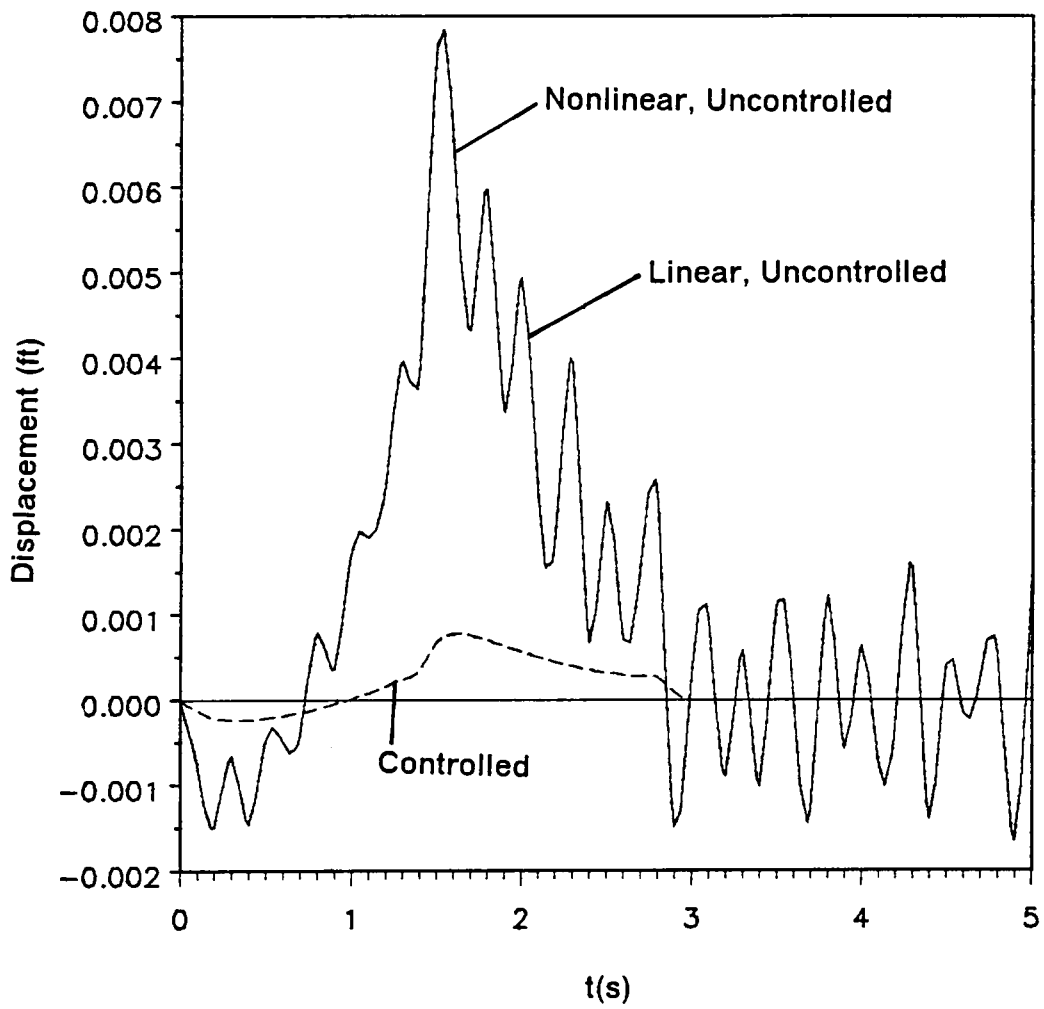


Figure 27. Elastic Displacements at the $r = 0.5 a$

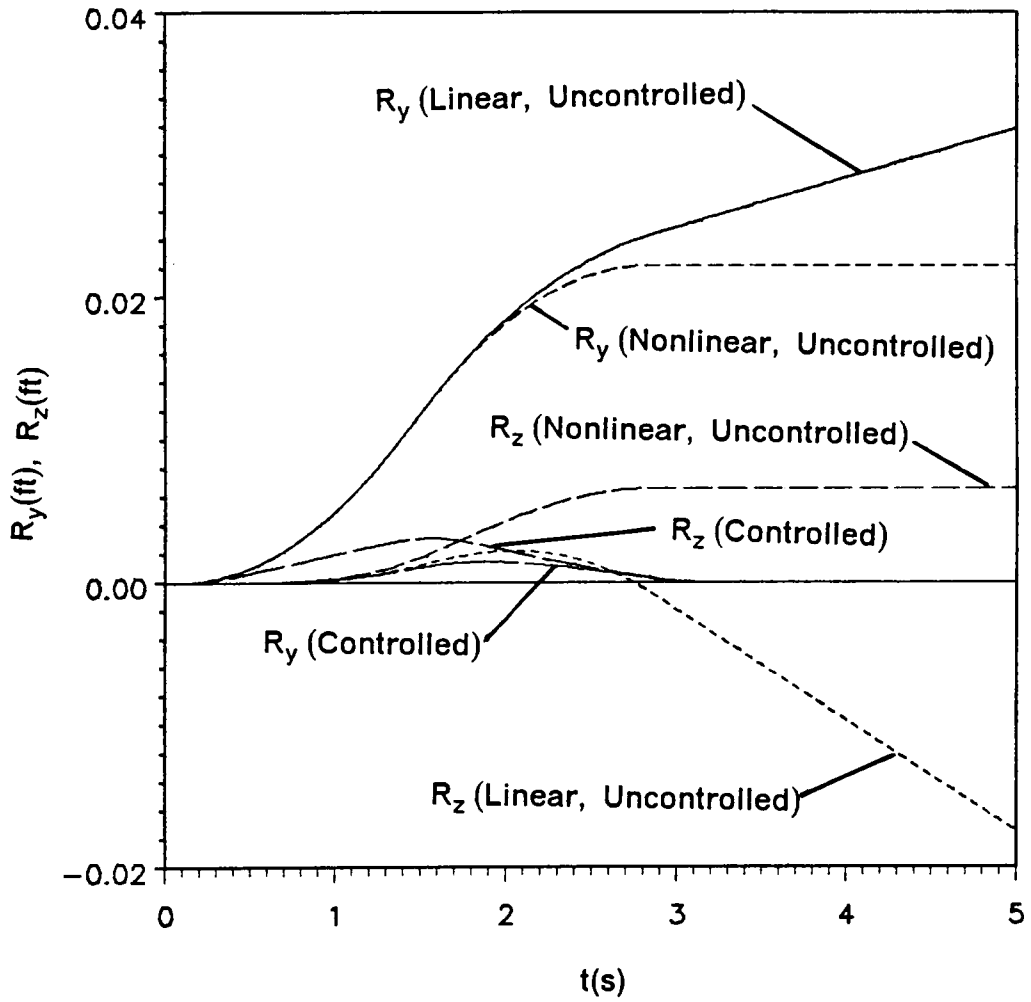


Figure 28. Time History of the Rigid-Body Translations

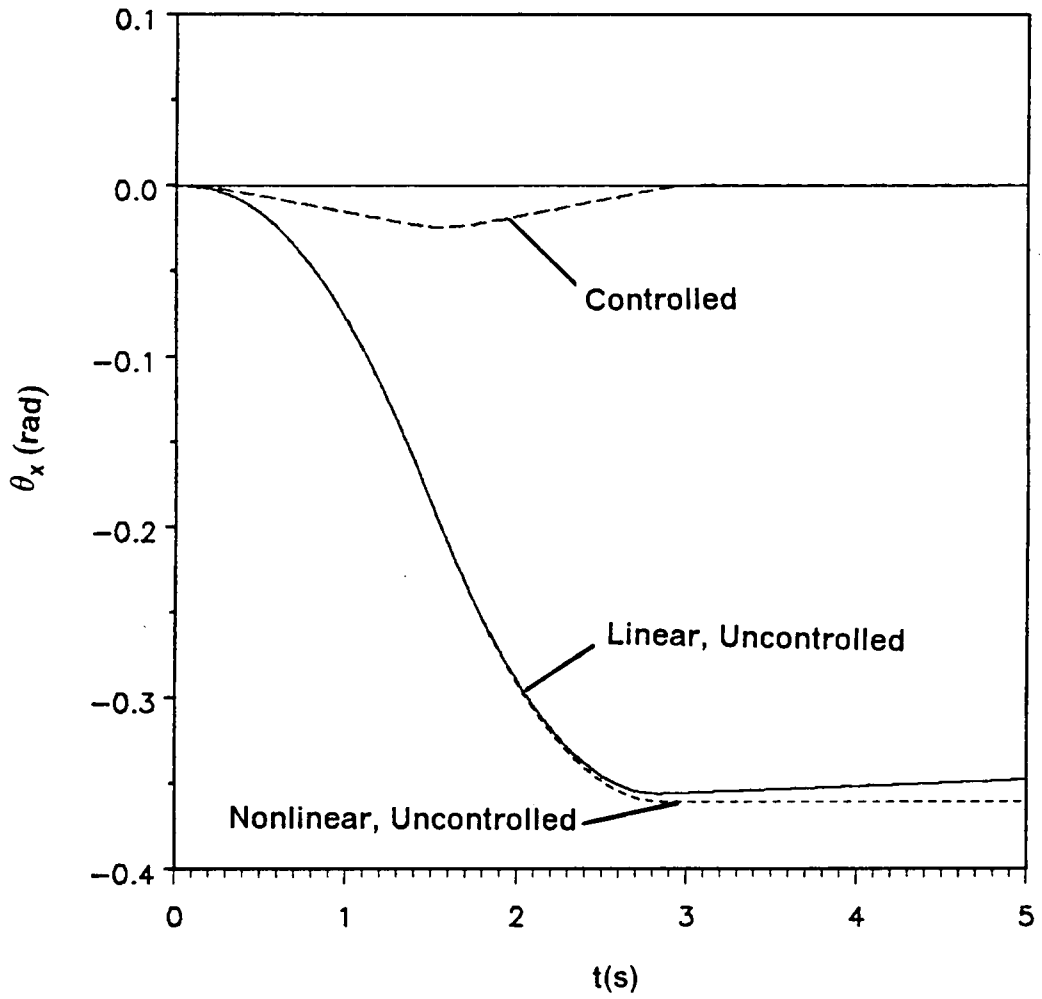


Figure 29. Time History of the Rigid-Body Rotations

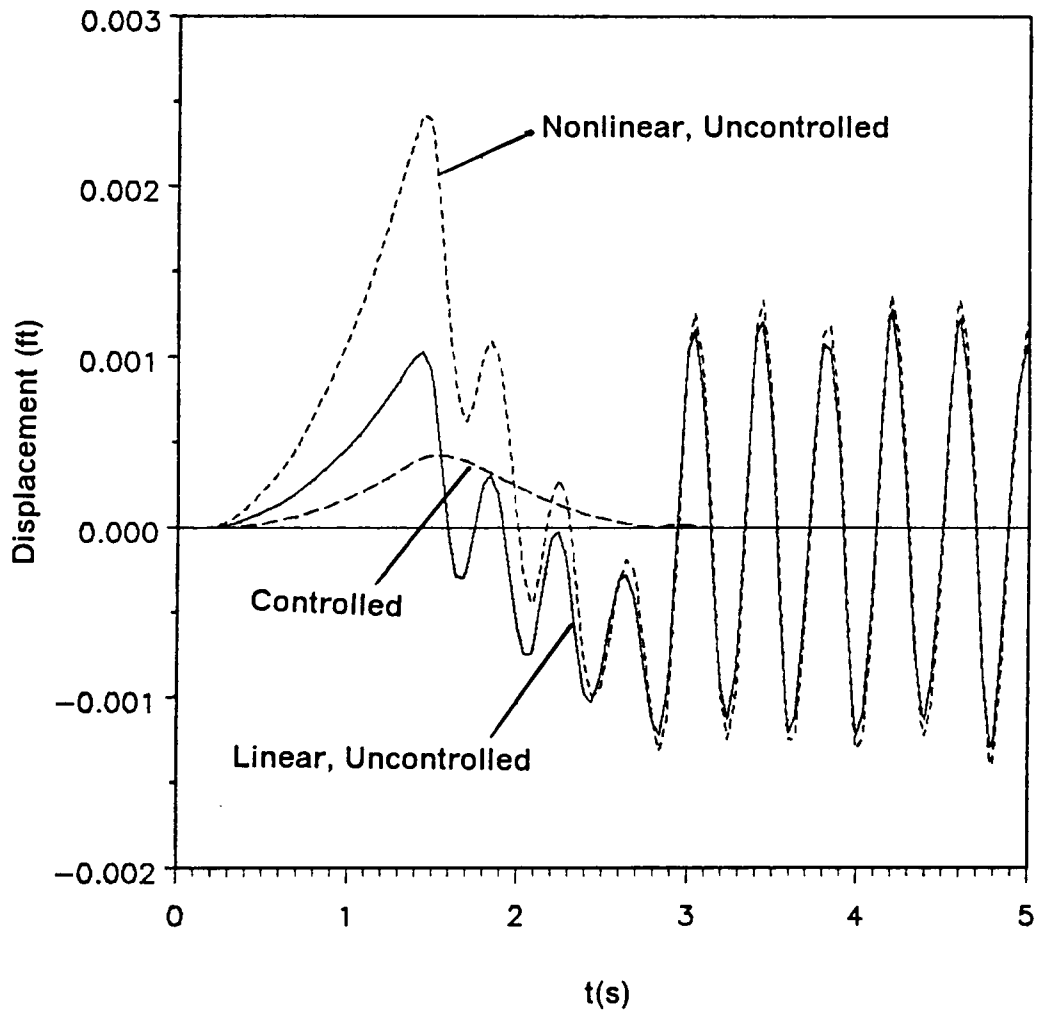


Figure 30. Elastic Displacements at the Center

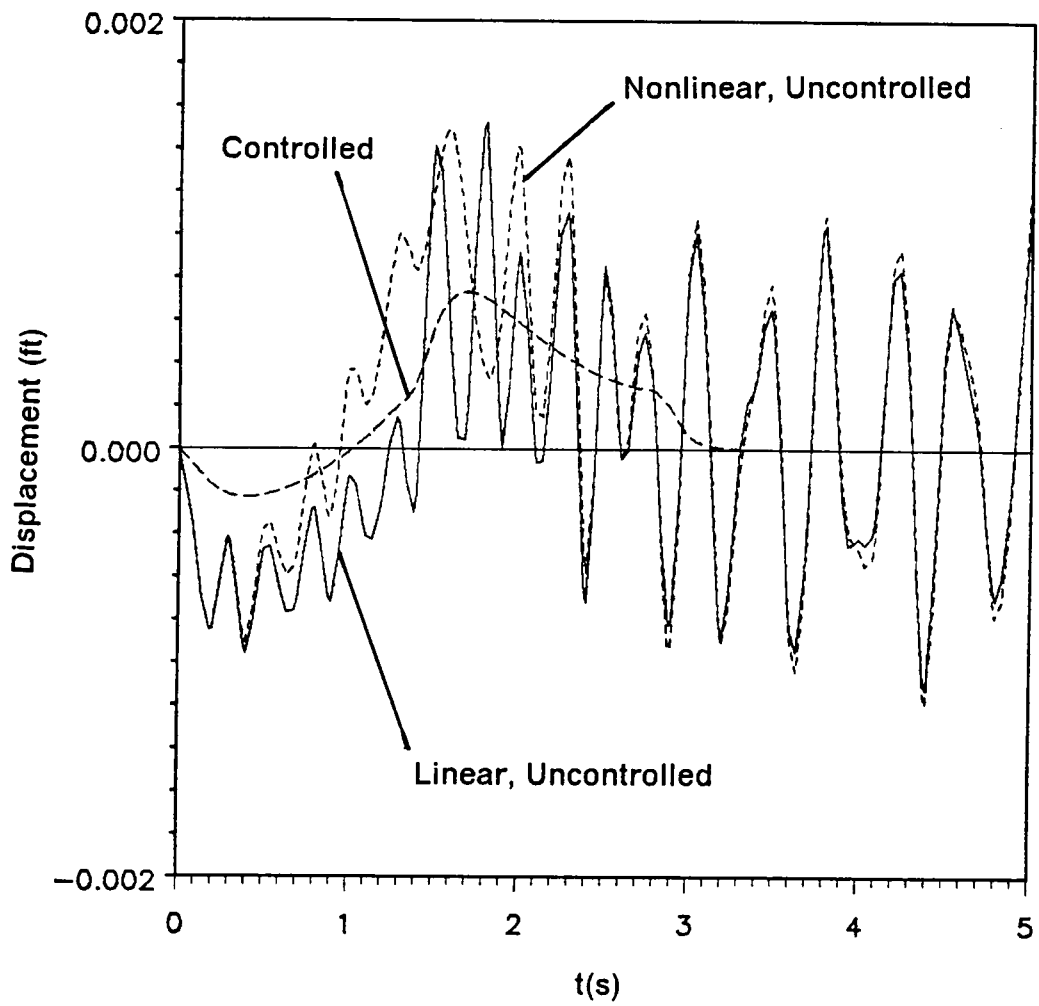


Figure 31. Elastic Displacements at the $r = 0.5 a$

Appendix A. Some Useful Properties

If \underline{a} is a three-dimensional vector, i.e., $\underline{a} = [a_1, a_2, a_3]^T$, then the skew symmetric matrix $\tilde{\underline{a}}$ is defined as

$$\tilde{\underline{a}} = \begin{bmatrix} 0 & -a_3 & a_2 \\ a_3 & 0 & -a_1 \\ -a_2 & a_1 & 0 \end{bmatrix} \quad (\text{A} - 1)$$

The cross product of two vectors can be expressed as

$$\underline{a} \times \underline{b} = \tilde{\underline{a}} \underline{b} = -\tilde{\underline{b}} \underline{a} \quad (\text{A} - 2)$$

Furthermore, the transpose of the cross product can be expressed in several ways, namely,

$$[\tilde{\underline{a}} \underline{b}]^T = -\underline{b}^T \tilde{\underline{a}} = -[\tilde{\underline{b}} \underline{a}]^T = \underline{a}^T \tilde{\underline{b}} \quad (\text{A} - 3)$$

The skew-symmetric matrix of the cross product is

$$[\tilde{\underline{a}} \underline{b}] = \tilde{\underline{a}} \tilde{\underline{b}} - \tilde{\underline{b}} \tilde{\underline{a}} \quad (\text{A} - 4)$$

Another useful relation is

$$[\tilde{a} \tilde{b} \tilde{c}] + [\tilde{b} \tilde{a} \tilde{c}] = \tilde{a} \tilde{b} \tilde{c} + \tilde{b} \tilde{a} \tilde{c} + \tilde{c} \tilde{b} \tilde{a} + \tilde{c} \tilde{a} \tilde{b} - 2(\tilde{b} \tilde{c} \tilde{a} + \tilde{a} \tilde{c} \tilde{b}) \quad (\text{A} - 5)$$

If I is a symmetric matrix, $I = I^T$, then following relation holds:

$$I \tilde{a} + \tilde{a} I + [I \tilde{a}] = \text{tr}(I) \tilde{a} \quad (\text{A} - 6)$$

where tr denotes the trace of the matrix.

The time derivative of the direction cosine matrix C given by Eq. (2-3a) can be expressed in either of the two forms

$$\dot{C} = -\tilde{\omega} C \quad \text{and} \quad \dot{C}^T = C^T \tilde{\omega} \quad (\text{A} - 7\text{a,b})$$

Finally, the direction cosine matrix E_e satisfies

$$E_e^T \tilde{a} E_e = [E_e^T \tilde{a}] \quad (\text{A} - 8)$$

Appendix B. Proof of Eq. (3-42)

Introducing the change of variables $t = t_f - \tau$, Eq. (3-52) becomes

$$P_1' = P_1 \hat{A}_{0C} + \hat{A}_{0C}^T P_1 + \Gamma(t_f - \tau) \quad (\text{B} - 1)$$

where

$$\Gamma(t_f - \tau) = P_0 \hat{A}_1(t_f - \tau) + \hat{A}_1^T(t_f - \tau) P_0 \quad (\text{B} - 2)$$

and prime denotes $d/d\tau$. Then, boundary condition (3-56) becomes $P_1(0) = 0$. Multiplying Eq. (B-1) on the left by $S_1(\tau)$ and on the right $S_2(\tau)$, we obtain

$$S_1 P_1' S_2 = S_1 P_1 \hat{A}_{0C} S_2 + S_1 \hat{A}_{0C}^T P_1 S_2 + S_1 \Gamma(t_f - \tau) S_2 \quad (\text{B} - 3)$$

Next, we consider

$$\frac{d}{d\tau} (S_1 P_1 S_2) = S_1' P_1 S_2 + S_1 P_1' S_2 + S_1 P_1 S_2' \quad (\text{B} - 4)$$

so that Eq. (B-3) can be rewritten as

$$\frac{d}{d\tau} (S_1 P_1 S_2) - S_1 P_1 (S_2' + \hat{A}_{0C} S_2) - (S_1' + S_1 \hat{A}_{0C}^T) P_1 S_2 = S_1 \Gamma(t_f - \tau) S_2 \quad (\text{B} - 5)$$

On the assumption that S_1 and S_2 satisfy

$$S_1' + S_1 \hat{A}_{0C}^T = 0 \quad , \quad S_2' + \hat{A}_{0C} S_2 = 0 \quad (\text{B} - 6a,b)$$

Eq. (B-5) reduces to

$$\frac{d}{d\tau} (S_1 P_1 S_2) = S_1 \Gamma(t_f - \tau) S_2 \quad (\text{B} - 7)$$

Integrating Eq. (B-7), we obtain

$$S_1(t') P_1(t') S_2(t') = \int_0^{t'} S_1(\tau) \Gamma(t_f - \tau) S_2(\tau) d\tau \quad (\text{B} - 8)$$

Equation (B-8) yields

$$P_1(t') = S_1^{-1}(t') \int_0^{t'} S_1(\tau) \Gamma(t_f - \tau) S_2(\tau) d\tau S_2^{-1}(t') \quad (\text{B} - 9)$$

Equations (B-6) have the solutions

$$S_1(\tau) = e^{-\hat{A}_{0C}^T \tau} S_1(0) \quad , \quad S_2(\tau) = e^{-\hat{A}_{0C} \tau} S_2(0) \quad (\text{B} - 10a,b)$$

so that, inserting Eqs. (B-10) into Eq. (B-9), we obtain

$$P_1(t') = \int_0^{t'} e^{\hat{A}_{0C}^T(t'-\tau)} \Gamma(t_f - \tau) e^{\hat{A}_{0C}(t'-\tau)} d\tau \quad (\text{B} - 11)$$

Introducing the changes of the variables $t'' = t_f - \tau$ and $t' = t_f - t$, we can rewrite Eq. (B-11)

as

$$P_1(t) = \int_t^{t_f} e^{\hat{A}_0(t^*-t)} \Gamma(t^*) e^{\hat{A}_0(t^*-t)} dt^* \quad (\text{B} - 12)$$

Finally, replacing t^* by τ , we obtain Eq. (3-42)

Appendix C. Derivation of Eq. (3-43)

The object is to discretize Eq. (3-42) in time. To this end, we let $t = t_k$ and $t = t_{k+1} = t_k + \Delta t$ in Eq. (3-42) and write

$$P_1(t_k) = \int_{t_k}^{t_f} e^{\hat{A}_T(\tau - t_k)} \Gamma(\tau) e^{\hat{A}_{0c}(\tau - t_k)} d\tau \quad (C - 1)$$

$$\begin{aligned} P_1(t_{k+1}) &= \int_{t_{k+1}}^{t_f} e^{\hat{A}_T(\tau - t_{k+1})} \Gamma(\tau) e^{\hat{A}_{0c}(\tau - t_{k+1})} d\tau = e^{-\hat{A}_T \Delta t} \int_{t_k}^{t_f} e^{\hat{A}_T(\tau - t_k)} \Gamma(\tau) e^{\hat{A}_{0c}(\tau - t_k)} d\tau e^{-\hat{A}_{0c} \Delta t} \\ &= e^{-\hat{A}_T \Delta t} [P_1(t_k) - \int_{t_k}^{t_{k+1}} e^{\hat{A}_T(\tau - t_k)} \Gamma(\tau) e^{\hat{A}_{0c}(\tau - t_k)} d\tau] e^{-\hat{A}_{0c} \Delta t} \\ &= e^{-\hat{A}_T \Delta t} [P_1(t_k) - \int_0^{\Delta t} e^{\hat{A}_T \xi} \Gamma(t_k + \xi) e^{\hat{A}_{0c} \xi} d\xi] e^{-\hat{A}_{0c} \Delta t} \end{aligned} \quad (C - 2)$$

where we introduced the change of variables $\tau = t_k + \xi$ in integral.

Appendix D. Expressions for Parameters

Inserting admissible functions given by Eq. (4-1) into Eqs. (2-22) and (2-24), we obtain

$$\bar{\phi}_e = m_e [0.783 \ 0.434 \ 0.254 \ 0.182 \ 0.141] \quad (D-1)$$

$$\tilde{\phi}_e = m_e l_e [0.569 \ 0.091 \ 0.032 \ 0.017 \ 0.010] \quad (D-2)$$

$$\bar{H}_e(\underline{a}) = a_3 m_e \begin{bmatrix} 0 & I \\ I & 0 \end{bmatrix}, \quad \tilde{H}_e(\underline{a}) = m_e \begin{bmatrix} -(a_2^2 + a_3^2)I & a_1 a_2 I \\ a_1 a_2 I & -(a_1^2 + a_3^2)I \end{bmatrix} \quad (D-3,4)$$

$$J_e(\underline{a}) = - \begin{bmatrix} a_3 \tilde{\phi}_e & 0 \\ 0 & a_3 \tilde{\phi}_e \\ a_1 \tilde{\phi}_e & a_1 \tilde{\phi}_e \end{bmatrix} \quad (D-5)$$

$$\int_{D_e} \rho_e \tilde{r}_e \tilde{a} \Phi_e dD_e = -a_3 m_e l_e \begin{bmatrix} \tilde{\phi}_e & 0 \\ 0 & \tilde{\phi}_e \\ 0 & 0 \end{bmatrix} \quad (D-6)$$

where I is the 5×5 identity matrix.

Appendix E. Expressions for Matrices

The matrices given by Eqs. (2-64) are computed by using the numerical data given in the Numerical Example 4. The resulting matrices are

$$M_0 = \begin{bmatrix} 15.75 & 0 & 0 & 0 \\ 0 & 15.75 & 0.435 & 0.117 \\ 0 & 0.435 & 14.574 & 0.474 \\ 0 & 0.117 & 0.474 & 0.150 \end{bmatrix}$$

$$K_0 = \begin{bmatrix} 0 & 0 & 0 & 0 \\ 0 & 0 & 0 & 0 \\ 0 & 0 & 0 & 0 \\ 0 & 0 & 0 & 49.449 \end{bmatrix}$$

$$M_s = \begin{bmatrix} 0 & 0 & -0.375 & -0.117 \\ 0 & 0 & 0 & 0 \\ -0.375 & 0 & 0 & 0 \\ -0.117 & 0 & 0 & 0 \end{bmatrix}$$

$$M_c = \begin{bmatrix} 0 & 0 & 0 & 0 \\ 0 & 0 & 0.375 & 0.117 \\ 0 & 0.375 & 0.3 & 0.047 \\ 0 & 0.117 & 0.047 & 0 \end{bmatrix}$$

$$K_{b1} = \begin{bmatrix} 0 & 0 & 0.375 & 0.117 \\ 0 & 0 & 0 & 0 \\ 0 & 0 & 0 & 0 \\ 0 & 0 & 0 & 0 \end{bmatrix}$$

$$K_{b2} = \begin{bmatrix} 0 & 0 & 0 & 0 \\ 0 & 0 & 0.375 & 0.117 \\ 0 & 0 & 0 & 0.047 \\ 0 & 0 & 0 & 0 \end{bmatrix}$$

$$K_{b3} = \begin{bmatrix} 0 & 0 & 0 & 0 \\ 0 & 0 & 0 & 0 \\ 0 & 0 & 0 & 0 \\ 0 & 0 & 0 & 0.15 \end{bmatrix}$$

$$G_s = \begin{bmatrix} 0 & 0 & 0 & 0 \\ 0 & 0 & 0.375 & -0.117 \\ 0 & 0 & 0.150 & -0.047 \\ 0 & 0 & 0 & 0 \end{bmatrix}$$

$$G_c = \begin{bmatrix} 0 & 0 & 0.375 & -0.117 \\ 0 & 0 & 0 & 0 \\ 0 & 0 & 0 & 0 \\ 0 & 0 & 0 & 0 \end{bmatrix}$$

The matrix of eigenvectors associated with the premaneuver state is

$$U = \begin{bmatrix} 0.2520 & 0 & 0 & 0 \\ 0 & 0.2521 & 0 & -0.0179 \\ 0 & -0.0075 & 0.2619 & -0.0883 \\ 0 & 0 & 0 & 2.7327 \end{bmatrix}$$

so that, using Eq. (2-62) and (2-64), the modal matrices are

$$\Lambda_0 = \begin{bmatrix} 0 & 0 & 0 & 0 \\ 0 & 0 & 0 & 0 \\ 0 & 0 & 0 & 0 \\ 0 & 0 & 0 & 369.2661 \end{bmatrix}$$

$$\bar{M}_s = \begin{bmatrix} 0 & 0.0007 & -0.0248 & -0.0722 \\ 0.0007 & 0 & 0 & 0 \\ -0.0248 & 0 & 0 & 0 \\ -0.0722 & 0 & 0 & 0 \end{bmatrix}$$

$$\bar{M}_c = \begin{bmatrix} 0 & 0 & 0 & 0 \\ 0 & -0.0014 & 0.0242 & 0.0715 \\ 0 & 0.0242 & 0.0206 & 0.0249 \\ 0 & 0.0715 & 0.0249 & -0.0306 \end{bmatrix}$$

$$\bar{K}_{b1} = \begin{bmatrix} 0 & -0.0007 & 0.0248 & 0.0722 \\ 0 & 0 & 0 & 0 \\ 0 & 0 & 0 & 0 \\ 0 & 0 & 0 & 0 \end{bmatrix}$$

$$\bar{K}_{b2} = \begin{bmatrix} 0 & 0 & 0 & 0 \\ 0 & -0.0007 & 0.0248 & 0.0713 \\ 0 & 0 & 0 & 0.0336 \\ 0 & 0.0001 & -0.0018 & -0.0165 \end{bmatrix}$$

$$\bar{K}_{b3} = \begin{bmatrix} 0 & 0 & 0 & 0 \\ 0 & 0 & 0 & 0 \\ 0 & 0 & 0 & 0 \\ 0 & 0 & 0 & 1.1201 \end{bmatrix}$$

$$\bar{G}_s = \begin{bmatrix} 0 & 0 & 0 & 0 \\ 0 & -0.0007 & 0.0245 & -0.0879 \\ 0 & -0.0003 & 0.0103 & -0.0371 \\ 0 & 0.0002 & -0.0052 & 0.0188 \end{bmatrix}$$

$$\bar{G}_c = \begin{bmatrix} 0 & -0.0007 & 0.0248 & -0.0889 \\ 0 & 0 & 0 & 0 \\ 0 & 0 & 0 & 0 \\ 0 & 0 & 0 & 0 \end{bmatrix}$$

Appendix F. Expressions for Parameters

For the given configuration, the position vector of a nominal point in the membrane appendage can be expressed as

$$\underline{r}_e = [r \sin \theta , r \cos \theta , h]^T \quad (F - 1)$$

Inserting the admissible functions given by Eqs. (4-17), together with Eq. (F-1), into Eqs. (2-22) and (2-24), we obtain

$$\overline{\Phi}_e^T = 2 a \sqrt{\pi \overline{\rho}_e} \begin{bmatrix} 0 & 0 & \frac{1}{\beta_{01} a} \\ 0 & 0 & \frac{1}{\beta_{02} a} \\ 0 & 0 & 0 \\ \cdot & \cdot & \cdot \\ \cdot & \cdot & \cdot \\ \cdot & \cdot & \cdot \\ 0 & 0 & 0 \end{bmatrix} \quad (F - 2)$$

$$\tilde{\Phi}_e^T = \sqrt{2\pi\bar{\rho}_e} a^2 \begin{bmatrix} 0 & 0 & 0 \\ 0 & 0 & 0 \\ 0 & -\frac{1}{\beta_{11}a} & 0 \\ 0 & -\frac{1}{\beta_{12}a} & 0 \\ 0 & 0 & 0 \\ 0 & 0 & 0 \\ \frac{1}{\beta_{11}a} & 0 & 0 \\ \frac{1}{\beta_{12}a} & 0 & 0 \\ 0 & 0 & 0 \\ 0 & 0 & 0 \end{bmatrix} \quad (\text{F} - 3)$$

and

$$\bar{H}_e(\underline{a}) = -(a_1^2 + a_2^2) I \quad (\text{F} - 4)$$

where I is 10×10 identity matrix. Moreover,

$$\tilde{H}_e(\underline{a}) = [0] \quad (\text{F} - 5)$$

$$J_e^T(\underline{a}) = 2a \sqrt{\pi \bar{\rho}_e}$$

$$\begin{bmatrix} \frac{2ha_1}{\beta_{01}a} & \frac{2ha_2}{\beta_{01}a} & 0 \\ \frac{2ha_1}{\beta_{02}a} & \frac{2ha_2}{\beta_{02}a} & 0 \\ \frac{-aa_3}{\sqrt{2}\beta_{11}a} & 0 & \frac{-aa_1}{\sqrt{2}\beta_{11}a} \\ \frac{-aa_3}{\sqrt{2}\beta_{12}a} & 0 & \frac{-aa_1}{\sqrt{2}\beta_{12}a} \\ 0 & 0 & 0 \\ 0 & 0 & 0 \\ 0 & \frac{-aa_3}{\sqrt{2}\beta_{11}a} & \frac{-aa_2}{\sqrt{2}\beta_{11}a} \\ 0 & \frac{-aa_3}{\sqrt{2}\beta_{12}a} & \frac{-aa_2}{\sqrt{2}\beta_{12}a} \\ 0 & 0 & 0 \\ 0 & 0 & 0 \end{bmatrix}$$

(F - 6)

$$\int_{D_e} \rho_e \Phi_e^T \tilde{a} \tilde{r}_e dD_e = 2 a \sqrt{\pi \bar{\rho}_e} \begin{bmatrix} \frac{ha_1}{\beta_{01}a} & \frac{ha_2}{\beta_{01}a} & 0 \\ \frac{ha_1}{\beta_{02}a} & \frac{ha_2}{\beta_{02}a} & 0 \\ 0 & 0 & \frac{-aa_1}{\sqrt{2} \beta_{11}a} \\ 0 & 0 & \frac{-aa_1}{\sqrt{2} \beta_{12}a} \\ 0 & 0 & 0 \\ 0 & 0 & 0 \\ 0 & 0 & \frac{-aa_2}{\sqrt{2} \beta_{11}a} \\ 0 & 0 & \frac{-aa_2}{\sqrt{2} \beta_{12}a} \\ 0 & 0 & 0 \\ 0 & 0 & 0 \end{bmatrix} \quad (F-7)$$

$$\int_{D_e} \rho_e [\Phi_e \tilde{q}_e] \Phi_e dD_e = [0] \quad (F-8)$$

where we note that the above null matrix is 3×1 . In addition,

$$\int_{D_e} \rho_e [\Phi_e \tilde{p}_e] dD_e = \begin{bmatrix} -\alpha_1 & 0 & 0 \\ 0 & -\alpha_1 & 0 \\ \alpha_2 & \alpha_3 & 0 \end{bmatrix} \quad (\text{F} - 9)$$

where

$$\alpha_1 = 2 a h \sqrt{\pi \bar{\rho}_e} \left[\frac{p_1}{\beta_{01} a} + \frac{p_2}{\beta_{02} a} \right] \quad (\text{F} - 10a)$$

$$\alpha_2 = a^2 \sqrt{2\pi \bar{\rho}_e} \left[\frac{p_3}{\beta_{11} a} + \frac{p_4}{\beta_{12} a} \right] \quad (\text{F} - 10b)$$

$$\alpha_3 = a^2 \sqrt{2\pi \bar{\rho}_e} \left[\frac{p_7}{\beta_{11} a} + \frac{p_8}{\beta_{12} a} \right] \quad (\text{F} - 10c)$$

$$\int_{D_e} \rho_e \tilde{u}_e \tilde{v}_e dD_e = - \sum_{i=1}^{10} q_i p_i \begin{bmatrix} 1 & 0 & 0 \\ 0 & 1 & 0 \\ 0 & 0 & 0 \end{bmatrix} \quad (\text{F} - 11)$$

$$\int_{D_e} \rho_e \Phi_e^T \tilde{\omega}_e \tilde{u}_e dD_e = \begin{bmatrix} -\omega_1 q_1 & \omega_2 q_1 & 0 \\ -\omega_1 q_2 & \omega_2 q_2 & 0 \\ \cdot & \cdot & \cdot \\ \cdot & \cdot & \cdot \\ -\omega_1 q_{10} & \omega_2 q_{10} & 0 \end{bmatrix} \quad (\text{F} - 12)$$

$$\int_{D_e} \rho_e \Phi_e q_e dD_e = 2 a \sqrt{\pi \bar{\rho}_e} \begin{bmatrix} 0 \\ 0 \\ \frac{q_1}{\beta_{01} a} + \frac{q_2}{\beta_{02} a} \end{bmatrix} \quad (\text{F} - 13)$$

$$\underline{S}_{ev} = 2 a \sqrt{\pi \bar{\rho}_e} \begin{bmatrix} 0 \\ 0 \\ \frac{p_1}{\beta_{01} a} + \frac{p_2}{\beta_{02} a} \end{bmatrix} \quad (\text{F} - 14)$$

**The vita has been removed from
the scanned document**